Carboxymethyl and periodate oxidative functionalization of cellulose fibers for textile applications

By

Martin Chewe Sichinga

A thesis submitted to McGill University in partial fulfillment of
the requirements for the degree of Doctor of Philosophy

Department of Chemistry
McGill University
Montreal, Quebec, Canada
11 April 2022

Table of contents

Abstract

Cellulosic products continue to advance the replacement of non-renewable polymeric products and provide a source of biobased materials. The quest to efficiently produce renewable and sustainable functional cellulosic products has prompted the development of an environmentally sensitive and cost-effective method to produce multi-functionalized cellulosic fibers for application in the textile industry. Current cellulose-based textiles, mainly manufactured by the rayon process, in which carbon disulfide, a highly toxic product, is used. In addition, textile dyeing is one of the most polluting processes in this industry.

Therefore, to tackle these drawbacks, Treeyon has been developed. One form of Treeyon is an imine carboxymethyl dialdehyde modified cellulose (ICDAMF) material, multi-functionalized in a sequential single-pot synthesis to obtain desired beneficial properties, without isolating and purifying intermediate products. Multi-functionalization allows for covalent addition of dye, thereby preventing leaching during the textile filament spinning process and products' lifetime use. Therefore, the present research explores color addition and wet textile spinning without production of dye waste. In addition, rheology and dye adsorption kinetics of modified fibers has been studied using break through curves, to optimize reaction conditions.

Furthermore, industrial production of carboxymethyl cellulose fibers (CMF) requires use of solvents (water and alcohols), which result in the hydrolysis of carboxymethylating agents and increase production cost. The present research also explores a solvent-free mechanosynthesis and characterization of CMF. Solvent-free reactions minimizes hydrolysis, resulting in higher yields. The CMF produced is further wet extruded into textile filaments that can be converted into yarn.

Résumé

Les produits cellulosiques continuent de faire progresser le remplacement des produits polymères non renouvelables et constituent une source de matériaux biosourcés. La quête pour produire efficacement des produits cellulosiques fonctionnels renouvelables et durables a incité le développement d'une méthode respectueuse de l'environnement et rentable pour produire des fibres cellulosiques multifonctionnelles pour les applications dans l'industrie textile. Textiles actuels à base de cellulose sont principalement fabriqués par le procédé de la rayonne, dans lequel le disulfure de carbone, un produit hautement toxique, est utilisé. De plus, la teinture de textile est l'un des procédés les plus polluants de cette industrie.

Par conséquent, pour remédier à ces inconvénients, Treeyon a été développé. Une forme de Treeyon est un matériau de cellulose modifiée en carboxyméthyldialdéhyde imine (ICDAMF), multifonctionnel dans une synthèse séquentielle en un seul pot pour obtenir les propriétés bénéfiques souhaitées, sans isoler ni purifier les produits intermédiaires. La multifonctionnalité permet l'ajout covalent de colorant, empêchant ainsi la lixiviation pendant le processus de filage des filaments textiles et l'utilisation pendant la vie des produits. Par conséquent, la présente recherche explore l'ajout de couleur et la filature de textile humide sans production de déchets de teinture. De plus, la rhéologie et la cinétique d'adsorption de colorant des fibres modifiées ont été étudiées à l'aide de courbes de percé afin d'optimiser les conditions de réaction.

De plus, la production industrielle de fibres de carboxyméthylcellulose (CMF) nécessite l'utilisation de solvants (eau et alcools), ce qui entraîne l'hydrolyse des agents carboxyméthylants et l'augmentation du coût de production. La présente recherche explore également une mécanosynthèse sans solvant et la caractérisation du CMF. Les réactions sans solvant minimisent l'hydrolyse, ce qui entraîne des rendements plus élevés. Le CMF produit est ensuite extrudé par voie humide en filaments textiles qui peuvent être convertis en fil.

Acknowledgements

Completing a PhD is seen as a singular endeavour with the praise focused on the writer almost exclusively. While I have worked hard for 5 years and I am infinitely proud of what I've accomplished, I've also been fortunate to have received help from so many incredible people along the way. It's now my greatest pleasure to share this accomplishment with them.

I am deeply indebted to my supervisor Professor Theo G.M. van de Ven. I knew from our first meeting that I would flourish in your lab. You approached my work with an open mind that let me explore my full potential and build my confidence as a scientist. Your guidance kept me on track while your trust in me allowed me to push my limits and grow. Research advise and helpful insight provided by Professor Ashok Kakkar and Professor Mattew J. Harrington from the infancy of the project greatly helped how I tackled problem solving. Your enthusiasm to research and new ideas is deeply inspirational. Gratitude goes to the PhD thesis examining committee, Professor Audrey Moores, Professor Dima Perepichka and Professor Gil Garnier, for their time and constructive feedback throughout the defence process.

The van de Ven lab saw years of amazing scientists pass through and each had an impact on my work. I'd especially like to acknowledge Kevin Conley, who initially taught me everything about the lab. Despite working on totally different projects, you took the time to train me patiently. You set the bar high for me as I took on more of this role in my later years at the lab. A big thank you to Jane Ebosetale, Md Shahidul Islam, Md Nur Alam, Mohammadhadi Moradian, Kayrel Edwards, Sierra Crammer-Smith, Yiwei Jiang and Mandana Tavakolian for the help, research advice, wonderful group meetings and making the van de Ven lab a pleasant place to work. Your contributions are invaluable.

I'm also incredibly appreciative of Roya Koshani. You have a special approach to work and set an inspiring example for me with your dedication and perseverance. You also showed me how important it is to grow as both a person and a scientist through this process. It's been a wonder to witness your ongoing evolution. You've achieved many great things while also striking a balance with life. You have been invaluable to me in times of stress and are always there to listen or help problem solve. You've taught me much more than you could ever know.

The Chemistry Department administrative staff, Chantal Marotte, Jennifer Marleau, Lina Alvarez, Chelsea Briand-Pitts provided great help in many instances, especially with the smooth running of my laboratory administrative duties. The characterization lab managers, Hatem Titi and Robin Stein, your help with XRD and NMR experiments, respectively, is greatly appreciated.

I would like to extend my sincere thanks to NSERC SRN on Green Fibers, NSERC SPG (506303-17), Centre for Advanced Materials (QCAM)/CQMF) and FPInnovations for providing the funding that allowed me to research this project and pursue my passion as a scientist. Organizations like yours are critical to Canada's research community, and I am honoured to have been in receipt of your assistance.

I came to McGill by way of University of Zambia, Mount Saint Vincent University (MSVU), and Acadia University. The lessons learned in those institutions went well beyond the classroom. Paula Barry and Nicolle Bowes Cashen, thank you for building a vibrant international student community and making the home away from home experience memorable. Mahsa, you were my first Chemistry Lab partner at MSVU. You helped me get my feet under me in a new country and new academic environment. Your partnership throughout my BSc helped me develop my love for research in Chemistry. Thank you. Chérif F. Matta, you are still the smartest and most humble person I know. Your supervision for my summer undergraduate project led to my first publication and set the stage for my future academic success. You are the mentor that every young scientist hopes to meet.

I must also thank my colleagues and friends at Tong's Lab at Acadia University, where I completed my MSc in Analytical Chemistry. It was here that I was first given the courage and opportunity to approach complex lab equipment and modify it for my needs. I realized I could design experiments in novel ways by learning the bones of each piece of machinery, which later proved invaluable in my PhD work. I would like to extend special thanks to Jim Ghoshdastidar and Crystal Sweeney, who both taught me so many things both inside and outside of the lab.

I can say with confidence that I would not be here without my friends. Marcus Bwalya Chitundu, Likezo Limbambala (deceased), Cholwe Buleze Francis Kayamba and Kingston Mbao, you are the best friends a guy could ask for. You are incredible people and I cherish your friendship, encouragement, and positivity. Life adventures without you would not be the same. To the friends I have made in Montreal (Hugo Antoine, Mitchell McNall, Lizbeth Moreno, Tobias Priemel, Christian Both, Monika Polakowska, David Kroeker-Maus, Konstandina Chalastara, Stephen George, Daniel Morales, Punit Singh, Mostafa Rammal and Tristan Borchers), the laughs we shared, the sports and games we played, and the adventures we went on, were what buoyed me through the most stressful periods. I'm a very lucky guy. Katherine Duckworth, a massive thank you for all the help in proofreading and formatting most of this work and taking the time from your busy schedule to offer support and encouragement. I am so grateful for everything you have done.

Finally, and foremost, I want to take a few moments to mention my family. My decision to become a scientist was most heavily influenced by my father, Henry Sichinga. Dad, while you passed when I was just 19, you had a passion for science that was ingrained in me early. You showed me what working at something you love can mean for your life. Thank you dad. My mother's, Catherine Nkonde, influence on my career cannot be understated. Mom, you always prioritized education, both ours and yours. You showed me what it is to sacrifice for your dream and set an example for what you can achieve if you put your mind to it. I credit you for my determination and resilience. To my grandparents, ba shikulu ba Levy Nkonde and ba mama ba Catherine Nkonde, I thank you for your tolerance of my curiosity and independence, both of which often got me in trouble. You never stifled my creativity, no matter how many broken telephones or radios resulted from it. My siblings, Jane Nachinga, Mirriam Nachinga and Henry Sichinga, your unwavering support, patience, belief, and dedication to the family is greatly appreciated. I love you all and thank you.

Contribution to original knowledge

1. Solvent-free synthesis of carboxymethyl cellulose

   Carboxymethylcellulose (CMC) is industrially produced using aqueous and organic solvents at elevated temperatures. The solvents constitute about 80% w/w during the process. Use and recovery of organic solvents, and high temperatures, increase the cost of production. Using similar reaction conditions used to produce CMC, our lab developed a protocol to synthesize low charge, non-water soluble carboxymethyl cellulose, herein called carboxymethyl fibers (CMF). This study further explored mechanical milling to produce CMF thereby eliminating the need to use organic solvents. The impact due to this process is energy saving, reduced cost and time of CMF production.

2. Kinetics of Fuchsine deposition on dialdehyde modified cellulose fibers packed beds

   The deposition kinetics is studied for a better understanding of amine dye loading capacity on modified cellulose fibers. The study explores physical and chemical adsorption of amine dyes using breakthrough curves and calculations from first principles. This process has potential to be applied in dye removal from wastewater generated from textile production. In current technologies, textile dyeing is done as a post-treatment step mainly relying on physisorption of dyes onto the fibers. The rates of chemisorption, obtained in this study, indicate that dyes applied prior to extrusion improves textile fastness thereby minimizing the environmental impact due to dye leaching.

3. One pot eco-friendly oxidative synthesis of Imine carboxymethyl dialdehyde cellulosic (ICDAC) fibers

This one pot synthesis investigated reactions to covalently dye cellulose fibers, in a process that minimizes the dyeing process environmental footprint. This protocol reinvents the order in which textile dyeing is done, i.e., as a pre-extrusion step. Chemical adsorption with a limited amount of dye is achieved first, followed by extrusion of fibers into textile filaments. The process developed can be applied in renewable textile and packaging materials as the economy moves towards development of more renewable and sustainable functional materials. Additionally, the high cost of producing dialdehyde cellulose (DAC) limits its applications in industry. To lower the cost, this study employed mildly modified dialdehyde cellulose fibers, herein referred to as dialdehyde modified fibers (DAMF) thereby making it cost effective for industrial applications in combination with recent achievements on sodium periodate recycling.

List of tables

List of figures

List of schemes

List of abbreviations

ATR-FTIR	Attenuated total reflectance Fourier transform infrared
BTC	Breakthrough curve
CDAMF	Carboxymethyl dialdehyde modified fibers
CMC	Carboxymethyl cellulose
CMF	Carboxymethyl fibers
CSTR	Continuously stirred batch reactors
DAC	Dialdehyde cellulose or 2,3-dialdehyde cellulose
DAMF	Dialdehyde modified fibers
DCC	Dicarboxylic acid cellulose
DFT	Density functional theory
DO	Degree of oxidation
DS	Degree of substitution
ICDAMF	Imine carboxymethyl dialdehyde modified fibers
LAG	Liquid-assisted grinding
MCA	Monochloroacetic acid
NMNO	N-methyl morpholine-N-oxide
NMR	Nuclear magnetic resonance
PBR	Packed bed reactor
RTD	Residence time distribution
UV-vis	Ultraviolet-visible
XRD	X-ray diffraction

1 Introduction

The textile industry is dominated by non-renewable materials, such as polyester, and processing techniques cause considerable CO_2 emissions thereby greatly contributing to climate change. Extensive efforts are being made to mitigate this effect and research into further applications of wood-based products provides a sustainable, renewable, and eco-friendly solution. The major consumers of wood-based products are construction, paper & board, and textile industries. However, due to a paperless economy transition, the pulp and paper industry has been negatively affected, leading to idle pulping mills. Through the pulping process, cellulose is extracted from wood which in turn is converted to other valuable bioproducts. Therefore, an investigation in developing novel functional cellulose products is essential and will contribute to sustaining the pulping industry. Cellulose is advantageous for a wide range of products because it is renewable, has low cost, is biodegradable and biocompatible.

Cellulose-based textiles, mainly produced by the rayon process, provide carbon-neutral textiles with high mechanical strength and stability. However, the manufacturing process uses and produces carbon disulfide, which is acutely toxic even at extremely low concentrations thereby creating a health risk to the workers. This has led to outsourcing rayon production to developing countries that have more relaxed environmental regulations. Additionally, the textile dyeing process is quite polluting due to poor binding affinity of the dyes to the fibers, which results in dye effluents leaching into the ecosystem. Canada’s vast forest reserves and the optimized pulping processes provides a suitable platform to develop a textile manufacturing process that mitigates the drawbacks of rayon production and address the dye-waste problem. Therefore, this research aims to develop an environmentally sensitive and economically viable technological to transform renewable carbon in textile manufacturing, as we gradually transition from a fossil fuel to a bio-based economy.

1.1 Research objectives

Main objective: To develop a novel cellulose-based textile filament manufacturing process, which is transformative in meeting the modern environmental interests of being renewable, economically viable and sustainable.

To achieve the main objective, the project was divided into subobjectives as follows:

(a) To investigate cellulose chemical modifications that will allow solubilization and regeneration of fibers in appropriate solvents.

(b) To develop and optimize a continuous extrusion process.

(c) To investigate a process to chemically bind dyes to the fibers without production of dye waste products.

(d) Investigate green chemistry techniques to lower production cost and improve efficiency.

1.2 Outline and scope of this thesis

This is a manuscript-based thesis consisting of two published papers (Chapters 4 and 5) and Chapter 3 has been submitted for publication and is under review in the journal Cellulose.

Chapter 2 provides a theoretical background and literature review on the principles used to develop the textile extrusion process and chemical analytical techniques employed to characterize the materials qualitatively and quantitatively.

Chapter 3 builds on the textile filament extrusion process [1, 2] by investigating the cellulose carboxymethylation reaction under solvent-free mechanosynthesis conditions. This process provides a green and more economical route to produce carboxymethyl cellulose fibers (CMF) offering an alternative to conventional CMF synthesis methods that employ organic solvents. In addition, this chapter also explores a reduction in procedural extrusion steps thereby making the process more efficient.

Chapter 4 explores the kinetics and mechanisms of chemisorption of diamine dyes onto aldehyde modified cellulosic fibers to determine applicability in textile dyeing and water purification.

Chapter 5 demonstrates an optimization of a one-pot synthesis and use of multi-functionalized cellulose in producing dyed textile filaments. Multi-functionalization allows the integration of desired functional groups with a particular purpose, while single-pot synthesis condenses the reaction steps.

Chapters 6 and 7 provides concluding remarks on the three manuscripts and protocols developed, with suggestions on future work to be done.

1.3 Contribution of authors

Below is a summary of the contributions by the authors:

(a) Martin Sichinga and Theo G.M. van de Ven, Mechanosynthesis of carboxymethyl cellulose fibers using ball and grind milling for applications in wet spinning textile extrusion, *Cellulose* (submitted March 2022).

Contributions: Martin Chewe Sichinga performed all carboxymethylation experiments, characterization, data analysis and wrote the manuscript. Theo van de Ven supervised the author, provided input during the research and edited the manuscipt.

(b) Martin Chewe Sichinga , Roya Koshani, and Theo G. M. van de Ven. 2022. 'Chemisorption of basic fuchsine in packed beds of dialdehyde cellulose fibres', *Colloids and Surfaces A: Physicochemical and Engineering Aspects,* 632: 127726. https://doi.org/10.1016/j.colsurfa.2021.127726.

Contributions: Martin Chewe Sichinga performed all adsorption experiments, data analysis and wrote the paper. Roya Koshani helped with Fourier transform infrared and nuclear magnetic resonance spectroscopic analysis. Theo van de Ven supervised both authors, provided input during the research and edited the manuscipt.

(c) Martin Chewe Sichinga, Timothy Kline, M.A. (Tony) Whitehead and Theo G.M. van de Ven. 2022. \`One-pot eco-friendly oxidative synthesis of imine carboxymethyl dialdehyde cellulosic fibers\` *Cellulose,* 29, 799-815. https://doi.org/10.1007/s10570-021-04352-1.

Contributions: Martin Chewe Sichinga performed all laboratory and some computational experiments, data analysis, trained and supervised Timothy Kline during his undergraduate research and wrote the manuscript. Timothy Kline performed some of the computational experiments and data analysis. M.A (Tony) Whitehead provided technical support and advise on computational methods and theories. Theo G. M. van de Ven supervised the project, provided input during research, and edited the manuscript.

2 Background

2.1 Cellulose fibres background – Uses and advantages

Cellulose is a major constituent of plant matter and generated yearly in large quantities through photosynthesis, though production is not limited to the vegetative kingdom only. Cellulose abundance makes it the most widely used organic chemical worldwide, in various forms such as wood, paper, cotton textiles, rayon, plastics, food and pharmaceuticals. As a renewable material, cellulose and its derivatives are ideal materials for sustainable development. Technologically, cellulose refers to the residue obtained after subjecting plant matter through a pulping process. Chemically, cellulose is a polysaccharide consisting of anhydroglucose units linked via a β-(1-4)-glucosidic linkage with three free hydroxyl groups at the 2, 3 and 6 positions [3], the repeat unit is shown in **Figure 2.1**. The polymeric linkage with high degree of polymerization leads to insolubility in water or dilute acids and alkalis at room temperature and pressure. Therefore, cellulose herein refers to bleached softwood kraft pulp as well as the polysaccharide from whence the fibres come, unless otherwise stated.

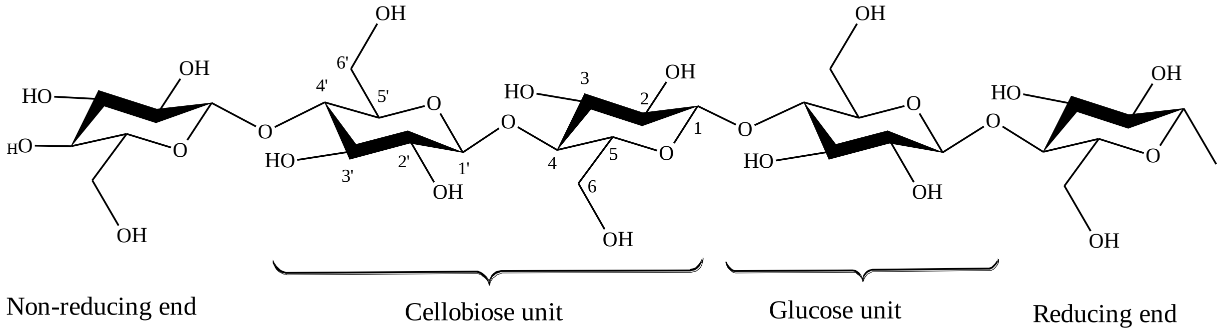

Figure 2.1: Steric configuration and numbering of the glucopyranose rings in cellulose.

As a naturally important material, cellulose has been subjected to enormous amounts of studies involving occurrence, chemical and physical structures, formation, isolation and purification, and chemical modifications. These investigations have led to a considerable understanding of its nature, behaviour, and development of value-added products in modern society. Cellulose in woody materials, mainly obtained from branches and trunks, constitutes 40 – 60% of dry mass with the other major components been 20 – 30% lignin and 10 – 30% hemicellulose [3, 4]. The pulping and bleaching process removes most of lignin and hemicellulose resulting in microfibrils consisting of bundles of nanofibrils with alternating amorphous and crystalline regions, with a degree of polymerization up to 20,000 units [5] and varying crystalline sizes depending on the source of fibres [6, 7]. This is schematically shown in **Figure 2.2**.

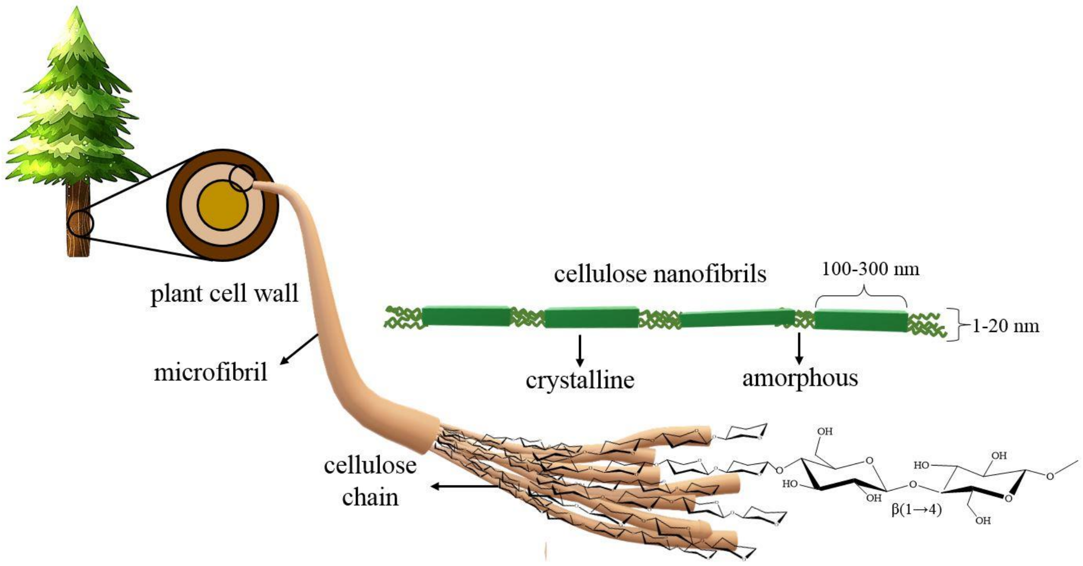

Figure 2.2: Schematic representation of cellulose assembly from a molecular level in plants.

Cellulose microfibrils structure can be modified via controlled mechanical, chemical or enzyme treatment that result in the hydrolysis of amorphous regions to obtain nanocrystalline cellulose [8]. Additionally, a novel class of nanocellulose with amorphous hairs protruding out of the crystalline ends have been developed. They are referred to as hairy nanocellulose [9]. Formation of nanocrystals conserves the cellulose chemical structure within the crystalloid, increase surface area and exhibit liquid crystalline properties. The precise control of hydrolysis has let to further understanding of the chirality of these nanoparticles, and by controlling the crystal size, it was observed that the handedness can be reversed [10, 11]. The changes in chemical and physical properties are advantageous in developing new materials with desired characteristics.

Most cellulose chemical alterations take advantage of the hydroxyl groups present on the carbons at positions 2, 3 and 6, as they have different reactivities. The variation in reactivity has a profound effect on the chemical and physical properties of the cellulose derivative. Therefore, a method to determine the average degree of substitution (DS) based on degree of polymerization and probability of attaching to the C2, C3 and C6 atoms was developed. The DS weight is averaged overall glucopyranose units of all molecules as a sum of the average probability of substitution of the hydroxyl group at the three positions [12]. The DS, determined via chemical analysis, nuclear magnetic resonance (NMR) and chromatography, has a profound effect on the physical and chemical properties of cellulose derivatives. Therefore, the ability to exist in different polymorphs, relatively easy to modify chemically and physically, biocompatibility, bioavailability, renewability, abundance and low cost makes cellulose a suitable material for many industrial and domestic applications.

2.2 Textile background and current technologies

2.2.1 Textile filament production methods

The Textile Institute defines fibers as units of matter characterized by flexibility, fineness and a high ratio of length to thickness, in addition high temperature stability if used in textile [13]. Textile fibers, which are polymeric compounds, are produced from natural (cotton, wool, silk, pulp fibers) and man-made sources (polyesters, nylon). The different types of fibers have different physical and chemical properties [14]. Fiber blending combines advantages of the different types of fibers, thereby minimizing the drawbacks of each. The major challenge with blending is in developing the best recycling solutions. The unique properties of the different types of fibers allows the development of varying functional products such as casual wear, sports clothing, high visibility safety clothing, water- and fire-resistant wear and lingerie.

Fibers are initially converted into filaments prior to making yarn, through a spinning process. The spinning process involves liquifying the polymer and then regenerating it into an ordered extruded fiber. There are two major spinning techniques, i.e., melt and wet spinning. Melt spinning involves heating the polymer to make it molten and then passed through an extruder at constant pressure. The spinneret forms fine filaments which are continuously drawn and wound when cooled down. Melt spinning is mainly used for synthetic fibers such as nylon [15]. The use of non-renewable starting materials, high energy consumption, suitability for thermoplastics and non-degradability of the final product are some of the major drawbacks in this process [16].

Wet spinning, also referred to as solution spinning, involves dissolving the polymer in an appropriate solvent to make a dope. The dope is then passed through a spinneret immersed in a coagulation bath, also known as a spin bath. The polymer coagulates and is drawn out of solution, dried and heat-set. This technique is employed in synthetic polymers such as aramid fibers and natural fibers that are challenging to form a melt, such as cellulose [15, 17]. Overall, in filament production, it is necessary to convert the polymer into a liquid and then regenerated continuously (**Figure 2.3**), with minimal fiber degradation in all the stages. The challenge lies in determining appropriate solvents and solvent combinations, including developing appropriate physical and/or chemical modifications of cellulose for this purpose.

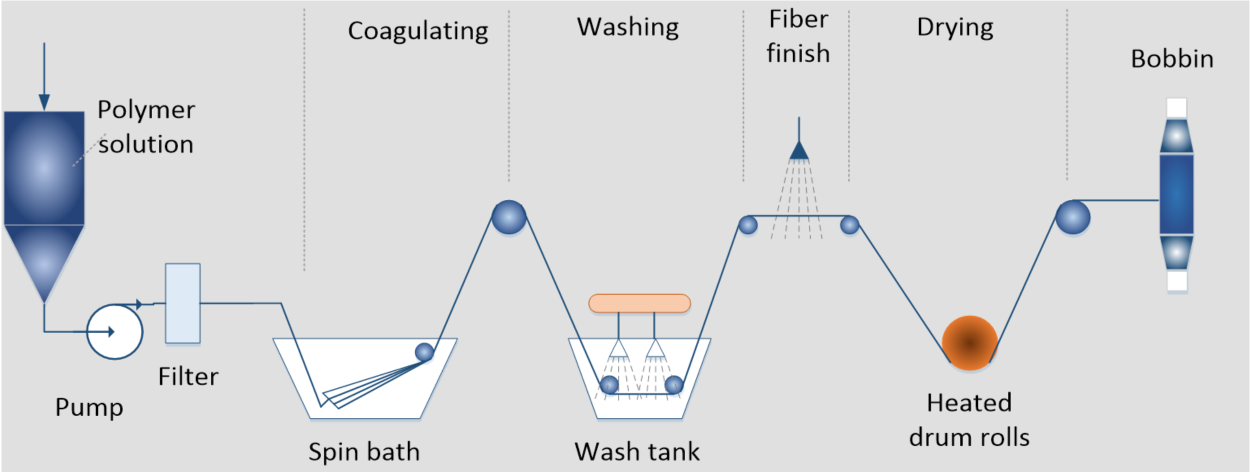

Figure 2.3: Schematic representation of filament production by the wet spinning process.

To this effect, various studies have been conducted on solubilization and regeneration of cellulose, with the most prominent techniques being the rayon (viscose) and lyocell procedures. The rayon process involves converting cellulose to a cellulose alkoxide in alkali solution, which is then converted to cellulose xanthate using carbon disulfide (CS_2). Cellulose xanthate is then solubilized into a highly viscose dope using NaOH. The product of NaOH solubilization is sodium cellulose xanthate, which then decomposes during wet spinning by regenerating cellulose in H_2SO_4 thus liberating CS_2 [18]. Therefore, the final product of this process is environmentally friendly and sustainable. The major drawback is the evolution of CS_2 which is poisonous to the viscose factory workers and surrounding communities [19, 20] in addition to dyeing challenges [18]. Steps have been undertaken to solve these problems, however, the low water solubility (0.2% at 20°C) and volatile nature of CS_2 makes it challenging [21, 22] and alternative approaches overall lead to increased production costs [23-25].

The lyocell process was developed to mitigate the major problem (CS_2) associated to the viscose process. The lyocell process employs the dry-jet wet spinning process by replacing CS_2 with a low toxicity, hot aqueous solution of N-methyl morpholine-N-oxide (NMMO) for polymer dissolving, via a physicochemical process [26]. Solubilization is achieved by disrupting the hydrogen bonding in cellulose fibers. During the dry-jet wet spinning, the dope is coagulated by cooling through an air gap and then filaments set in a dilute aqueous amine oxide solution [22]. The process is relatively green, and the final product has been considered to have improved physical properties and better aesthetic qualities than viscose [27]. The major drawbacks are: (1) energy intensive, as the dope is prepared at 90 - 120 °C and NMMO recycling is conducted by distillation. (2) degradation of NNMO at high temperatures and cellulose due to formation of by-products and use of stabilizers. (3) Increased use of stabilizers and NMMO increases the cost of the final product [22, 26]. To address some of these problems, use of ionic liquids [27, 28] or NMMO concentration via use ion-exchange resins and condensation and reuse of distilled water have been proposed [29], largely adding to the number of production steps and production cost. Therefore, future technologies need to enhance these processes further or develop novel techniques that address the current environmental and economical demands.

Fiber finishing stage of the textile production process involves post treatment of fibers, which involve dyeing. Textile dyeing is a process of adding dyes or pigments to fabrics, to obtain desired colors, which is one of the main attractions to the consumer. Dyes contain a chromophore and electron donating or withdrawing functional groups, such as azo, nitro carbonyl or amine, which intensify colors [30]. The chromophore has a covalently unsaturated group and UV-visible radiation absorption result in movement of the π-electrons, the impact on color due this excitation depends on the radiation wavelength [31].

2.2.2 Textile dyeing and its challenges

Dyes are classified as either natural (e.g., quinones and carotenoids) or synthetic (e.g., amines and azo). Natural dyes tend to be less reactive as they may contain less reactive end groups and lower decomposition temperatures. Synthetic dyes are tailored to be more reactive and water soluble by functionalizing with reactive groups and/or a charge [32], making them more toxic to the environment [33]. Thus, natural dyes are more challenging to adsorb on cellulosic textiles due to poor binding affinity, compared to synthetic counterparts. The high absorbance of cellulose makes it easy to infuse dyes resulting in deep rich colors but they fade over lifetime use [18]. The fastness properties of the dye depend on the type of bonding used in the fiber finish.

There are various techniques used to fix dyes onto textile fibers, and the choice depends on quality of finish, cost, type of fiber and availability of technology. Overall, dyes are adsorbed onto fibers by hydrogen bonding, van der Waals attraction, thermal fixation and chemisorption. The process involves fiber preparation to remove impurities, aqueous application of dyes and then finishing to improve fiber quality, permanent press or enhance desired characteristics [30]. For cellulosic textiles, the absence of highly reactive functional groups makes chemisorption of natural dyes challenging. Consequently, natural dye fixation techniques, such as mordanting treatment, have been developed to improve fastness. In this case, a binding agent such as a polyelectrolyte, salts or coordinating agents are applied onto the fibers prior to passing it through a dye aqueous solution. The procedure involves pre-treatments of fibers to bleach and remove impurities and then a soaping treatment after dye application to remove residual dyes and other auxiliary chemicals. The whole process ranges from 60 – 120 minutes at temperatures of 70 – 100 °C [32].

This process result in high water consumption which is in the range of 21 – 645 L kg^{-1} of product in cotton mills and the more optimized systems averaging ~100 L kg^{-1} [34]. Technological improvements, such as recycling, flow automation and onsite water purification, have been proposed to reduce water consumption to < 80 L kg [35]. Furthermore, high temperature dye fixation has limited application for natural dyes due to their lower decomposition temperatures, in addition to higher cost compared to synthetic ones. Conversely, natural dyes are more environmentally friendly. Textiles with natural dyes using metallic mordants demonstrates improved ultraviolet protection factor and anthraquinone-based fabrics have insect repelling characteristics [32].

Synthetic dyes are chemically designed to be water solubility, easier to adsorb on textiles using chemical functionalization, higher thermal stability, cheaper due to mass production techniques and can be tailored for specialized applications [32]. Synthetic dyes are either acid (anionic) possessing acidic groups such as SO_3H or COOH or cationic. Basic dyes are cationic, which are salts generated from aromatic bases, most frequently containing primary, secondary or tertiary amines or nitrogen-containing heterocyclic rings [36]. Reactive dyes form ionic or covalent bonds with cellulosic fibers to improve wet-fastness properties, using simpler reaction techniques due to an increased dye-fiber affinity [37]. Basic dyes have been described as having a beautiful shiny crystalline structure giving brilliant and high intensity colors that are unmatched by other synthetic dyes [37], resulting in extensive use in various industries such as textile, paper, photography, pharmaceutical, food and cosmetics [38].

Therefore, use of colors is one the major attractions for textile consumers, however, extensive use of water and dyes in textiles is one of the major aquatic polluting concerns. To mitigate the environmental impact, various degradation, filtration and adsorption techniques have been developed to process and treat dye wastewater [38, 39]. Most techniques emphasize on wastewater management and dye degradation, rather than preventing generation of waste. Therefore, it is critical to develop efficient technologies in which textile dyeing is achieved with minimal use of water and inhibit production of waste.

It was observed that Kraft pulp contains hemi-cellulose (~1%), which has carboxyl groups with a charge content of 0.06 mmol g^{-1} of cellulose [40], giving the fibers a negative charge. Therefore, this study focused on four basic dyes with 1° amines (**Figure 2.4**), examples of which are acridine yellow G (3,6-diamino-2,7-dimethylacridine), basic fuchsine (4-[(4-Aminophenyl)-(4-imino-1-cyclohexa-2,5-dienylidene)methyl]aniline hydrochloride), Bismarck brown (1, 4,4′-(m-Phenylenebisazo)bis-m-phenylenediamine dihydrochloride) and safranine (3,7-Diamino-2,8-dimethyl-5-phenylphenazin-5-ium chloride). Ionic bonding improves dye fixation which is easier to achieve between cellulosic fibers with a negative charge and cationic dyes, thereby improving material fastness. This has been taken advantage of in the rayon fibers although fading is observed with prolonged use of the fabrics [18]. However, covalent attachment of dyes to the fibers makes the dye be part of the fiber chemical structure [41], and this can further improve fastness as long as the reaction is not reversible under the conditions in which the material is used.

Therefore, this research explores the kinetics of chemisorption of basic amine dyes onto Kraft pulp in a Schiff base reaction, which is supplemented by ion exchange, with the aim of applying the method to textile dyeing in a continuous flow process. Exploring chemisorption methods would be advantageous in preventing dye leaching during and after production, while minimizing the quantities of dyes and water utilized. This was achieved by introducing aldehyde functionality to cellulose and then reduce it to imine in Schiff base reactions.

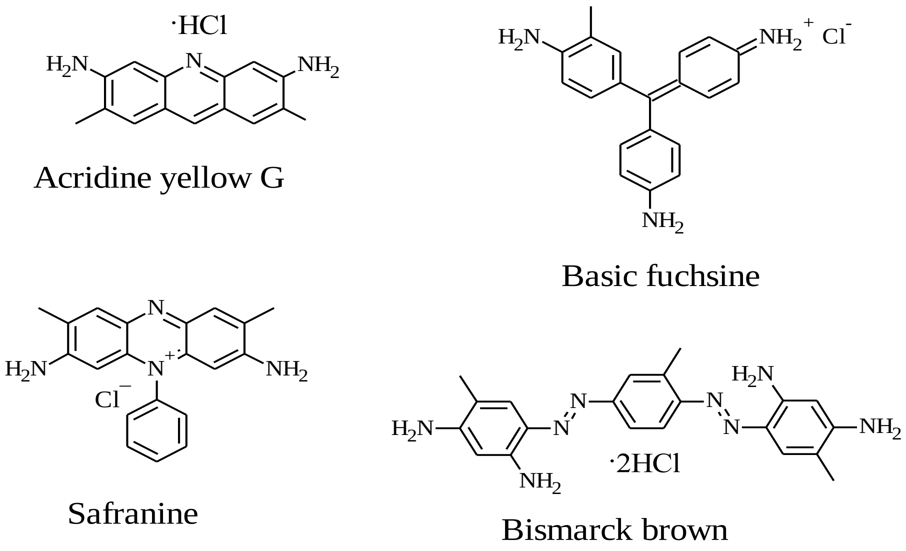

Acridine yellow G

Basic fuchsine

Safranine

Bismarck brown

Figure 2.4: Primary amine synthetic dyes with benzylic chromophores used in chemisorption to modified cellulose.

2.3 Cellulose chemical modifications and characterization

2.3.1 Carboxymethylation reaction

This research hinges on further exploration and improvement of the process developed using mildly modified carboxymethyl cellulose fibers (CMF) in producing textile filaments. The van de Ven research group determined that CMF with a charge content ~1 – 2 mmol g^{-1} of cellulose could be solubilized in NaOH and extruded in H_2SO_4 forming filaments [1, 2]. Carboxymethyl cellulose (CMC) is a non-toxic ether derivative of cellulose, which has various industrial applications depending on the degree of substitution. Low-substituted types are soluble in alkali solution but insoluble or partially soluble in water [42, 43]. As a result, low-substituted CMC, herein referred to as CMF, is ideal for textile applications. In this project, we explored the use of CMF, dialdehyde modified fibers (DAMF) and imine in a multi-functionalized product to improve processing efficiency. CMC and CMF are mainly synthesized using organic solvents and heat [44], this research also explored solvent-free synthesis via mechanical milling as a greener approach.

Carboxymethylation is performed by etherification of the cellulose hydroxyl groups using monochloroacetic acid (MCA). The initial step in the reaction is alkalization (mercerization) using NaOH, which is an equilibrium reaction that forms a cellulose alkoxide [45]. Use of alkaline conditions reduces the conversion amounts due to MCA hydrolysis. Optimization studies have been done [44, 46], yet, use of organic solvents has not been eliminated.

We investigate a protocol to produce CMF without use of organic solvents via mechanical milling. Mechanical treatment in biomass (i.e., cellulose, hemi-cellulose, lignin, chitin and starch) chemical modification has been applied as a pre-treatment technique to prepare materials for further chemical modification. This allows for homogeneous and accelerated reaction rates. Mechanochemistry, also known as mechanosynthesis, has been explored as a method to chemically modify biomass into functional materials. Mechanochemical-assisted synthesis employs forces such as shear, friction or compression to perform chemical reactions, and the success of this technique has witnessed an explosive growth in recent years [47]. In solvent-free mechanochemistry, it has been observed that adding a small amount of liquid, 1 µL mg^{-1}, accelerates the reactions. This is referred to as liquid-assisted grinding (LAG) and is advantageous for materials containing moisture and/or assist in solubilizing a reactant. Some other factors that influence mechanochemical processes include milling frequency, catalysts, temperature and pressure, therefore, each reaction must be optimized for a specific application to control the input energy [48]. Therefore, we investigated CMF synthesis via dry and aqueous LAG mechanochemistry as a way to eliminate use of organic solvents.

2.3.2 Periodate oxidation reaction

Periodate oxidation is a stereospecific oxidative cleavage of 1,2-diols to form two carbonyl compounds i.e. aldehydes or ketones, via formation of a cyclic intermediate which lead to cleavage of the C-C bond [49]. The simplified general mechanism is shown in **Figure 2.5** and the reaction has been applied to cellulose (carbohydrates) by acting on the hydroxyl groups in the 2,3-positions resulting in anhydro D-glucopyranose ring opening producing 2,3-dialdehyde cellulose (DAC).

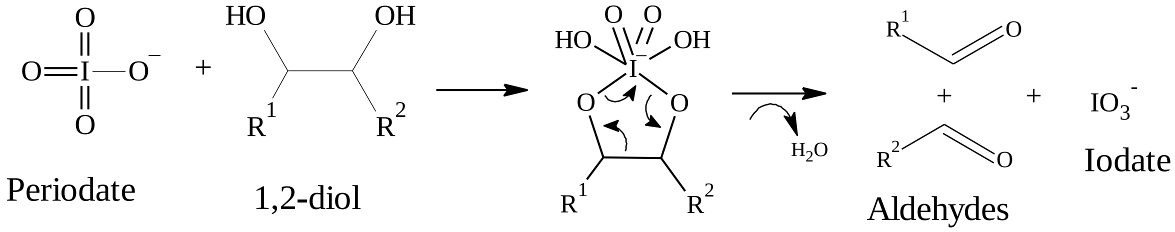

Figure 2.5: Simplified periodate oxidation mechanism of vicinal diols.

Long reaction time, cost of periodate and generation of iodate has hampered the industrial application. However, reaction time has been improved by use of elevated temperatures, salts and mechanical treatments [50, 51]. Additionally, methods to regenerate periodate have been developed [52, 53]. These achievements in addition to formation of reactive aldehyde groups has attracted interest to investigate industrial applications of DAC. DAC is used as an intermediate in synthesizing imines [50, 54], dicarboxylic acid cellulose (DCC) [55] and the novel hairy cellulose nanocrystals [9, 11, 56]. Highly oxidized DAC forms a stable solution after heating above 60 °C for 6 hours, therefore, our research aimed to investigate DAC with a low degree of oxidation (DO), referred to as DAMF, extensively discussed in **Chapter 5**. Therefore, by using lower quantities of periodate, and potentially recovering the by-product, mild periodate oxidation cost could be lowered. Solubilization by heat and β-alkoxy fragmentation under alkaline condition [57] could be minimized as the mild oxidation retains some properties of unmodified cellulose [55].

2.3.3 Schiff base reaction

A Schiff base, also known as imine, is a nitrogen analog of a ketone with a general structure $R^1R^2C{=}NR^3$ where $R^3 \neq H$. Imines are synthesized from primary amines and aldehydes or ketones, in a mild acid (pH of 4 – 5) catalyzed Schiff base reaction [58]. A condensed general reaction mechanism is shown in **Figure 2.6**. The reaction is relatively fast, from a few minutes to hours depending on reaction conditions, and is carried out at room temperature in aqueous media. This is advantageous in minimizing energy consumption, achieving high conversion rates and using a green solvent. Schiff base reactions have been applied on DAC using various types of primary amines [54, 59-61], and the final product is an insoluble cellulosic imine, unless solubilized DAC is used. The coupling of various types of aldehyde modified cellulosic materials and/or composites with amine dyes via a Schiff base reaction has been studied as an efficient way purify dye wastewater in batch reactors [62-64]. Therefore, recovering a solid product with water as the only biproduct is advantageous in reusing the water by simply adjusting the pH, which is ideal in conjugating dyes in textile production.

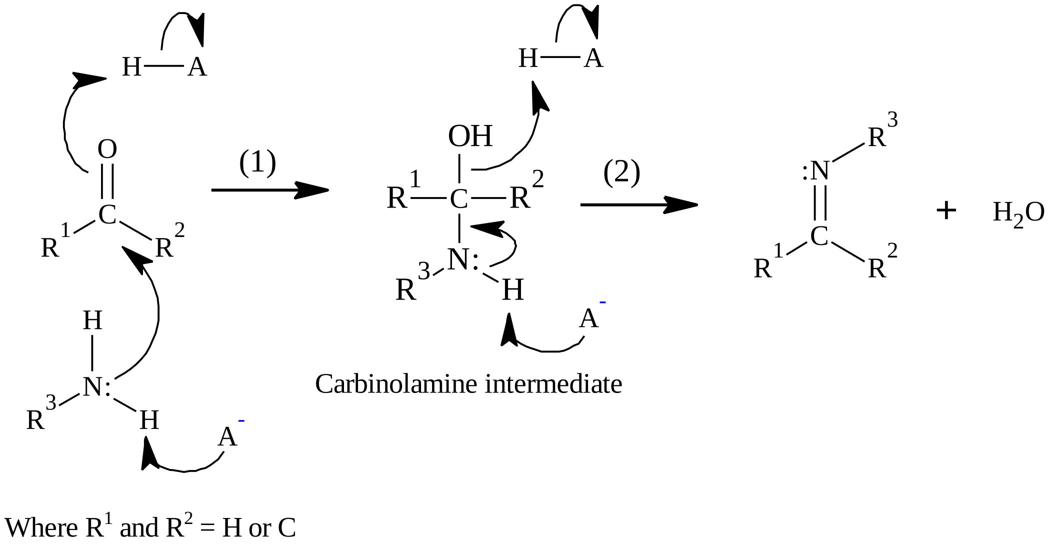

Figure 2.6: Concerted Schiff base reaction mechanism between an aldehyde or ketone and a 1° amine.

2.3.4 Qualitative chemical analysis

Consequently, the products of the reaction are qualitatively characterized using spectroscopy to determine chemical functionality and morphology relative to the starting materials.

2.3.4.1 Infrared spectroscopy

Most compounds containing covalent bonds absorbs electromagnetic radiation in the infrared (IR) region which is in the wavelength (λ) range of ~2.5 – 25 µm. Absorption in this region results in molecular vibration, with characteristics functional groups having specific vibrational frequencies, as λ is inversely proportional to frequency (ν), whereas the energy (E) is directly proportional to the frequency with the proportionality constant being Planck's constant (h = 6.626×10-34 m^2kg/s), shown in *Equations 2.1* and *2.2*. Thus, IR spectroscopy is a vibrational technique and wavelength results are often reported in wavenumber (cm^{-1}), which is simply a reciprocal of wavelength.

$$\nu = {}^{c}/_{\lambda} \tag{2.1}$$

$$E = h\nu \tag{2.2}$$

Since every bond in a molecule has a unique vibrational frequency, different molecules give rise to different IR patterns even if the same wavelength is absorbed. As a result, IR spectroscopy is used as molecular fingerprint technique. Most importantly, IR spectra contain information about what type of bond is present, or absent, in a molecule by using correlation charts. Absorption of IR result in stretch modes, which are high energy vibrations and bend modes, which are of low energy. Modern IR spectrometers, Fourier transform IR (FTIR), collects time series interferograms which are converted into a frequency-domain spectrum. The outcome is a well resolved spectrum with low noise-to-signal ratio [65].

2.3.4.2 Nuclear magnetic resonance *spectroscopy*

Whereas IR spectroscopy provides information about the functional groups present in a molecule, nuclear magnetic resonance (NMR) shows the number of magnetically distinct atoms of a particular type. Although many nuclei are magnetically active, this technique is mostly applied to hydrogen and carbon. For example, when the carbon nuclei are studied, information is obtained about the number of each distinct type of carbon atom present and the nature of the immediate environment. The two methods complement each other in qualitative chemical characterization of compounds.

Atomic nuclei have spin which is quantized and applying a magnetic field in a specified direction which results in either spin alignment with the field (low energy state) or opposed (high energy state). The energy difference is a function of the strength applied field and the magnitude of the nuclei energy-level separation depend on the particular nucleus involved. Electromagnetic radiation causing nucleus spin are in the radio frequency range of 60 – 600 MHz, hence a low energy technique compared IR.

In carbon NMR, the most abundance isotope (^{12}C) has spin of zero and hence is NMR inactive. On the other hand, ^{13}C is active with a spin of ½, however the low abundance gives an observation challenge compared to the proton (^{1}H). Therefore, a ^{13}C NMR spectrum is developed from a collection of molecules to determine the number of non-equivalent carbons and identify the functional types that are present using correlation charts. The chemical shifts, expressed in parts per million (ppm), in the range 0 – 220 ppm are determined using tetramethylsilane (TMS) as a reference standard. The longer range allows for determination of many carbon environments without peak overlap, which is advantageous compared to ^{1}H NMR [65].

2.3.4.3 Ultraviolet-visible spectroscopy

In ultraviolet-visible (UV-vis) spectroscopy, a photon is absorbed by an atom or molecule from an electromagnetic radiation resulting in an increase in the internal energy by the equivalent amount of the photon energy. The result of absorption lead to the species transition from a lower energy state to an excited state. The quantization of energy result in absorption and excitation at specific wavelengths (λ) within the UV (180 – 380 nm) and visible (~380 - 750) ranges, which mainly affect the valence electrons. A compound absorptivity is wavelength-dependent which is proportional to the concentration of the absorbing species, experimentally measured under specified conditions. The ratio of absorbed or transmitted radiation at the maximum absorption wavelength (λ_{max}) is related by the Beer-Lambert's law for dilute solutions ($A = \varepsilon l C$, where A is absorbance, ε is molar absorptivity, *l* is path length and C is the concentration) [66].

Highly conjugate molecules, like dyes strongly absorb in the visible region due to π-π* transitions, therefore are easily characterized and quantified by this technique. Additionally, ab initio computational methods such as DFT can be used to predict molecular UV-vis absorption spectra by solving the time dependent Schrödinger wave equation in an energy calculation [67].

2.3.4.4 X-ray powder diffraction

Powder X-ray diffraction (XRD) is a non-destructive qualitative and quantitative method to analyze material properties such as phase composition, structure and texture of pure substances or mixtures. X-rays are electromagnetic waves in the range of 0.01 – 10 nm. Like other electromagnetic waves, the λ of X-rays is inversely proportional to its energy as shown in *Equations 2.1* and *2.2*, above. When X-rays of specific λ and intensity I_0 interact with matter, they penetrate and get attenuated, absorbed and scatter giving a combined effect called attenuation coefficient (μ). The μ of the material depends on atomic number, density, material packing and λ. The X-ray interaction with a material results in the transmitted intensity (I) depending on I_0, μ and the material pathlength, d, which are related according to *Equation 2.4* [68].

$$I = I_0 e^{-\mu d} \tag{2.4}$$

The scattered transmitted photon intensities are plotted against the Bragg angle (2θ) displaying a diffractogram, which contains peaks commonly referred to as reflections. The 2θ, obtained from Bragg's law (2d sinθ = nλ, where n = 1,2,3… which is the reflection of order n), θ is the angle between the incident and reflected beam. The reflections are characterized by position, intensity and profile. This gives rise to interpreting crystalline and amorphous domains in materials. Crystalline domains have atoms periodically and regularly arranged in 3-D with long range order, giving diffractograms with sharp pronounced peaks. Amorphous states have short range order resulting in broad humps in the diffractogram. For samples prepared similarly, the peak position and intensity can be used quantitatively to determine the crystallite preferred orientation and material texture [69, 70].

2.4 Textile filament extrusion

2.4.1 Dope preparation and extrusion

Following cellulose chemical modification and characterization, dope solutions were prepared for extrusion into filaments, shown in **Figure 2.7**. The cellulosic materials were solubilized in NaOH solutions and regenerated in acids (HCl and H_2SO_4). Use of NaOH to form dopes result in a highly viscous gel, which is challenging to filter. Optimization methods involved varying the charge content and concentration of base, to determine suitable conditions for solubilization and filtration. Potential acids and varying concentrations were examined to achieve continuous flow extrusion using syringes, while maintaining conditions suitable for large scale production. It was determined that it was suitable to use 6% NaOH solution to make an 8% dope, filtered with a 40 µm nylon cloth, then extruded in 10% H_2SO_4 and finally washed in water.

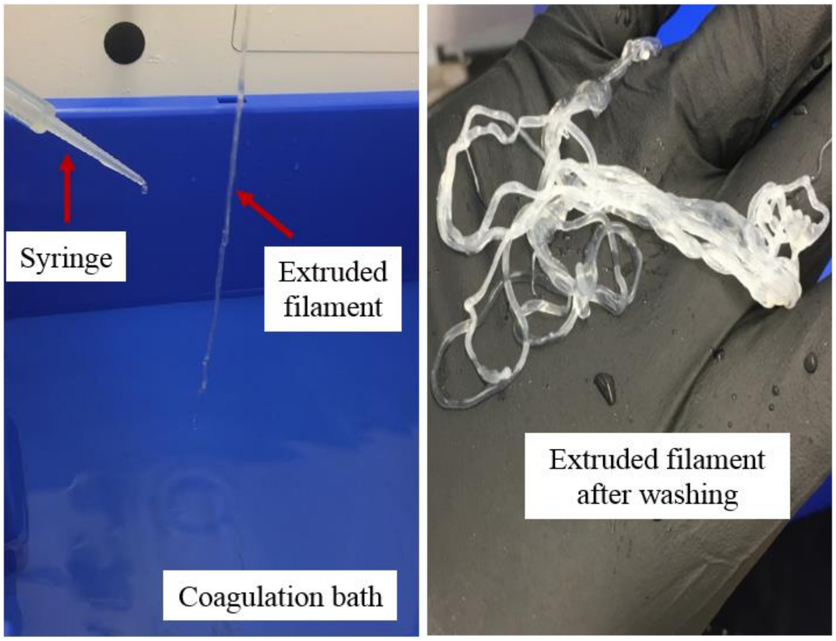

Figure 2.7: Photographic images of CMF extrusion during process optimization of continuous flow fiber regeneration.

2.4.2 Lab scale spinneret and operating parameters

After developing the syringe extrusion method described in **Section 2.4.1 above**, a custom-made laboratory scale spinneret (**Figure 2.8**) fabricated from high grade steel to withstand the acid/base environment was acquired. The design was based on mimicking the flow of the industrial wet spinning process described in **Section 2.2.1** and shown in **Figure 2.3**, above. The spinneret is air-operated to force the dope out of the reservoir into the coagulation bath and the filaments are wound by hand and then washed after collection. The extrusion is achieved with a pressure range of 0.35 – 0.70 MPa depending on the dope viscosity. The spinneret has a maximum operating pressure of 6.4 MPa.

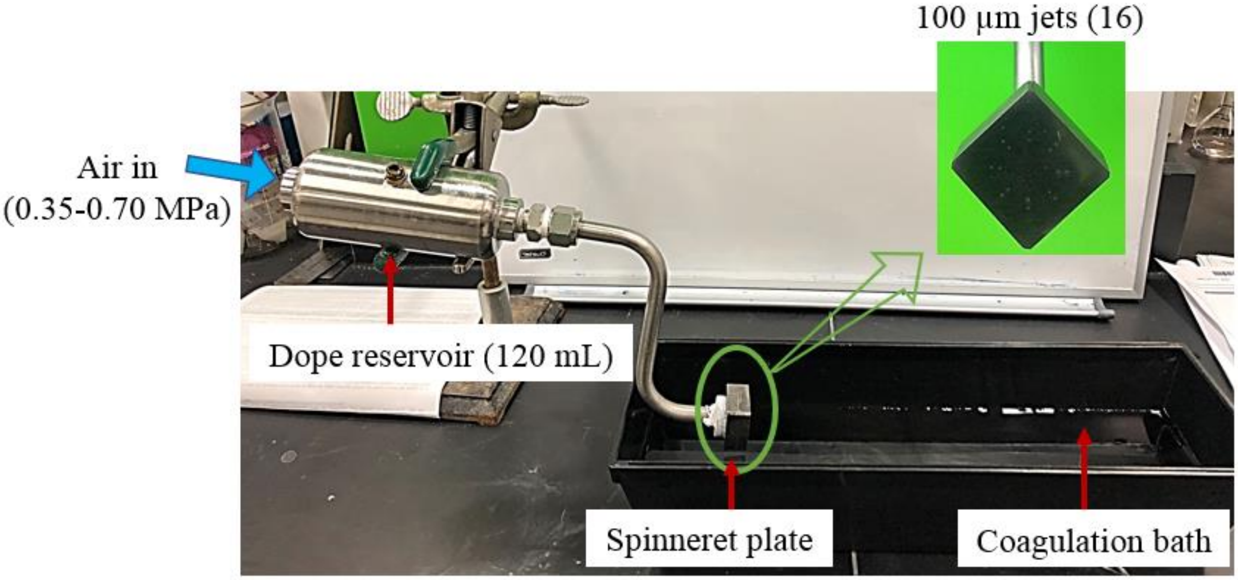

Figure 2.8: Stainless steel laboratory scale spinneret and 100 µm spinneret head.

References

[1] M.S. Islam, M.N. Alam, T.G.M. van de Ven, Production of textile filaments from carboxymethylated cellulosic pulps, Cellulose 28 (2021) 9475-9488.

[2] M.N. Alam, M.S. Islam, T.G.M.v.d. Ven, J.-P. Lumb, Cellulose-based filaments and methods of production thereof, in: USPTO (Ed.)USA, 2020.

[3] E. Ott, H.M. Spurlin, M.W. Grafflin, N.M. Bikales, L. Segal, Cellulose and cellulose derivatives, Interscience Publishers1954.

[4] K. Kamide, 1 - Introduction, in: K. Kamide (Ed.), Cellulose and Cellulose Derivatives, Elsevier, Amsterdam, 2005, pp. 1-23.

[5] Y. Habibi, L.A. Lucia, O.J. Rojas, Cellulose Nanocrystals: Chemistry, Self-Assembly, and Applications, Chemical Reviews 110 (2010) 3479-3500.

[6] D. Fengel, G. Wegener, Wood: chemistry, ultrastructure, reactions, De Gruyter2011.

[7] S. Beck-Candanedo, M. Roman, D.G. Gray, Effect of Reaction Conditions on the Properties and Behavior of Wood Cellulose Nanocrystal Suspensions, Biomacromolecules 6 (2005) 1048-1054.

[8] J. George, S.N. Sabapathi, Cellulose nanocrystals: synthesis, functional properties, and applications, Nanotechnol Sci Appl 8 (2015) 45-54.

[9] T.G.M. van de Ven, A. Sheikhi, Hairy cellulose nanocrystalloids: a novel class of nanocellulose, Nanoscale 8 (2016) 15101-15114.

[10] K. Conley, M.A. Whitehead, T.G.M. van de Ven, Probing the structural chirality of crystalline cellulose with induced circular dichroism, Cellulose 24 (2017) 479-486.

[11] K. Conley, M. Whitehead, T.G.M. van de Ven, Chemically peeling layers of cellulose nanocrystals by periodate and chlorite oxidation, Cellulose 23 (2016) 1553-1563.

[12] K. Kamide, 2 - Characterization of Molecular Structure of Cellulose Derivatives, in: K. Kamide (Ed.), Cellulose and Cellulose Derivatives, Elsevier, Amsterdam, 2005, pp. 25-188.

[13] W.E. Morton, J.W.S. Hearle, 1 - An introduction to fibre structure, in: W.E. Morton, J.W.S. Hearle (Eds.), Physical Properties of Textile Fibres (Fourth Edition), Woodhead Publishing2008, pp. 1-81.

[14] M.M. Houck, Identification of textile fibers, Woodhead Publishing Limited, Cambridge, England, 2009.

[15] B.L. Deopura, N.V. Padaki, Chapter 5 - Synthetic Textile Fibres: Polyamide, Polyester and Aramid Fibres, in: R. Sinclair (Ed.), Textiles and Fashion, Woodhead Publishing2015, pp. 97-114.

[16] Q. Mao, T.P. Wyatt, A.T. Chien, J. Chen, D. Yao, Melt spinning of high-strength fiber from low-molecular-weight polypropylene, Polymer Engineering & Science 56 (2016) 233-239.

[17] J.K. Fink, Chapter 13 - Aramids, in: J.K. Fink (Ed.), High Performance Polymers (Second Edition), William Andrew Publishing2014, pp. 301-320.

[18] T. Shaikh, S. Chaudhari, A. Varma, Viscose rayon: a legendary development in the manmade textile, International Journal of Engineering Research and Application 2 (2012) 675-680.

[19] E.C. Vigliani, Carbon disulphide poisoning in viscose rayon factories, Br J Ind Med 11 (1954) 235-244.

[20] M. Davidson, M. Feinleib, Carbon disulfide poisoning: A review, American Heart Journal 83 (1972) 100-114.

[21] U.S.E.P.A. (EPA), Preliminary Study of Carbon Disulfide Discharges from Cellulose Products Manufacturers U.S. Environmental Protection Agency Office of Water (4303T), Washington, DC, 2011.

[22] S. Zhang, C. Chen, C. Duan, H. Hu, H. Li, J. Li, Y. Liu, X. Ma, J. Stavik, Y. Ni, Regenerated cellulose by the Lyocell process, a brief review of the process and properties, BioResources 13 (2018) 1-16.

[23] H. Li, S. Legere, Z. He, H. Zhang, J. Li, B. Yang, S. Zhang, L. Zhang, L. Zheng, Y. Ni, Methods to increase the reactivity of dissolving pulp in the viscose rayon production process: a review, Cellulose 25 (2018) 3733-3753.

[24] Q. Miao, C. Tian, L. Chen, L. Huang, L. Zheng, Y. Ni, Combined mechanical and enzymatic treatments for improving the Fock reactivity of hardwood kraft-based dissolving pulp, Cellulose 22 (2015) 803-809.

[25] M. Hummel, A. Michud, M. Tanttu, S. Asaadi, Y. Ma, L.K.J. Hauru, A. Parviainen, A.W.T. King, I. Kilpeläinen, H. Sixta, Ionic Liquids for the Production of Man-Made Cellulosic Fibers: Opportunities and Challenges, in: O.J. Rojas (Ed.), Cellulose Chemistry and Properties: Fibers, Nanocelluloses and Advanced Materials, Springer International Publishing, Cham, 2016, pp. 133-168.

[26] T. Rosenau, A. Potthast, H. Sixta, P. Kosma, The chemistry of side reactions and byproduct formation in the system NMMO/cellulose (Lyocell process), Progress in Polymer Science 26 (2001) 1763-1837.

[27] L.K.J. Hauru, M. Hummel, A. Michud, H. Sixta, Dry jet-wet spinning of strong cellulose filaments from ionic liquid solution, Cellulose 21 (2014) 4471-4481.

[28] A. Michud, M. Tanttu, S. Asaadi, Y. Ma, E. Netti, P. Kääriainen, A. Persson, A. Berntsson, M. Hummel, H. Sixta, Ioncell-F: ionic liquid-based cellulosic textile fibers as an alternative to viscose and Lyocell, Textile Research Journal 86 (2015) 543-552.

[29] K.E. Perepelkin, Lyocell fibres based on direct dissolution of cellulose in N-methylmorpholine N-oxide: Development and prospects, Fibre Chemistry 39 (2007) 163-172.

[30] F.D. Chequer, G.R. De Oliveira, E.A. Ferraz, J.C. Cardoso, M.B. Zanoni, D.P. de Oliveira, Textile dyes: dyeing process and environmental impact, Eco-friendly textile dyeing and finishing 6 (2013) 151-176.

[31] B. Chaudhary, T. VIOLET, Chemistry of synthetic dyes: A review, J. Interdiscipl. Cycle Res 12 (2020) 390-396.

[32] A.K. Samanta, N. Awwad, H.M. Algarni, Chemistry and Technology of Natural and Synthetic Dyes and Pigments, BoD–Books on Demand2020.

[33] R. Kant, Textile dyeing industry an environmental hazard. J Nat Sci 4 (1): 22–26, 2012.

[34] E. Ozturk, H. Koseoglu, M. Karaboyacı, N.O. Yigit, U. Yetis, M. Kitis, Minimization of water and chemical use in a cotton/polyester fabric dyeing textile mill, Journal of Cleaner Production 130 (2016) 92-102.

[35] A.M. Kocabaş, Improvements in energy and water consumption performances of a textile mill after bat applications, 2008.

[36] H. Zollinger, Color chemistry: syntheses, properties, and applications of organic dyes and pigments, John Wiley & Sons2003.

[37] K. Venkataraman, The Chemistry of Synthetic Dyes V4, Elsevier2012.

[38] H. Ali, Biodegradation of Synthetic Dyes—A Review, Water, Air, & Soil Pollution 213 (2010) 251-273.

[39] S. Rodríguez Couto, Dye removal by immobilised fungi, Biotechnology Advances 27 (2009) 227-235.

[40] M. Moradian, M.S. Islam, T.G.M. van de Ven, Insoluble Regenerated Cellulose Films Made from Mildly Carboxylated Dissolving and Kraft Pulps, Industrial & Engineering Chemistry Research 60 (2021) 5385-5393.

[41] J. Aspland, Reactive dyes and their application, Textile Chemist and Colorist 24 (1992) 31-36.

[42] C.B. Hollabaugh, L.H. Burt, A.P. Walsh, Carboxymethylcellulose. Uses and Applications, Industrial & Engineering Chemistry 37 (1945) 943-947.

[43] R. Ergun, J. Guo, B. Huebner-Keese, Cellulose, in: B. Caballero, P.M. Finglas, F. Toldrá (Eds.), Encyclopedia of Food and Health, Academic Press, Oxford, 2016, pp. 694-702.

[44] W. Im, S. Lee, A. Rajabi Abhari, H.J. Youn, H.L. Lee, Optimization of carboxymethylation reaction as a pretreatment for production of cellulose nanofibrils, Cellulose 25 (2018) 3873-3883.

[45] C. Eyholzer, N. Bordeanu, F. Lopez-Suevos, D. Rentsch, T. Zimmermann, K. Oksman, Preparation and characterization of water-redispersible nanofibrillated cellulose in powder form, Cellulose 17 (2010) 19-30.

[46] H. Almlöf, K. Schenzel, U. Germgård, Carboxymethyl Cellulose Produced at Different Mercerization Conditions and Characterized by NIR FT Raman Spectroscopy in Combination with Multivariate Analytical Methods, Bioresources 8 (2013) 1918-1932.

[47] F. Hajiali, T. Jin, G. Yang, M. Santos, E. Lam, A. Moores, Mechanochemical Transformations of Biomass into Functional Materials, ChemSusChem 15 (2022) e202102535.

[48] G. Margoutidis, F.M. Kerton, Biomass Processing via Mechanochemical Means, Biomass Valorization2021, pp. 343-365.

[49] G. Dryhurst, Periodate oxidation of diol and other functional groups: analytical and structural applications, Elsevier2015.

[50] E. Esen, M.A.R. Meier, Sustainable Functionalization of 2,3-Dialdehyde Cellulose via the Passerini Three-Component Reaction, ACS Sustainable Chemistry & Engineering 8 (2020) 15755-15760.

[51] M.N. Alam, M. Antal, A. Tejado, T.G.M. van de Ven, Salt-induced acceleration of chemical reactions in cellulose nanopores, Cellulose 19 (2012) 517-522.

[52] H. Liimatainen, J. Sirviö, H. Pajari, O. Hormi, J. Niinimäki, Regeneration and Recycling of Aqueous Periodate Solution in Dialdehyde Cellulose Production, Journal of Wood Chemistry and Technology 33 (2013) 258-266.

[53] A. Besemer, Recovery process for spent periodate, Google Patents, 2003.

[54] Z. Sabzalian, M.N. Alam, T.G.M. van de Ven, Hydrophobization and characterization of internally crosslink-reinforced cellulose fibers, Cellulose 21 (2014) 1381-1393.

[55] U.-J. Kim, S. Kuga, M. Wada, T. Okano, T. Kondo, Periodate Oxidation of Crystalline Cellulose, Biomacromolecules 1 (2000) 488-492.

[56] R. Koshani, T.G.M. van de Ven, Electroacoustic characterization of trimmed hairy nanocelluloses, Journal of Colloid and Interface Science 563 (2020) 252-260.

[57] P. Calvini, G. Conio, M. Lorenzoni, E. Pedemonte, Viscometric determination of dialdehyde content in periodate oxycellulose. Part I. Methodology, Cellulose 11 (2004) 99-107.

[58] J. MacMurry, Organic chemistry, Brooks/Cole Publishing Company, Pacific Grove, California, 1992.

[59] L. Zhang, P. Yan, Y. Li, X. He, Y. Dai, Z. Tan, Preparation and antibacterial activity of a cellulose-based Schiff base derived from dialdehyde cellulose and L-lysine, Industrial Crops and Products 145 (2020) 112126.

[60] L. Zhang, Q. Zhang, Y. Zheng, Z. He, P. Guan, X. He, L. Hui, Y. Dai, Study of Schiff base formation between dialdehyde cellulose and proteins, and its application for the deproteinization of crude polysaccharide extracts, Industrial Crops and Products 112 (2018) 532-540.

[61] H. Zhang, P. Liu, X. Peng, S. Chen, K. Zhang, Interfacial Synthesis of Cellulose-Derived Solvent-Responsive Nanoparticles via Schiff Base Reaction, ACS Sustainable Chemistry & Engineering 7 (2019) 16595-16603.

[62] X. Zheng, X. Li, J. Li, L. Wang, W. Jin, J. liu, Y. Pei, K. Tang, Efficient removal of anionic dye (Congo red) by dialdehyde microfibrillated cellulose/chitosan composite film with significantly improved stability in dye solution, International Journal of Biological Macromolecules 107 (2018) 283-289.

[63] S. Kumari, D. Mankotia, G.S. Chauhan, Crosslinked cellulose dialdehyde for Congo red removal from its aqueous solutions, Journal of Environmental Chemical Engineering 4 (2016) 1126-1136.

[64] H. Yang, A. Sheikhi, T.G.M. van de Ven, Reusable Green Aerogels from Cross-Linked Hairy Nanocrystalline Cellulose and Modified Chitosan for Dye Removal, Langmuir 32 (2016) 11771-11779.

[65] L.D. Pavia, M.G. Lampman, S.G. Kriz, R.J. Vyvyan, Introduction to Spectroscopy, 4 ed., Brooks/Cole Cengage Learning, United States of America, 2009.

[66] H.-H. Perkampus, UV-VIS Spectroscopy and its Applications, Springer Science & Business Media 2013.

[67] E.G. Lewars, Computational Chemistry, Introduction to the theory and applications of molecular and quantum mechanics, Springer International Publishing, Switzerland, 2016, pp. 387-388.

[68] M. Ermrich, D. Opper, X-Ray powder diffraction, PANalytical GmbH, 2011.

[69] N. Iwashita, Chapter 2 - X-ray Powder Diffraction, in: M. Inagaki, F. Kang (Eds.), Materials Science and Engineering of Carbon, Butterworth-Heinemann2016, pp. 7-25.

[70] C. Hammond, The basics of crystallography and diffraction, International Union of Crystal 2015.

Preface to Chapter 3

Chapter 3 discusses the use of ball and grind milling in preparation of carboxymethyl cellulose fibers (CMF) under organic solvent-free and water assisted milling conditions. This is done in an effort to process biomass into a functional material by utilizing the carboxylate functional groups to prepare a dope solution that is subsequently extruded into textile filaments. Studies have shown that solvent-free and water assisted milling processes are environmentally friendly and energetically conservative. In this study, we demonstrate that CMF can be synthesized under these conditions, in addition to reducing the number of processing steps involved in textile filament production. This research has been submitted for publication to Cellulose.

Martin Sichinga and Theo G.M. van de Ven, Mechanosynthesis of carboxymethyl cellulose fibers using ball and grind milling for applications in wet spinning textile extrusion, *Cellulose* (submitted March 2022).

3 Mechanosynthesis of carboxymethyl cellulose fibers using ball and grind milling for applications in wet spinning textile extrusion

3.1 Abstract

The continued exploration for green and sustainable chemical modifications led to the development of solvent-free mechanochemical synthesis of carboxymethylated cellulose fibres (CMF) from Kraft cellulose pulp. The elimination of organic solvents and shortened reaction time makes the mechanosynthesis carboxymethylation process economical and efficient. Nuclear magnetic resonance and Fourier transform infrared spectroscopy confirmed the successful etherification of cellulose under solvent-free mechanochemical conditions, in comparison with the conventional process. Using similar mole ratios for reactants, the conversion rates (-COOH charge content) for conventional (1.26 mmol g^{-1}), ball (1.30 mmol g^{-1}) and grind (1.91 mmol g^{-1}) milling processes were 46, 47 and 69%, respectively. The higher conversion rate for grind milling is due to minimization in hydrolysis of monochloacetic acid in aqueous media. The produced CMF was wet extruded into textile filaments with and without purification after the synthesis, thereby reducing the number of processing steps involved in textile spinning. Therefore, solvent-free carboxymethylation provides a green, efficient, cost effective and sustainable synthesis route to the conventional method.

Keywords: · Cellulose pulp · Carboxymethyl cellulose · Mechanochemistry · Textile · Solvent-free modification· Wet spinning

3.2 Introduction

The natural abundance, renewability, low cost of cellulose is advantageous in producing biobased materials. The textile industry is one of the major consumers of cellulosic pulps, holding ~40% of the total market share [1] and fibers are mainly regenerated by the rayon and lyocell processes. The volatile carbon disulfide employed in the rayon process makes it highly toxic with the Lyocell process being advantageous from an environmental viewpoint [2]. Surface chemical modification of cellulose allows to tailor desired physical and chemical properties of the final product. To this effect, a novel method to produce textile filaments from carboxymethylated cellulose has been developed [3] by taking advantage of the pH dependence on gelation in aqueous media [4].

Carboxymethyl cellulose (CMC) is a commercially available, non-toxic and the most used cellulose ether, with applications in textile, food, pharmaceutical, paint and paper industries [5]. CMC is produced by an alkali-catalyzed etherification of cellulose by monochloroacetic acid with varying degrees of substitution (DS = 0 – 3 or equivalently 0 – 18.5 mmol –COOH/g of cellulose), shown in **Figure 3.1**. The DS regulates its functional properties; CMC with low DS (<0.4) is insoluble in water and is commonly referred to as carboxymethyl cellulose fibers (CMF) [5-8]. Under basic conditions, CMF is soluble and forms an ideal gel for wet spinning and/or molding by regenerating in acid. Cellulose fibers do not rapidly degrade in 10% H_2SO_4 and the fiber quality, strength and tenacity are retained [4, 7].

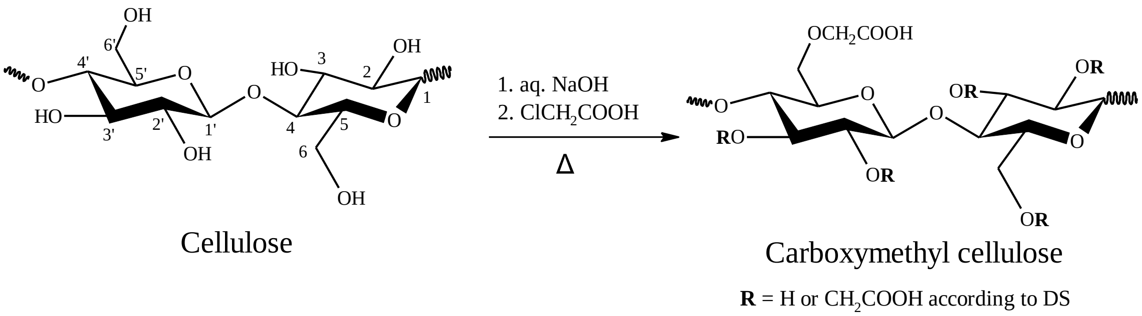

Figure 3.1: Reaction scheme for carboxymethylation of cellulose to form CMC or CMF.

Traditionally, CMF and CMC production require the use of aqueous and organic solvents, elevated temperatures, and long reaction time. One of the most common methods for CMF and CMC is by dispersion of cellulose and sodium hydroxide solution in 2-propanol at 45 °C for 60 minutes. This is followed by addition of monochloroacetic acid solution reacting at 55 °C for 120 minutes, and the product is purified using ethanol [9]. It has been recognized that the process uses surplus of 2-propanol and/or ethanol [10]. Furthermore, industrial use of volatile and flammable organic solvents requires installation of fireproof systems on the production line, which adds to increased equipment expenditure in addition to the cost and regulations gouverning these solvents. Therefore, eliminating organic solvents from CMF synthesis has the potential to reduce cost and increase reaction efficiency. This can be achieved by using mechanochemistry, in which the reactants are mechanically milled to produce desired products.

Mechanosynthesis is a growing field due to its potential application as a “green” methodology which allows for solvent-free, faster and energy efficient reactions. It is a technology that uses mechanical energy such as compression, shear or friction to achieve chemical transformation [11]. It has been observed that solvent-free reactions achieved via microwave or ball milling methods lead to higher chemical kinetics with lower energy consumption and the conditions for “green” synthesis qualification well described by Sarkar *et al* (2016) [12]. It has been observed that there are limited mechanochemical studies on polymers in general, including cellulose. The major drawback in applying mechanosynthesis to polymers is the thermoplastic characteristics which result in melting of materials due to the heat generated during the milling process. However, since cellulose is a non-melting polymer, it has recently attracted attention in this field [13].

Some of the studies involving mechanochemical modification of cellulose by ball milling are phosphorylation of cellulose nanocrystals [14], effect of solvent on morphology [15], dilute acid hydrolysis effect of crystallinity [16] and reaction of cellulose with styrene [17]. Therefore, ball milling is a promising technique in cellulose modification. However, the large volume to mass ratio of cellulose makes it challenging to scale-up the process for mass production. Therefore, in addition to ball milling proof of concept, this research demonstrates the use of a grinding mill as a scale-up technique in a solvent-free environment, similar to a study on preparation of carboxylate-functionalized cellulose using a pan-mill reactor [18]. Furthermore, the product is solubilized and extruded into textile filaments.

Grinding mills are specially designed for reducing materials particle size by mechanical force, i.e., shear or cutting, to the desired size as they pass through a predetermined aperture size sieve. Considering that most cellulose-based reactions begin with finely ground pulp [9, 19, 20], we can take advantage of the mechanical action for a dual purpose, i.e., particle size reduction and chemical modification. This combination has the potential to reduce energy consumption and increase efficiency, by reducing the number of steps in filament production.

3.3 Materials and Methods

3.3.1 Materials

Bleached soft wood Kraft pulp sheets (Q-90), supplied by Domtar Canada, was ground using GlenMills-SM300 mill equipped with a 0.5 mm sieve. This pulp was used as a cellulose starting raw material for all carboxymethylation reactions. Monochloroacetic acid (MCA) ($C_2H_3ClO_2$), sulfuric acid (H_2SO_4) and sodium chloride were supplied by Sigma Aldrich, Ontario Canada. Sodium hydroxide (NaOH) pellets, ethanol (100%) and 2-propanol were purchased from Fisher Scientific, Ontario Canada. For quantitative analysis purposes, certified analytical grade sodium hydroxide solution (0.01 *N*) and hydrochloric acid (0.5 M) were acquired from Sigma Aldrich, Ontario Canada. These chemicals were used in the analysis of starting materials and final products.

3.3.2 Solvent carboxymethylation of cellulose pulp

Cellulose ground pulp was dispersed in 2-propanol to make an 8% w/w suspension and the temperature raised to 40 °C. An aqueous NaOH solution (10 mmol equivalent per gram of cellulose) was added, and the mixture stirred for 1 hour while maintaining the temperature. The temperature was raised to 60 °C and freshly prepared aqueous monochloroacetic acid (2.76 mmol equivalent per gram of cellulose) was added. The reaction proceeded for 2 hours. The carboxymethylation product was washed twice in ethanol-water mixture (60:40, w/w) and finally with 100% ethanol and then air dried. This protocol result in a charge content of about 1 mmol carboxylic acid groups per gram of cellulose (1 mmol/g), commonly referred to as carboxymethyl cellulose fibers (CMF) [9]. This charge content is equivalent to degree of substitution (DS) of 0.16, where the theoretical maximum is 18.5 mmol/g (DS = 3). This procedure herein is referred to as the conventional method.

3.3.3 Solvent-free carboxymethylation of cellulose pulp

The solvent-free mechanosynthesis of carboxymethyl cellulose was conducted on a Retsch MM200 ball mill operated at 25 Hz, shown in **Figure 3.2**. The reagents in milligram quantities (cellulose, NaOH and MCA) were loaded in a 15 mL PTFE milling jar and insert an 8.5 mm zirconia ball to provide the collision energy necessary for the reaction.

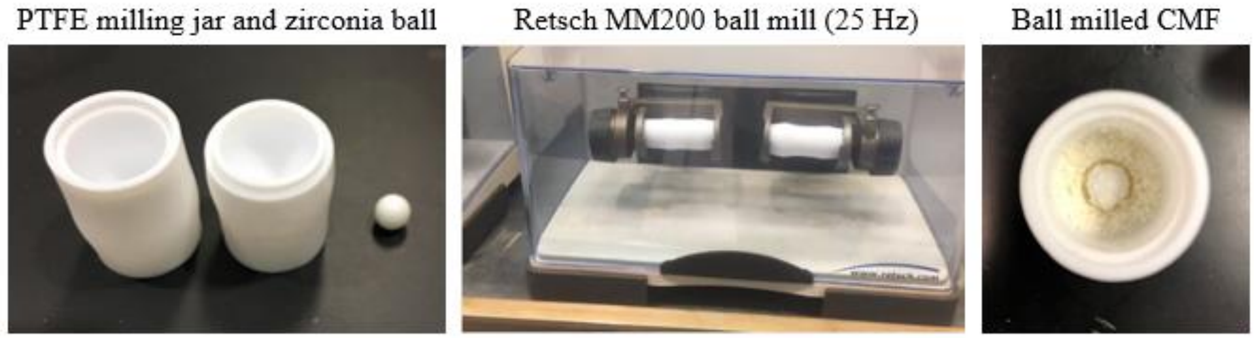
PTFE milling jar and zirconia ball
Retsch MM200 ball mill (25 Hz)
Ball milled CMF

Figure 3.2: Experimental setup for ball milling carboxymethylation.

Reaction quantities were increased to 20 g and mechanosynthesis experiments were conducted on a GlenMills SM-300 grinding mill (**Figure 3.3**), operated at 2800 rpm, with a blocked sieve. The rotating blade provides the shear mechanical action and reagents are circulated within the grinding chamber. To ensure homogeneous distribution of reactants, the dissolved NaOH and MCA were added dropwise with the mill operated at 300 rpm. The products were washed as described in **Section 3.3.2** above. Varying milling times and effect of washing solvents were evaluated in all experiments.

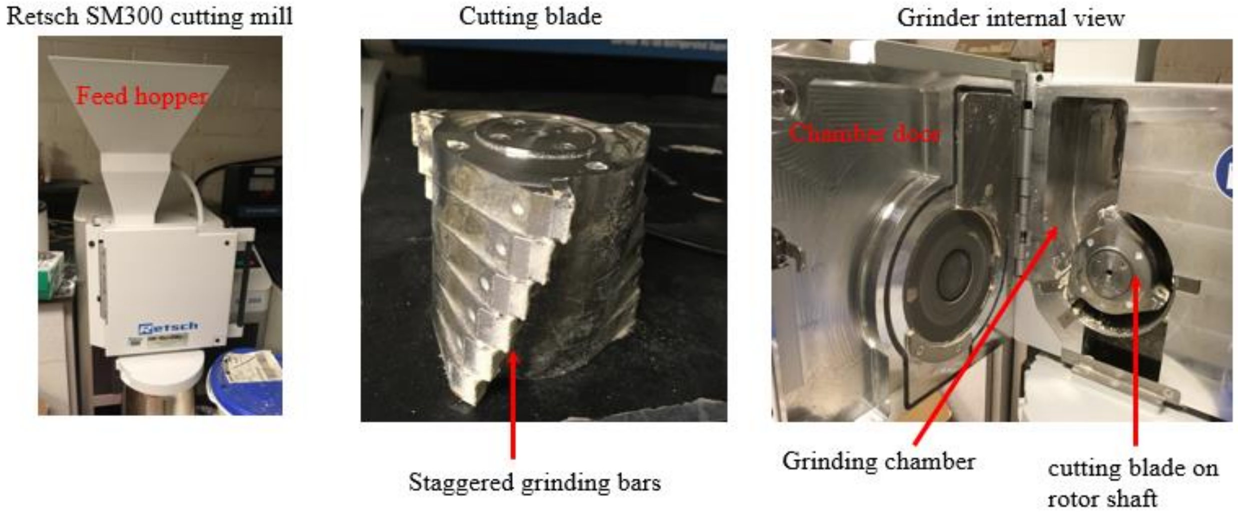

Figure 3.3: Retsch SM300 cutting grinding meal used in solvent-free carboxymethylation reaction.

3.3.4 Quantitative determination of carboxyl content

An automated Metrohm 836 Titrando titrator (Ontario, Canada) was used to measure the CMF charge density by conductometric titration. The obtained titration curves (**Figure S3.1**) were also used to estimate the pK_a values. The CMF pH was initially adjusted to ~3.5 and when necessary, salt was added to ensure that the conductivity was significantly above the instrument detection limit. The solution was titrated against 10 mM NaOH at a rate of 0.1 mL/min until a final pH of ~11 [21, 22]. Data graphing was performed using OriginPro® 2018 graphing software and statistical analysis done at a 95% confidence level.

3.3.5 Surface chemical characterization

Infrared vibrational spectra were acquired using a Bruker Attenuated Total Reflectance Fourier Transform Infrared (ATR-FTIR) spectrometer, with a single bounce diamond ATR accessory and

Opus software for peak analysis. The data was collected in a wavenumber range of 400 – 4000 cm^{-1} with a resolution of 4 cm^{-1}.

Chemical functionalization was also studied using solid-state ^{13}C NMR spectroscopy, with data acquired from a Varian/Agilent VNMRS-400 operated at 100.5 MHz, according to the method described by Koshani (2018) [23].

The crystallinity effect on modified cellulose was investigated using a Bruker Discover D8 two-dimensional diffractometer, equipped with CuKα radiation (λ= 1.54 Å) and VANTEC 2D detector. The X-ray diffractograms were acquired with a 2Θ angle range of 5 – 50°, at a scan rate of 0.005° s^{-1}. The crystallinity index (CI) was determined according to [24], using the conventional peak height method as follows:

$$\mathrm{CI}(\%) = \frac{I_{200} - I_{am}}{I_{200}} \times 100$$

where I_{200} is the intensity obtained from the (2 0 0) plane reflection, while I_{am} is the minimum reflection between the (1 0 0) and (2 0 0) planes.

3.3.6 Preparation of dope solution and filament extrusion

The dried CMF was solubilized in 6% w/w NaOH to make an 8% w/w highly viscous gel, herein referred to as a dope solution. The dope was mechanically homogenized using a Polytron PT2500E homogenizer operated between 4,000 –10,000 rpm until well-mixed. The dope was left to further solubilize at 4 °C for 24 hours and the solubility checked via a polarized light microscope. The undissolved pulp was removed using a 40 µm nylon filter. The dope was then loaded into a custom-made laboratory scale filament spinneret, fitted with a 16-hole 100 µm extrusion spinneret head, shown in **Figure 2.8**. The dope was pumped out, using air pressure at 0.35 – 0.70 MPa (maximum operating pressure is 6.4 MPa), for extrusion in a 10% w/w H_2SO_4 coagulation bath. The filaments were washed in excess warm water to remove the residual acid and salts, and then air dried.

3.3.7 Physical properties of the dope and extruded filaments

A HighRes LDA02 fiber quality analyzer (OpTest Equipment Inc., Hawkesbury, ON, Canada) was used to measure fiber count and length distribution in cellulose and dope solutions, using the TAPPI T271 method and weighted average lengths determined according to Ferritsius O *et al* [25]. The method parameters for minimum and maximum measurements were; length (0.1 – 7.2 mm), fines (0.07 – 0.2 mm), and count all fibers in a 600 mL solution operated in auto-dilution mode. Data processing was done after water blank correction and statistical confidence intervals determined at 95% confidence level. The dope stability fluid dynamics was measured acoustically using an Electroacoustic Spectrometer DT-1202 (Dispersion Technology, Bedford Hills, NY, USA). Using an acoustic sensor, the sound attenuation was measured in the range 1 – 100 MHz, to determines the fluid rheology [26] and the particle size distribution determined acoustically. Furthermore, a Nikon Eclipse LV100POL polarizing light microscope (Tokyo, Japan) was used to analyze the morphological changes in the starting cellulosic materials, dope solutions and extruded filaments.

3.4 Results and Discussion

3.4.1 Solvent and solvent-free carboxymethylation of cellulose

Conductometric titration curves (**Figure 3.4**) for weak acids were used to determine the carboxyl group charge content and degree of substitution (DS). Conventional CMF synthesis resulted in CMF with a -COOH charge content of 1.26 ± 0.19 mmol/g or equivalently a DS of 0.20 ± 0.03 (n = 7) **(Figure S3.1**) with a total reaction time of 3 hours and 46% conversion. To solvate the pulps and ease stirring, 2-propanol constituted 78 wt% of the total reaction mass, in the presence of aqueous solutions NaOH and MCA. The conversion is comparable with observations by Islam *et al* (2021) [3] when sodium chloroacetate and 2-propanol are used while use of sodium chloroacetate in aqueous media reduced the conversion to ~25% [27].

Using aq. NaOH and aq. MCA, with comparable mole ratios as the conventional method, the ball milling procedure resulted in a charge content of ~0.4 –1.3 mmol/g within 2 hours (**Table S3.1)**. It was observed that milling solid NaOH and/or MCA negatively affect the CMF charge content, therefore, reagents were dissolved in a minimal amount of water. The solubilities at room temperature of NaOH and MCA are 1.00 and 0.86 g/mL, respectively. Freshly prepared MCA was necessary to minimize the hydrolysis process, which is accelerated under basic conditions [28]. Therefore, the increased charge content in solvent-free systems is due to MCAs' reduced residence time under solvated conditions. Additionally, increasing the amount of NaOH in the first step led to a reduction in charge content, which is also attributed to high rates of hydrolysis, rendering MCA inactive for carboxymethylation according to **Scheme 3.1**.

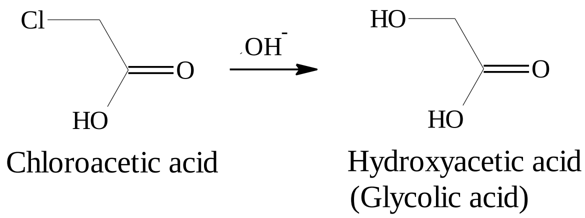

Scheme 3.1: Hydrolysis of monochloroacetic acid to glycolic acid under basic media.

Scaling up from milligram to gram quantities employed a cutting mill grinder under the same reaction conditions with the highest conversion rates achieved in the ball mill. Similar -COOH content (~1.3 mmol/g) was observed for unwashed products within a reaction time of 20 minutes (**Figure 3.5**) and summarized in **Table 3.1**. This observation also confirms that the reaction is initiated and sustained under solvent-free conditions, and the temperature naturally generated in the mill is sufficient. Washing resulted in further reaction progress, resulting in a charge content increase to 1.84 ± 0.04 mmol g^{-1} (DS = 0.30 ± 0.01) (n = 7), improving the conversion to 67%. The increase in charge content compared to conventional CMF is due to minimization of the hydrolysis process of MCA. Therefore, solid state synthesis of CMF saves time and give higher yields.

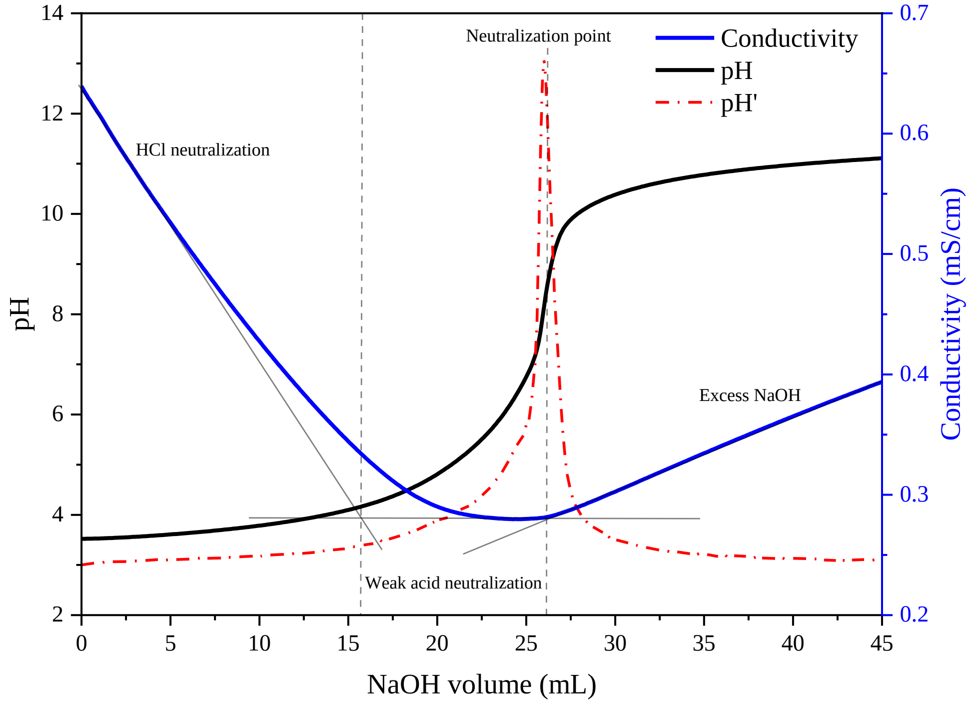

Figure 3.4: Example of pH and conductivity titration curves used to determine carboxyl charge content, degree of substitution and estimate the weak acid pK$_a$ in CMF produced by SM300 grinding mill.

Table 3.1: Carboxymethylation reaction conditions under solvent (conventional method) and solvent-free systems.

Method	Kraft pulp (g)	NaOH (g)	Reaction time (min)	MCA (g)	Reaction time (min)	-COOH (mmol/g)	DS
Conventional	30	12.0	60	9.60	120	1.33	0.22
Ball milling	0.2	0.06 solid*	60	0.05	60	1.26	0.20
	0.2	0.06	60	0.05	60	1.17	0.19
	0.2	0.06	50	0.05	All milled together	1.30	0.21
SM-300 grinder	20$^{\$\$}$	6.25	30	5.00	70	1.91	0.31
	20	6.25	30	5.00	70	1.87	0.30

*NaOH was added as a solid and drops of water added

$^{\$\$}$Sample not washed after the reaction

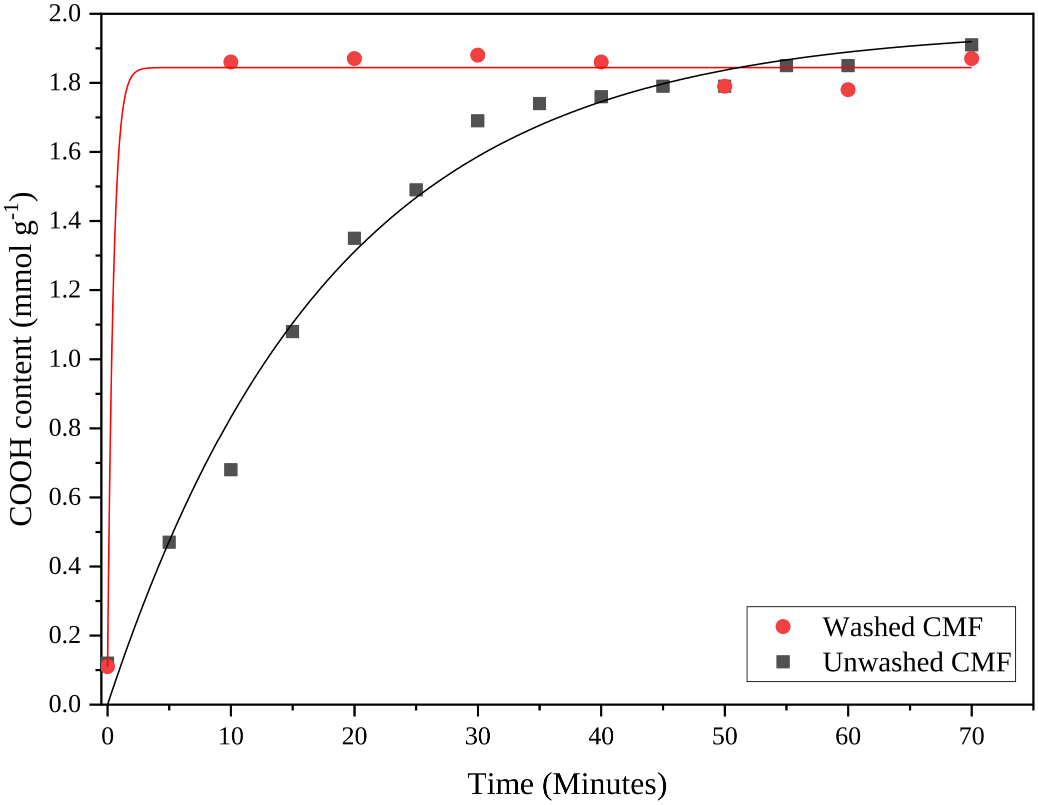

Figure 3.5: Grinding mill carboxymethylation reaction progress for washed and unwashed CMF samples. The curve for unwashed CMF is best fit to an exponential function with a plateau value of 1.91 mmol g^{-1} and $R^2 = 0.968$.

Comparing the pH curves for the three systems (conventional, ball milling and grinding mill), there is formation of a diprotic acid during ball milling, shown in **Figure S3.1**. Ball milling provides mechanical energy by material impact and shear, whereas, grinding mill energy is by shear and friction. Therefore, ball milling being a vibrational technique has been described as a high-energy method [13] of which it has been observed that the impact affects morphology by disrupting the hydrogen bonds [15]. In our experiments, the mill had a fixed vibrational frequency of 25 Hz. The supplied energy could be sufficient to overcome the reaction energy barrier on the C2 and C3 positions of the anhydro D-glucopyranose ring or could result in the formation of carboxylated nanoparticles, as similar titrations curve shapes (**Figure S3.1**) are often observed in cellulose nanomaterials [23, 29]. It has been observed that the hydroxyl groups on the C6 carbons is more easily accessible due to reduced steric hinderance [30], hence the monoprotic acid is commonly formed.

Using the Henderson-Hasselbalch equation ($pH = pK_a + \log_{10} [R–COO^-]/[R–COOH]$) at the titration point(s) of neutralization [31], the pK_a values for CMF produced conventionally, by grinding and by ball milling were determined. The pK_a values for conventional and grinding mill CMF were 4.8, and 4.6, respectively, whereas the diprotic ball milled CMF had pK_a values of 4.3 and 6.4. CMC pK_a values have been reported in the range of 3.2 – 4.7 [32], and has been characterized as a weak polyelectrolyte which pK_a value is greatly influenced by vicinal carboxyl groups, degree of substitution and solution ionic strength [33, 34].

3.4.2 Surface chemical properties

3.4.2.1 Characterization by infrared spectroscopy

Chemical modification via carboxymethylation was confirmed obtaining and comparing FTIR spectra (**Figure 3.6**) of softwood pulp and CMF produced conventionally, by grinding and ball milling. The broad peak at about 3300 cm^{-1} is due to –OH stretching influenced by hydrogen bonding, with corresponding bending modes at 1325 cm^{-1}. The C–H stretching, scissoring and CH_2–CH_2 stretching vibrational modes are observed at 2890, 1412 and 1016 cm^{-1}, respectively. These peaks are observed in both modified and unmodified cellulose and consistent with peak in previous studies [35, 36]. Formation of carbonyl carbon due to carboxylate ion is verified by the development of the peak at 1593 cm^{-1} associated with C=O stretch in acidic form (–COONa), observed in both conventional and solvent-free reactions. Additionally, the conventional method shows a minor peak at 1730 cm^{-1} which correlates with C=O stretch in salt form (–COOH). These observations and peak assignments were also observed by Moradian *et al* (2021) [37]and Islam *et al* (2020) [38]. Therefore, these similarities prove a successful formation of CMF using mechanical energy, without use of organic solvents.

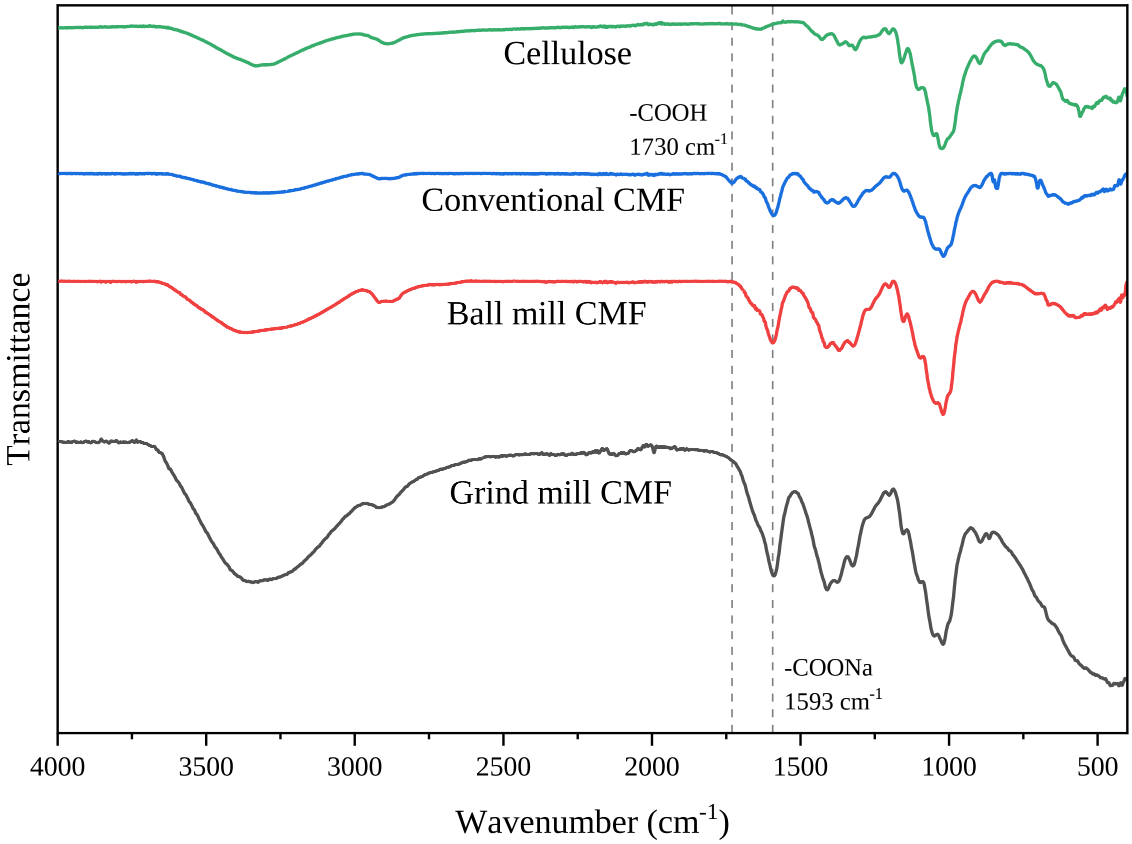

Figure 3.6: FTIR spectra of cellulose and carboxymethyl cellulose fibers produced by in solvent and solvent-free environments.

3.4.2.2 Characterization by solid-state NMR spectroscopy

The ^{13}C NMR spectra for cellulose Kraft pulp and CMF produced conventionally and through solid state milling are compared in **Figure 3.7**. The characteristic ^{13}C chemical shift at 177 ppm is due to –COOH in CMF in both conventional and solvent-free milling methods, which is absent in unmodified cellulose. The carbonyl carbon peak in organic acids is expected in the range of 155 – 185 [39] and observed in carboxymethyl cellulose at 173 – 178 ppm [3, 6]. This further confirms the formation of CMF under solvent-free conditions. Unmodified cellulose has glucopyranoside ring chemical shifts in the range of about 60 – 110 ppm, with the C4 (89 ppm) and C4´ (84 ppm) peaks well resolved, which are assigned to more ordered crystalline parts and less ordered structures [40], respectively. This 13C NMR spectrum is typical of cellulose I, the peak at 89 ppm disappears in all CMF spectra, with a slight right shift of all the peaks. This change is attributed to formation of less crystalline cellulose II, due to conformation changes on the C4 and C6 positions[41, 42]. The crystallinity changes are also confirmed by XRD in **Section 3.4.2.3** below.

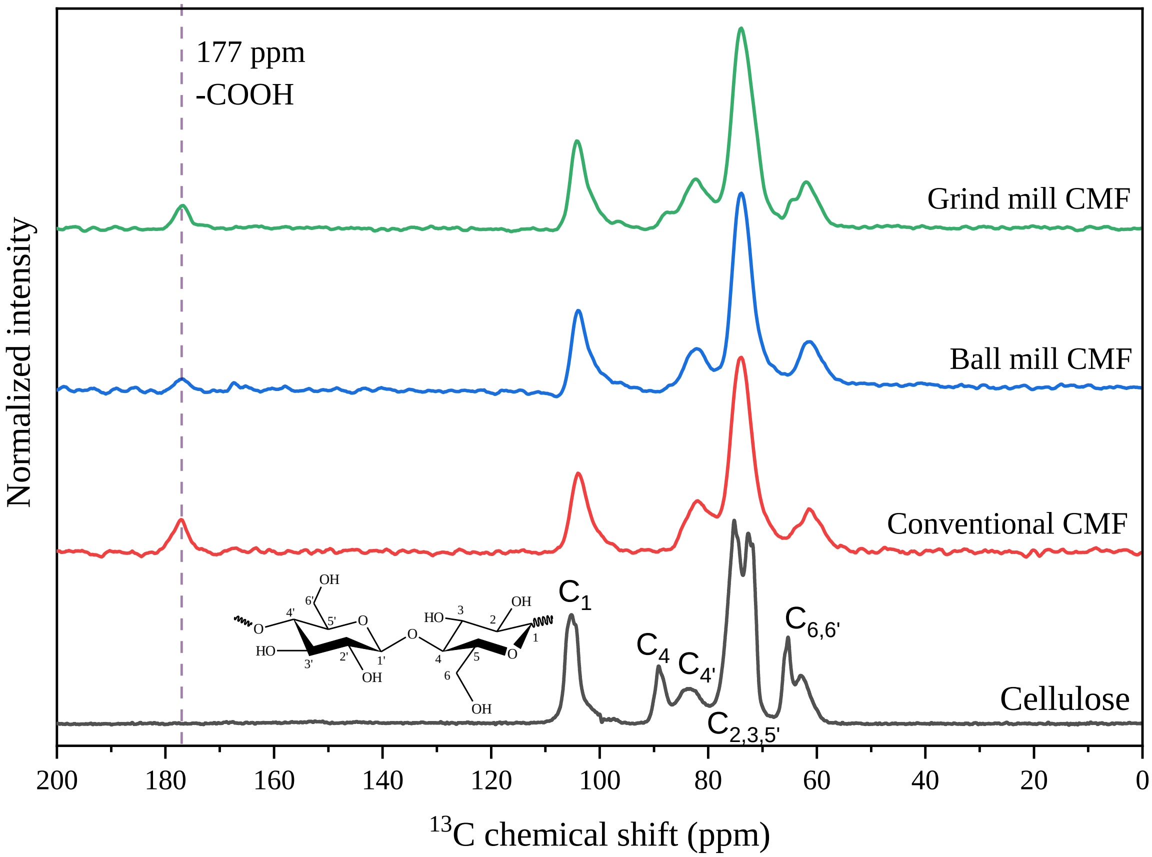

Figure 3.7: Solid-state ^{13}C NMR spectra for cellulose Kraft pulp and CMF produced conventionally in 2-propanol as the solvent and under solvent free conditions in a grinding mill and a ball mill.

3.4.2.3 Crystalline properties by X-ray diffraction spectroscopy

Figure 3.8 shows X-ray diffractograms of unmodified cellulose Kraft pulp and CMF. Kraft pulp has the characteristic peaks [43] at 2θ angles of about 15.5°, 22.5° and 34.5° which represent the crystallographic planes of 1 1 0, 2 0 0 and 0 4 0, respectively. The crystallinity index (CI) for cellulose was 73%. Modified cellulose has left shifted peaks to ~20° and ~12° in conventional, grind and ball milled CMF, otherwise, the diffractograms after carboxymethylation are similar. The slight shift of both peaks has been attributed to partial conversion of cellulose I to cellulose II during the reaction [27] and the CI reduced to 66, 62 and 65% for conventional, grind milled and ball milled CMF, respectively. Therefore, both the solvent and solvent-free reaction conditions have a similar effect on crystallinity and the lower CI for grind milled CMF could be due to a higher charge content. Conventional and grind milled CMF were wet extruded, there is a significant change in the peaks for the grind milled, while the conventional CMF retained its CI (64%). A low CI (14%) for regenerated grind milled CMF can be attributed to a higher charge content which makes it easier to go into solution and form nanofibers. The XRD pattern is similar to observations made by Mahrous F. *et al* (2021) for regenerated nanocrystals with a charge content >1.4 mmol g^{-1} [44].

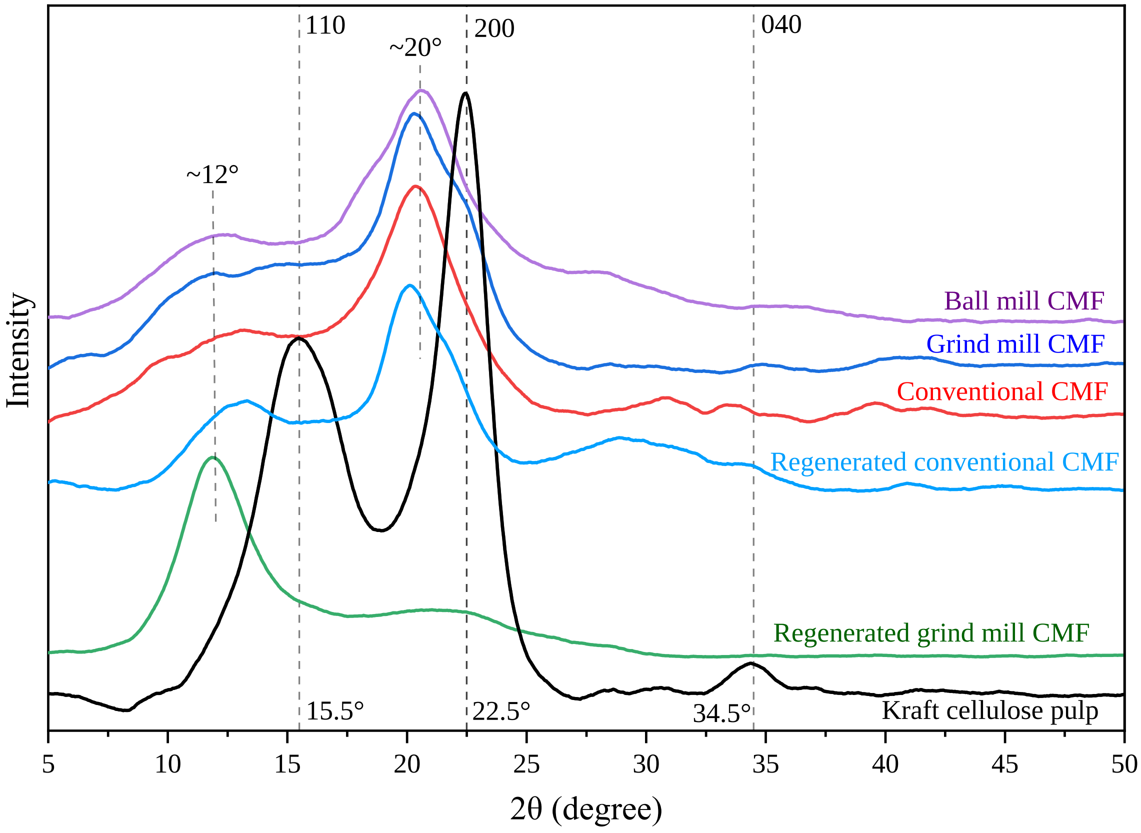

Figure 3.8: XRD patterns for unmodified and modified cellulose.

3.4.3 Dope solution and filament wet extrusion characteristics

The dope viscosity measured acoustically was 7.9 mPa s, which is high relative to that of the solvent (0.94 mPa s) at 22.6 °C. Additionally, the dope exhibited shear-thinning characteristics (**Figure S3.2**) and remains stable over long periods of storage (**Figure S3.3**), and forms a clear and colorless gel, significantly different from the appearance of CMF dispersed in water (**Figure 3.9**). The average particle size, and distribution shown in **Figure S3.4**, measured acoustically was 24.5 and 19.1 nm for conventional CMF and SM300 grinding mill CMF, respectively. There is no significant difference in the solubilized particle size, hence the similarity in rheology properties. The minor difference can be attributed difference in charge content or experimental error, as acoustic measurements greatly depend on temperature as sound attenuation linearly decreases with increase in temperature [45].

Furthermore, using a fiber quality analyzer, the fiber count for cellulose pulp in water was 32,768 fibers/mL in water with an average length of 0.119 ± 0.001 mm. This shows the ground pulp consist of > 95% fines (**Figure S3.5**), which is beneficial in reaction and dope homogenization. Furthermore, under alkaline conditions, the average fiber count and length were 31,515 fibers/mL, and 0.144 ± 0.003 mm, respectively. This indicates the non-solubility of unmodified fibers under alkaline conditions. While, conventional and SM300 grind milled CMF dopes had non-solubilized average fiber count of 2,218 and 2,434 fibers/mL, with an average length of 0.148 ± 0.007 mm and 0.075 ± 0.001 mm, respectively. This represents a solubility of > 90%, prior to filtration. The increase in size of the conventional CMF non-solubilized fibers is due to non-uniformity in reaction and bundling up of the larger chunks of cellulose pulp, whereas in SM300 CMF, this is prevented during the milling process as the fibers are continuously subjected to a cutting blade.

This observation is also confirmed in microscopy images (**Figure 3.9)**, as 1% solutions of cellulose pulp shows fibers dispersed in solution and the absence of fibers in the dopes. Upon regeneration in an acid bath using the wet spinning process, the fibers are ordered in a cotton-like form and retain the white colour with an average wet diameter of ~170 µm (**Figure 3.9**). The increase in size is due to fiber swelling via water absorption during the extrusion and wash procedures.

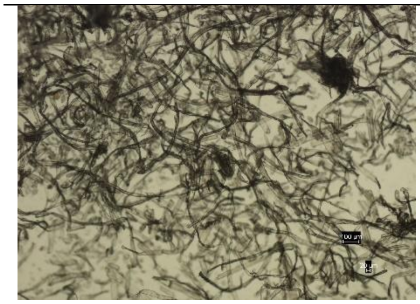

Cellulose in water

Cellulose in NaOH

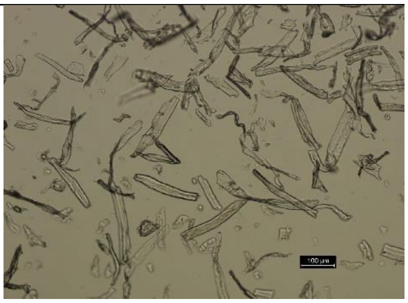

Conventional CMF in water

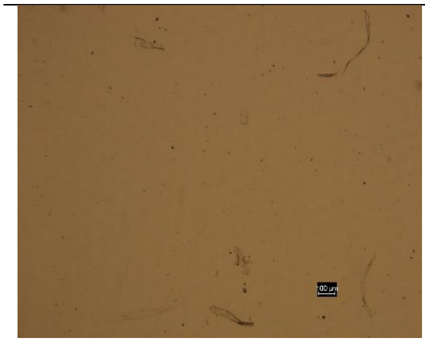

Conventional CMF dope before filtration

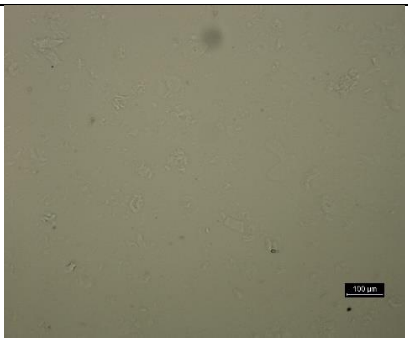

SM300 CMF dope before filtration

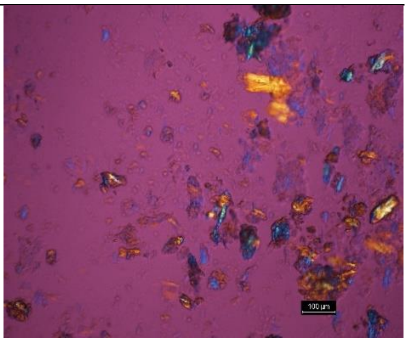

SM300 CMF in water

Extruded CMF filament

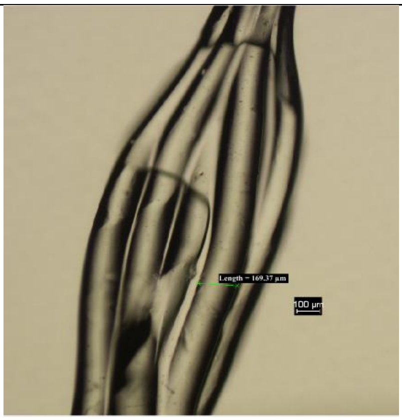

Microscopy image of extruded conventional CMF

Microscopy image of extruded grinding mill CMF

Figure 3.9: Optical light microscopy images of 1% solutions of cellulose fibers dispersed in water and NaOH, as well as photographic image of filaments extruded from CMF prepared conventionally and by solid state grinding mill. Scale bar is 100 µm.

Organic solvents (2-propanol or ethanol) are used in conventional CMF reaction to prevent gelation observed in aqueous media. Therefore, CMF must be washed thoroughly prior to forming dope solutions. The process from chemical modification to filament extrusion involves eight steps (1: Grinding 2: reacting with NaOH 3: reacting with sodium chloroacetate 4: washing 3× with ethanol 5: drying 6: dope formation 7: extrusion and 8: washing with water) [3]. However, since 2-propanol was not used in solvent-free mechanosynthesis of CMF, the dope solutions were also prepared without washing the samples, thereby eliminating the use of ethanol as a wash solvent. CMF disperses in ethanol and prevents the formation of a gel, hence the necessity to dry the CMF after washing in the conventional method. After extrusion, the filaments were washed with water and then dried. The mechanosynthesis process reduces the number of steps to six (**Scheme 3.2**), with a possibility to reduce to five by optimizing the reaction in which NaOH and MCA are milled together, see **Table S3.1** on ball milling the reagents together. Additionally, the conventional process would require organic solvent reclamation via distillation which would drive the energy and cost requirements higher. Therefore, the mechanosynthesis route is likely to be more efficient through cost effective use of materials, lowering production cost and processing time.

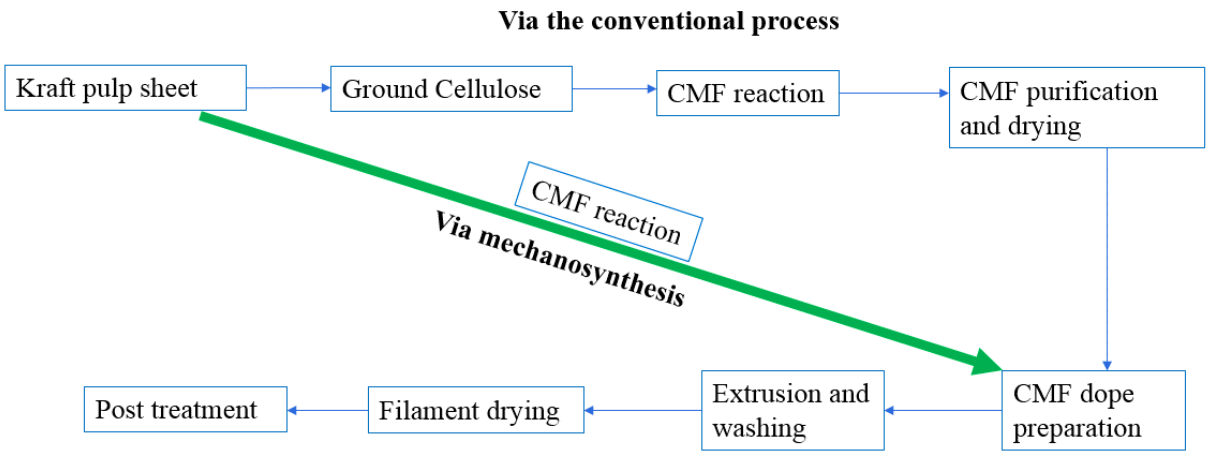

Scheme 3.2: Textile filament extrusion process for CMF

3.5 Conclusions

A novel method to prepare carboxymethyl cellulose fibers (CMF) using ball and grind milling under solvent-free conditions has been developed and compared to the conventional synthesis method employing 2-propanol as a solvent. Using comparable mole ratios of reactants, the average carboxyl group (-COOH) charge content of 1.26 (DS = 0.20) and 1.84 mmol g^{-1} (DS = 0.30) for conventional and grind milled CMF, respectively, was achieved. Under optimal conditions, the ball milling highest conversion was 1.30 mmol g^{-1} (DS = 0.21). The conventional method reaction time was 3 hours, whereas highest conversions for grind and balling milling procedures were within ~1.5 and 2 hours, respectively. Therefore, solvent-free reaction conditions reduce cost by eliminating use of organic solvents and higher conversions in a shorter time. Additionally, the products were qualitatively chemically characterized by nuclear magnetic resonance (NMR) and Fourier transform infrared spectroscopy (FTIR). The characteristic peaks for CMF formation at 177 ppm in NMR and 1593 cm^{-1} in FTIR were observed in both conventional and solvent-free methods, indicating successful carboxymethylation of cellulose under the newly developed methods.

Furthermore, CMF produced conventionally and by the grinding milling process were solubilized in 6% w/w NaOH solution to make an 8% w/w dope solution and regenerated in 10% w/w H_2SO_4 by extrusion into textile filaments. Organic solvents prevent gelation in aqueous media, therefore, conventional CMF had to be washed thoroughly and dried prior to making the dope. Since the grinding mill process does not use organic solvents, dope solutions were prepared without sample purification. There are eight steps involved in textile filament production, from cellulose preparation, chemical modification, purification and drying, and then wet extrusion. Therefore, the solvent-free process is more efficient as it eliminates the purification and drying steps, with the potential to eliminate the pulp preparation step. Overall, the process steps are reduced from eight to six. Solvent-free carboxymethylation and production of textile filaments has the potential to be a greener and more efficient process, providing an alternative to the conventional method.

3.6 Acknowledgements

The authors acknowledge funding support by a NSERC SRN on Green Fibers and a NSERC SPG (506303-17), supported by FPInnovations. User fees were partly covered by the FRQNT Centre for Advanced Materials (QCAM/CQMF).

References

[1] M.C. Sichinga, R. Koshani, T.G.M. van de Ven, Chemisorption of basic fuchsine in packed beds of dialdehyde cellulose fibres, Colloids and Surfaces A: Physicochemical and Engineering Aspects 632 (2022) 127726.

[2] S. Zhang, C. Chen, C. Duan, H. Hu, H. Li, J. Li, Y. Liu, X. Ma, J. Stavik, Y. Ni, Regenerated cellulose by the Lyocell process, a brief review of the process and properties, BioResources 13 (2018) 1-16.

[3] M.S. Islam, M.N. Alam, T.G.M. van de Ven, Production of textile filaments from carboxymethylated cellulosic pulps, Cellulose 28 (2021) 9475-9488.

[4] R. Barbucci, A. Magnani, M. Consumi, Swelling Behavior of Carboxymethylcellulose Hydrogels in Relation to Cross-Linking, pH, and Charge Density, Macromolecules 33 (2000) 7475-7480.

[5] V. Pushpamalar, S.J. Langford, M. Ahmad, Y.Y. Lim, Optimization of reaction conditions for preparing carboxymethyl cellulose from sago waste, Carbohydrate Polymers 64 (2006) 312-318.

[6] G. Joshi, S. Naithani, V.K. Varshney, S.S. Bisht, V. Rana, P.K. Gupta, Synthesis and characterization of carboxymethyl cellulose from office waste paper: A greener approach towards waste management, Waste Management 38 (2015) 33-40.

[7] N. Haleem, M. Arshad, M. Shahid, M.A. Tahir, Synthesis of carboxymethyl cellulose from waste of cotton ginning industry, Carbohydrate Polymers 113 (2014) 249-255.

[8] G. Sim, Y. Liu, T.G.M. van de Ven, Transparent composite films prepared from chemically modified cellulose fibers, Cellulose 23 (2016) 2011-2024.

[9] M. Moradian, M.S. Islam, T.G.M. van de Ven, Insoluble Regenerated Cellulose Films Made from Mildly Carboxylated Dissolving and Kraft Pulps, Industrial & Engineering Chemistry Research 60 (2021) 5385-5393.

[10] M.P. Adinugraha, D.W. Marseno, Haryadi, Synthesis and characterization of sodium carboxymethylcellulose from cavendish banana pseudo stem (Musa cavendishii LAMBERT), Carbohydrate Polymers 62 (2005) 164-169.

[11] A. Perona, P. Hoyos, Á. Farrán, M.J. Hernáiz, Current challenges and future perspectives in sustainable mechanochemical transformations of carbohydrates, Green Chemistry 22 (2020) 5559-5583.

[12] A. Sarkar, S. Santra, S.K. Kundu, A. Hajra, G.V. Zyryanov, O.N. Chupakhin, V.N. Charushin, A. Majee, A decade update on solvent and catalyst-free neat organic reactions: a step forward towards sustainability, Green Chemistry 18 (2016) 4475-4525.

[13] S. Kuga, M. Wu, Mechanochemistry of cellulose, Cellulose 26 (2019) 215-225.

[14] B.G. Fiss, L. Hatherly, R.S. Stein, T. Friščić, A. Moores, Mechanochemical Phosphorylation of Polymers and Synthesis of Flame-Retardant Cellulose Nanocrystals, ACS Sustainable Chemistry & Engineering 7 (2019) 7951-7959.

[15] M. Ago, T. Endo, K. Okajima, Effect of Solvent on Morphological and Structural Change of Cellulose under Ball-Milling, Polymer Journal 39 (2007) 435-441.

[16] H. Zhao, J.H. Kwak, Y. Wang, J.A. Franz, J.M. White, J.E. Holladay, Effects of Crystallinity on Dilute Acid Hydrolysis of Cellulose by Cellulose Ball-Milling Study, Energy & Fuels 20 (2006) 807-811.

[17] I. Solala, U. Henniges, K.F. Pirker, T. Rosenau, A. Potthast, T. Vuorinen, Mechanochemical reactions of cellulose and styrene, Cellulose 22 (2015) 3217-3224.

[18] W. Zhang, C. Li, M. Liang, Y. Geng, C. Lu, Preparation of carboxylate-functionalized cellulose via solvent-free mechanochemistry and its characterization as a biosorbent for removal of Pb2+ from aqueous solution, Journal of Hazardous Materials 181 (2010) 468-473.

[19] U.-J. Kim, S. Kuga, M. Wada, T. Okano, T. Kondo, Periodate Oxidation of Crystalline Cellulose, Biomacromolecules 1 (2000) 488-492.

[20] R. Koshani, M. Tavakolian, T.G.M. van de Ven, Natural Emulgel from Dialdehyde Cellulose for Lipophilic Drug Delivery, ACS Sustainable Chemistry & Engineering 9 (2021) 4487-4497.

[21] H. Yang, A. Tejado, N. Alam, M. Antal, T.G.M. van de Ven, Films Prepared from Electrosterically Stabilized Nanocrystalline Cellulose, Langmuir 28 (2012) 7834-7842.

[22] J. Araki, M. Wada, S. Kuga, Steric Stabilization of a Cellulose Microcrystal Suspension by Poly(ethylene glycol) Grafting, Langmuir 17 (2001) 21-27.

[23] R. Koshani, T.G.M. van de Ven, A. Madadlou, Characterization of Carboxylated Cellulose Nanocrytals Isolated through Catalyst-Assisted H2O2 Oxidation in a One-Step Procedure, Journal of Agricultural and Food Chemistry 66 (2018) 7692-7700.

[24] L. Segal, J.J. Creely, A.E. Martin, C.M. Conrad, An Empirical Method for Estimating the Degree of Crystallinity of Native Cellulose Using the X-Ray Diffractometer, Textile Research Journal 29 (1959) 786-794.

[25] O. Ferritsius, R. Ferritsius, M. Rundlöf, Average fibre length as a measure of the amount of long fibres in mechanical pulps – ranking of pulps may shift, Nordic Pulp & Paper Research Journal 33 (2018) 468-481.

[26] R. Koshani, T.G.M. van de Ven, Electroacoustic characterization of trimmed hairy nanocelluloses, Journal of Colloid and Interface Science 563 (2020) 252-260.

[27] M.N. Alam, M.S. Islam, L.P. Christopher, Sustainable Production of Cellulose-Based Hydrogels with Superb Absorbing Potential in Physiological Saline, ACS Omega 4 (2019) 9419-9426.

[28] L. Nanninga, Velocity of hydrolysis of sodium chloroacetate in alkaline medium and concentrated solutions), Recueil des Travaux Chimiques des Pays-Bas 69 (2010).

[29] P. Criado, C. Fraschini, S. Salmieri, D. Becher, A. Safrany, M. Lacroix, Evaluation of Antioxidant Cellulose Nanocrystals and Applications in Gellan Gum Films, Industrial Biotechnology 11 (2015) 59-68.

[30] H. Kono, K. Oshima, H. Hashimoto, Y. Shimizu, K. Tajima, NMR characterization of sodium carboxymethyl cellulose: Substituent distribution and mole fraction of monomers in the polymer chains, Carbohydrate Polymers 146 (2016) 1-9.

[31] M. Spaic, D.P. Small, J.R. Cook, W. Wan, Characterization of anionic and cationic functionalized bacterial cellulose nanofibres for controlled release applications, Cellulose 21 (2014) 1529-1540.

[32] L.F.W. Vleugels, S. Ricois, I.K. Voets, R. Tuinier, Determination of the ‘apparent pKa’ of selected food hydrocolloids using ortho-toluidine blue, Food Hydrocolloids 81 (2018) 273-283.

[33] I. Aggeryd, Å. Olin, Determination of the degree of substitution of sodium carboxymethylcellulose by potentiometric titration and use of the extended henderson-hasselbalch equation and the simplex method for the evaluation, Talanta 32 (1985) 645-649.

[34] A.M. Zhivkov, Electric Properties of Carboxymethyl Cellulose, Cellulose - Fundamental Aspects2013, pp. 197-226.

[35] K. Conley, M. Whitehead, T.G.M. van de Ven, Chemically peeling layers of cellulose nanocrystals by periodate and chlorite oxidation, Cellulose 23 (2016) 1553-1563.

[36] T. Zheng, X. Yu, S. Pilla, Mechanical and moisture sensitivity of fully bio-based dialdehyde carboxymethyl cellulose cross-linked soy protein isolate films, Carbohydrate Polymers 157 (2017) 1333-1340.

[37] M. Moradian, M.N. Alam, T.G.M. van de Ven, Influence of Carboxyl Charge Density on Properties of Extruded Cellulose Films, Industrial & Engineering Chemistry Research 60 (2021) 13756-13763.

[38] M.S. Islam, M.N. Alam, T.G.M. van de Ven, Sustainable cellulose-based hydrogel for dewatering of orange juice, Cellulose 27 (2020) 7637-7648.

[39] L.D. Pavia, M.G. Lampman, S.G. Kriz, R.J. Vyvyan, Introduction to Spectroscopy, 4 ed., Brooks/Cole Cengage Learning, United States of America, 2009.

[40] R. Koshani, T.G.M. van de Ven, Carboxylated Cellulose Nanocrystals Developed by Cu-Assisted H2O2 Oxidation as Green Nanocarriers for Efficient Lysozyme Immobilization, Journal of Agricultural and Food Chemistry 68 (2020) 5938-5950.

[41] G. Sèbe, F. Ham-Pichavant, E. Ibarboure, A.L.C. Koffi, P. Tingaut, Supramolecular Structure Characterization of Cellulose II Nanowhiskers Produced by Acid Hydrolysis of Cellulose I Substrates, Biomacromolecules 13 (2012) 570-578.

[42] A. Isogai, M. Usuda, T. Kato, T. Uryu, R.H. Atalla, Solid-state CP/MAS carbon-13 NMR study of cellulose polymorphs, Macromolecules 22 (1989) 3168-3172.

[43] Z. Sabzalian, M.N. Alam, T.G.M. van de Ven, Hydrophobization and characterization of internally crosslink-reinforced cellulose fibers, Cellulose 21 (2014) 1381-1393.

[44] F. Mahrous, R. Koshani, M. Tavakolian, K. Conley, T. van de Ven, Formation of hairy cellulose nanocrystals by cryogrinding, Cellulose 28 (2021).

[45] A.S. Dukhin, P.J. Goetz, Characterization of liquids, nano- and microparticulates, and porous bodies using ultrasound, Elsevier, Amsterdam, 2017.

3.7 Supplementary information for mechanosynthesis of carboxymethyl cellulose fibers using ball and grind milling for applications in wet spinning textile filament extrusion

Martin Sichinga and Theo G. M. van de Ven[*]

Department of Chemistry, Pulp and Paper Research Centre, McGill University, 3420 Rue University, Montreal, Quebec, H3A 2A7, Canada

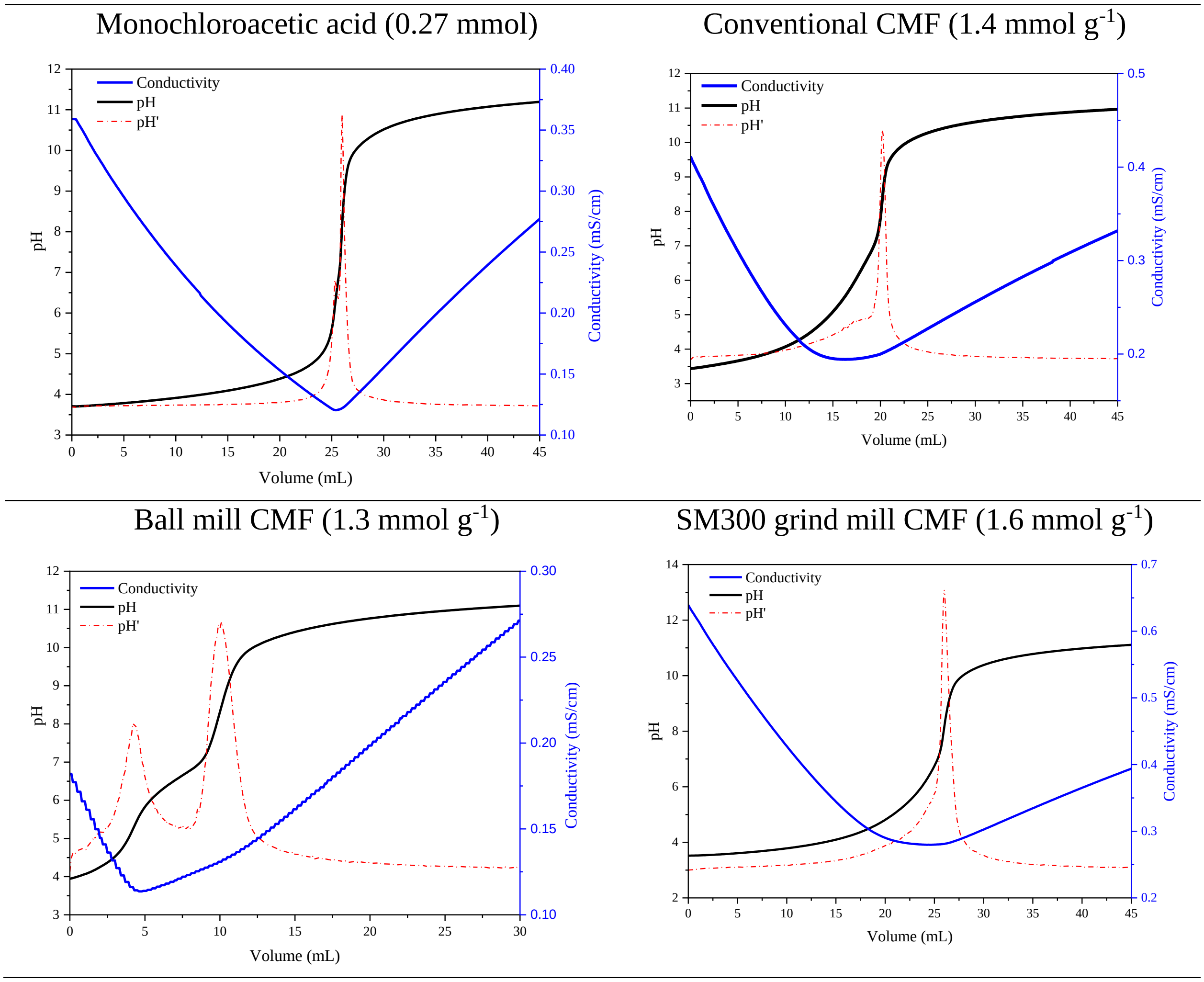

Figure S3.1: Titration curves for monochloacetic acid and CMF produced conventionally and by solid state milling, used for the determination of charge content of a weak carboxylic acid.

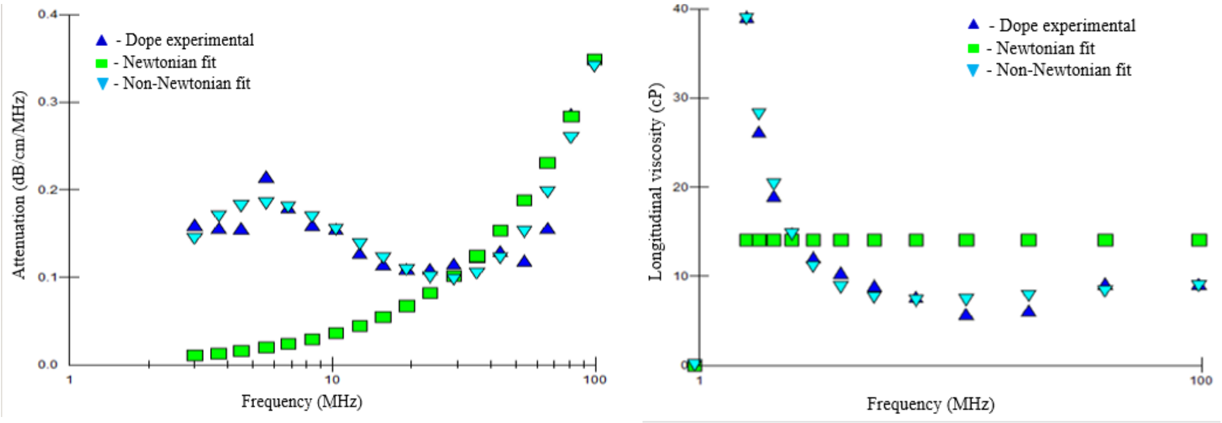

Figure S3.2: Rheology properties of an 8 wt% CMF dope solution.

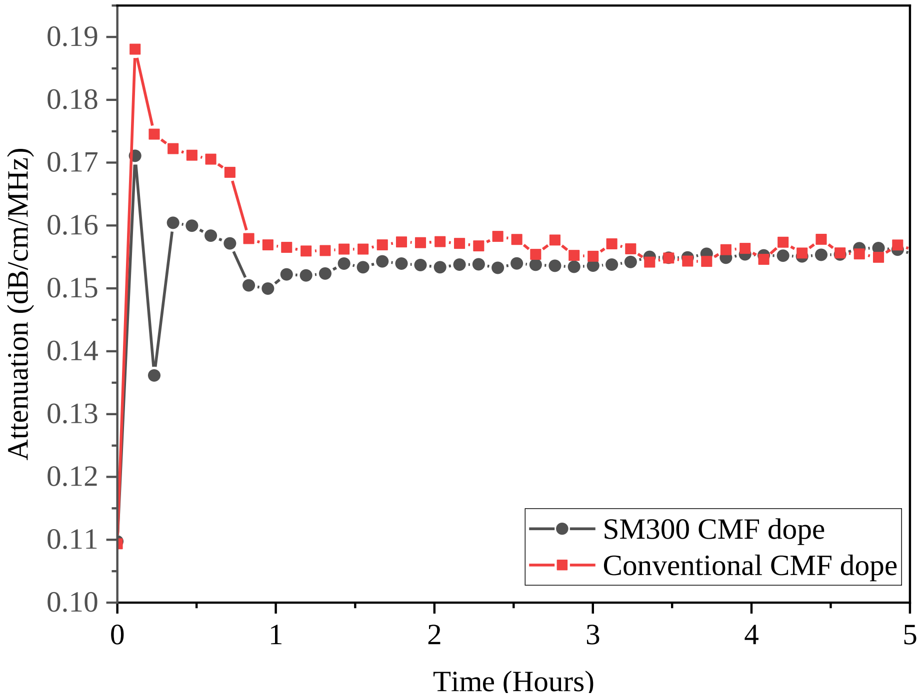

Figure S3.3: CMF dope stability under basic conditions.

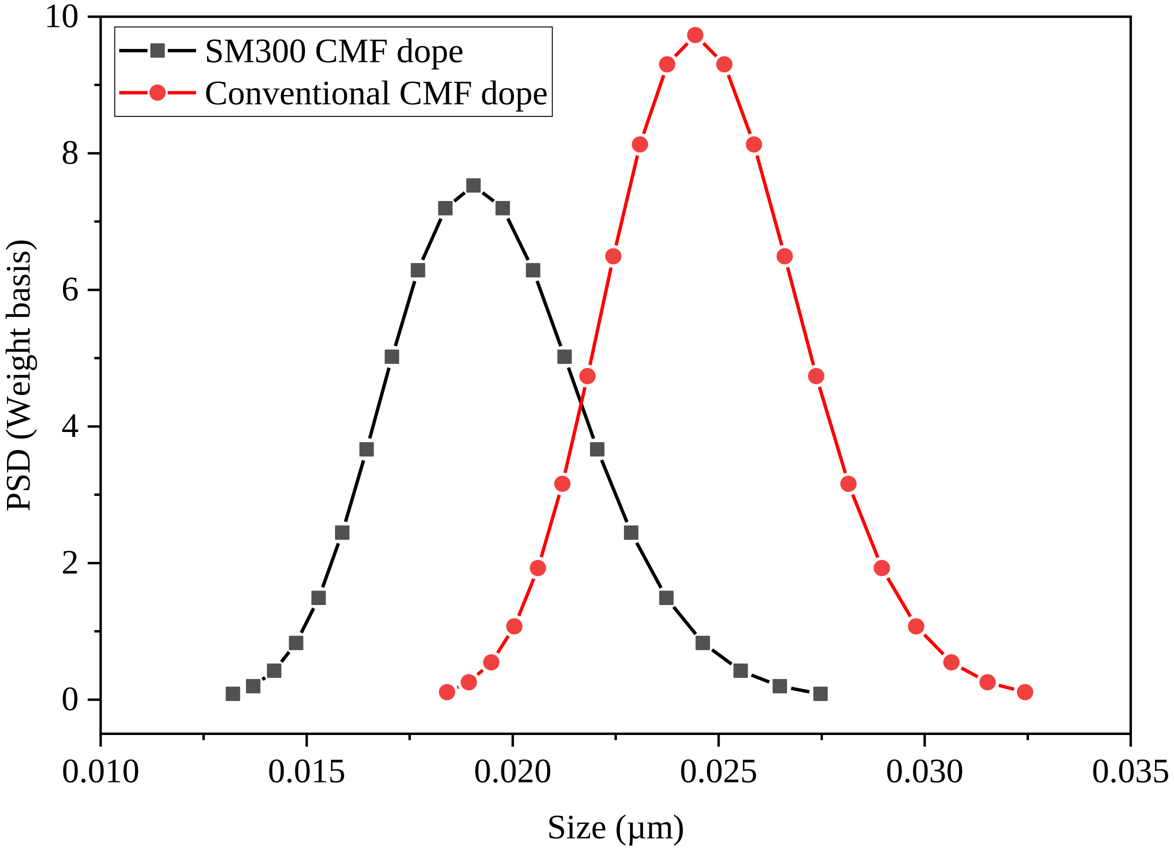

Figure S3.4: Particle size distribution of CMF dope measured acoustically.

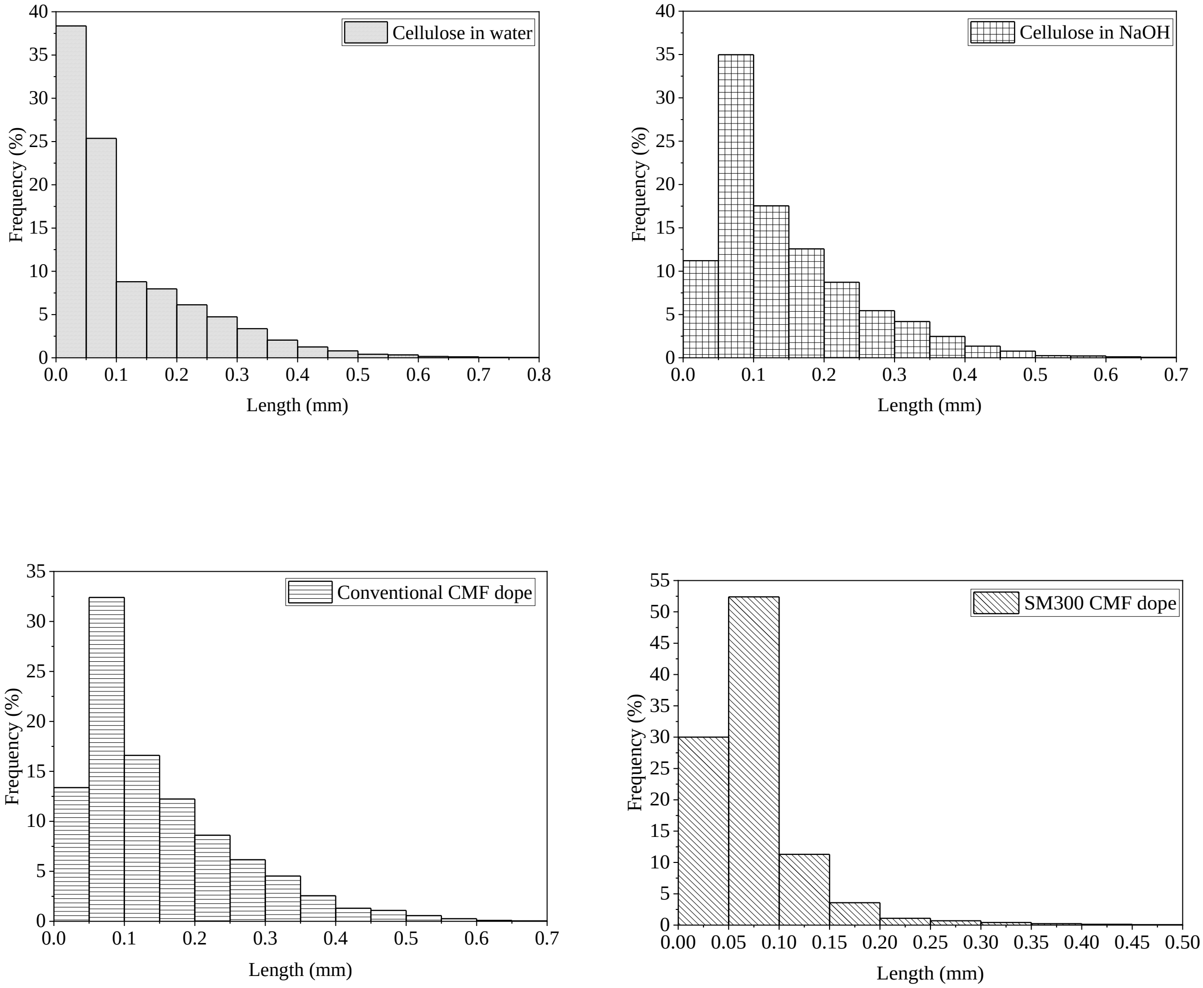

Figure S3.5: Fiber quality analysis of particle length distribution of non-solubilized cellulose fibers in water and dope solutions.

Table S3.1: Carboxymethylation reaction conditions under solvent (conventional method) and solvent-free systems (ball and SM300 grinder milling). NaOH and MCA were added as solutions, unless otherwise stated.

Method	Kraft pulp (g)	2-propanol (g)	NaOH (g)	Temp. (°C)	Reaction time (min)	MCA (g)	Temp. (°C)	Reaction time (min)	-COOH (mmol/g)	DS	Wash
Conventional	30	510	12.0	40	60	9.60	60	120	1.33	0.22	Yes
Ball milling	0.2	0	0.06 solid	-	60	0.05 solid	-	60	0.37	0.06	Yes
	0.2	0	0.06 solid*	-	60	0.05 Solid	-	60	0.42	0.07	Yes
	0.2	0	0.06 solid*	-	60	0.05	-	60	1.26	0.20	Yes
	0.2	0	0.06	-	60	0.05	-	60	1.17	0.19	Yes
	0.2	0	0.09	-	60	0.075 Solid	-	60	0.49	0.08	Yes
	0.2	0	1.25 solid*	-	60	0.075 Solid	-	60	0.48	0.08	Yes
	0.2	0	0.06	-	30	0.05	-	20	0.73	0.12	Yes
	0.2	0	0.06	-	30	0.05	-	15	0.64	0.10	Yes
	0.2	0	0.06	-	30	0.05	-	10	0.60	0.10	Yes
	0.2	0	0.06	-	30	0.05	-	5	0.39	0.06	Yes
	0.2	0	0.06	-	30	0.05	-	0	0.31	0.05	Yes
	0.2	0	0.06	-	5	0.05	-	30	0.56	0.09	Yes
	0.2	0	0.06	-	10	0.05	-	30	0.99	0.16	Yes
	0.2	0	0.06	-	15	0.05	-	30	0.79	0.13	Yes
	0.2	0	0.06		50	0.05		All milled together	1.30	0.21	Yes
SM-300 grinder	20	0	6.25	37	30	5.00	37	70	1.91	0.31	No
	20	0	6.25	37	30	5.00	37	70	1.87	0.30	Yes

*NaOH was added as a solid and drops of water added

- Temperature could not be measured inside the milling jar

Preface to Chapter 4

The Chapter 3 discussed the use of carboxymethyl cellulose fibers (CMF) as the base functionalized material in the extrusion of textile filaments. The filament extrusion process is reduced by eliminating the use of organic solvents, in comparison to the conventional method of CMF synthesis. In addition, the process side product is a non-toxic salt, Na_2SO_4, unlike the rayon process that releases CS_2. Having developed a method to produce the textile filaments, Chapter 4 moves on to address the problem of dyeing in textile manufacturing. Dyes are mainly applied to textiles as a post-treatment step, with physisorption and ion exchange as the main mechanisms of adsorption. Chapter 4 focusses on the feasibility of using a Schiff base reaction as a method to chemically adsorb dyes. This was achieved using a continuous amine dye flow process on dialdehyde cellulose packed beds, to understand the kinetics and mechanisms of adsorption. A continuous flow process, unlike batch reactors, was utilized to mimic industrial practice in textile manufacturing. This research has been published in the following paper:

Martin Chewe Sichinga, Roya Koshani, and Theo G. M. van de Ven. 2022. 'Chemisorption of basic fuchsine in packed beds of dialdehyde cellulose fibres', *Colloids and Surfaces A: Physicochemical and Engineering Aspects*, 632: 127726.

4 Chemisorption of basic fuchsine in packed beds of dialdehyde cellulose fibres

4.1 Abstract

The discharge of textile dyes in water systems, due to poor binding to fabrics, is a major health and environmental concern. The majority of synthetic dyes used in textile are hazardous and carcinogenic. Despite efforts in addressing challenges associated with covalent binding of dyes to fibers and effluent filtration, there has been no promising green solution based on green materials and chemistry. Here, we demonstrate that dialdehyde cellulose (DAC) engineered through the chemical functionalization of cellulose fibres provides great functionality for Schiff base dye conjugation. Breakthrough curves (BTCs) of basic fuchsine in packed beds of DAC fibers were fitted to a Langmuir model and pseudo-first order kinetics. DAC fibers with an aldehyde density of 10.8 mmol g^{-1} had an adsorption capacity, adsorption and desorption rates of 204 mg g^{-1}, 0.05 min^{-1} and 9.0×10^{-5} min^{-1}, respectively. For cellulose fibers, used as a control, these values are 61 mg g^{-1}, 0.15 min^{-1} and 2.6×10^{-3} min^{-1}, respectively. It is shown that all dye is chemisorbed on DAC fibres, after initial physisorption and ion-exchange. Addition of 1M NaCl to the dye solution resulted in coagulation of the dye and the removal capacity through filtration increased to 489 mg g^{-1}, a process ideal for dye recovery or water purification.

Keywords: adsorption, cellulose, dialdehyde cellulose, fuchsine dye, Schiff base, textile

4.2 Introduction

The demand for clean water from domestic and industrial effluent remains a priority for a sustainable modern society. Aquatic pollution due to dyes is of major concern as it threatens human health, ecosystem, and aquatic life. The textile industry is one of the principal contributors, contributing about 20% of total industrial pollution [1], to surface and ground water contamination due to large water quantities (100 L kg^{-1} of fabric) required for finishing [2, 3]. Typically, textile effluents have dye concentrations in the range 10-50 mg L^{-1} and some studies have reported concentrations exceeding 300 mg L^{-1}. These effluents are highly colored and visually identifiable even at concentrations as low as 1 mg L^{-1}, affecting water transparency [4]. The main reason for high pollution is the poor binding affinity of dyes to fabrics, with dye loss ranging from 2-50%, for basic dyes to reactive dyes [5, 6]. It has also been observed that cationic dyes, such as methylene blue and basic fuchsine, are more toxic than anionic dyes [7, 8]. Application of dye as a finish, after production of yarns, results in large quantities of dye wastewater. Therefore, understanding the kinetics of adsorption/desorption and developing an approach that adds only the required amount of dye and which would reduce/eliminate waste generation, is highly required.

The high solubility and stability of molecular dye solutions makes it challenging to filter them. Consequently, various dye decontamination techniques have been explored, with each method having both pros and cons. Some of these techniques are Fenton reagents, ozonation, photochemical oxidation, electrochemical destruction, activated carbon, membrane filtration, ion exchange and electrocoagulation. The pros and cons are well summarized by Rodriguex Couto (2009) [9] with some of the major concerns being high operation costs, chemical break-down [10] and high sludge retention. A variety of studies have also focused on biological degradation using various bacterial cultures and fungi [2, 4, 9]. These techniques are based on decolorizing water by breaking dye molecules, thus destroying conjugation and hence are chemical degradation methods. The degradation products have the potential to be toxic or have a negative environmental effect, high residence time, in addition to leading to higher bioreactor operation and maintenance costs [11-13].

Dye adsorption methods have also been explored with non-destructive techniques. Some of the dye adsorption materials that have been studied include carbon nanotubes [14], kaolin [7], pineapple leaf powder [15], sawdust [16], polyurethane foam [17] and cellulose [18-21]. Cellulosic and other biobased adsorbents are advantageous due to low cost, high abundance, renewability, non-toxicity, biodegradability and versatility in surface modification [22, 23]. Cellulose fibres are usually negatively charged due to hemicellulose [24] with a high porous structure [25], making it a suitable natural precursor to develop adsorbents for cationic dyes. However, high crystallinity [26] of cellulose fibres poses as a barrier for efficient dye diffusion. Therefore, chemical functionalization of cellulose is proposed to create covalent attachment sites and reduce crystallinity.

Cellulose as a raw biomaterial is highly employed in textile manufacturing with a market share of about 40% of total world textile production, accounting for >99% among the renewable biomaterials [27]. Cellulose is used in its raw, regenerated or functionalized form [28]. In all cases, the dye is physically bound to the textile material, which leads to dye leaching during both processing and lifetime use. Here, we engineer an aldehyde-bearing version of functionalized cellulose and demonstrate that it can function as a green solution in addressing dye leaching problems through chemical binding via a Schiff base reaction. A Schiff base reaction is a quick and straight-forward approach for covalent attachment, which can be exploited at high industrial processing rates.

To synthesize 2,3-dialdehyde cellulose (DAC), periodate oxidation is used resulting in anhydro D-glucopyranose ring opening [29]. Aldehyde functionalization enhances reactivity that can be manipulated further [30, 31]. By taking advantage of cellulose characteristics, this study explores using DAC fibres as (i) an adsorbent for cationic basic fuchsine dye to covalently dye textile, thereby preventing leaching and (ii) an efficient aqueous dye decontaminant. Furthermore, the majority of dye decontamination techniques explore wastewater effluent treatment [32], hence not addressing the root-cause of the problem. Therefore, understanding rates of covalent dye fixation would lead to exploration of efficient methods to produce dyed products, thereby minimizing or eliminating the production of dye wastewater.

Dye adsorption capacity is influenced by charge, hydrogen bonds, π-π bonds and covalent interactions [33]. Electrostatic interactions in porous media often lead to an ion-exchange process, in which dye ions replace the counterions initially present. These interactions are useful in exploiting target species based on charge and size [34, 35]. Overall, mechanisms of adsorption are categorized as (i) physisorption which relies mainly on van der Waals interactions or hydrogen bonding; (ii) ion exchange in which the counterions are exchanged with adsorbing ions, and (iii) covalent bonding or chemisorption where new chemical bonds are formed between the adsorbent and adsorber. By taking advantage of various adsorption mechanisms, selective adsorption and separation of complex dye mixtures can be achieved [36].

Basic fuchsine (a triaminotriphenylmethane dye), see **Figure 4.1**, is a molecular cationic dye commonly used as a biological stain [37], as it readily adsorbs on many surfaces, including cellulose. It is also employed in textile dyeing, causing a negative aquatic environmental impact.

Additionally, the dye possess antibacterial (Gram-positive) and antifungal properties [38, 39]. Basic fuchsine has been studied as a Schiff reagent using formaldehyde [40] to generate imines, commonly referred to as Schiff bases. Therefore, by modifying cellulose to DAC, basic fuchsine can covalently be grafted onto DAC fibres, supplementing ion exchange and physisorption, thereby improving the cellulose adsorption capacity. Furthermore, as a triamine, basic fuchsine has the potential to crosslink the DAC fibres, thus potentially increasing the mechanical strength of the cellulosic product.

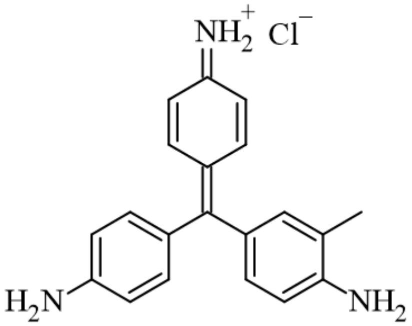

Figure 4.1: Chemical structure for basic fuchsine ($C_{20}H_{20}N_3Cl$, molar mass 337.86 g mol^{-1}).

Typically, adsorption reactions are conducted in continuously stirred batch reactors (CSTR) or packed bed reactors (PBR). The major advantages of PBRs in wastewater treatment are low operating costs owing to ability to operate continuously, thereby minimizing downtime. Moreover, PBRs are compact and can easily be integrated into existing technologies [41]. These PBR's advantages have prompted us to evaluate the potential of DAC as a dye scavenger in PBRs. The data are analyzed with the axial dispersion model for particle deposition, described by transport and deposition process equations [41-44].

The transport behaviour of continuous flow systems was described by Danckwerts [45], in which the residence time distribution (RTD) function in a packed bed is obtained from an inert tracer. An inert tracer must be a non-reactive and non-adsorbing compound that is flown through the packed bed [46]. In this study, sucrose was used as an inert tracer to acquire the RTD, which is obtained by solving the transport *Equation 4.1*. All mechanisms contributing to the RTD are consolidated in the axial dispersion coefficient (D_d).

$$\frac{\partial c}{\partial t} + \frac{U}{\varepsilon}\frac{\partial c}{\partial x} = D_d \frac{\partial^2 c}{\partial x^2} \tag{4.1}$$

Here, c is inert tracer concentration, t is the time (seconds), x is axial direction of flow, U (m s^{-1}) is the superficial fluid velocity through the bed and ε is the bed void volume (porosity). By normalizing *Equation 4.1* as described by Colli *et al.* (2011) [42] and Al-Jarabi *et al.* (1994) [43], a Peclet (Pe) number is obtained as a single parameter that is needed to specify the shape of the RTD function. For a closed system with Danckwert boundary conditions [43], the Pe number is defined as follows:

$$Pe = \frac{HU}{D_d \varepsilon} \tag{4.2}$$

where H is the packed bed height (m). The limits of $Pe \rightarrow \infty$ and $Pe \rightarrow 0$ describe systems for an ideal plug flow and a CSTR, respectively. The analytical solution was obtained by Brenner who showed that Pe and the RTD can be determined from the exit concentration of an inert tracer [47].

A plug flow model for particle deposition describes adsorption rates and quantities on a porous medium at a constant velocity. The primary driving forces for deposition are the attractive forces, i.e. van der Waals and electrostatic, between the flowing particles and pore walls [48]. Particle deposition is gouverned by a transport equation (*Equation 4.3*) obtained by performing a mass balance over an incremental suspension volume until a steady state is reached [43]. Monitoring concentration changes in either effluent or the packed bed allows for the determination of breakthrough curves (BTCs).

$$\varepsilon \frac{\partial n}{\partial t} + (1-\varepsilon)\rho_c \frac{\partial N}{\partial t} + U \frac{\partial n}{\partial x} = 0 \tag{4.3}$$

Here ρ_c is the density (kg m^{-3}) of the fibres in the bed, with porosity ε; N (g g^{-1}) and n (kg m^{-3}) are particle concentrations in the packed bed and suspension, respectively.

Langmuir kinetics (*Equation 4.4*) can relate N and n, which describe the kinetics of adsorption and desorption. At steady state, the rates of particle adsorption and desorption are equal [46, 49]. Therefore, a Langmuir isotherm provides information on adsorption efficiency and capacity in a packed bed [18, 43, 50]. It is expected that dye adsorption on cellulosic fibres in a PBR would follow similar kinetics.

$$\frac{1}{N_e} = \frac{(1-\varepsilon)\rho_c}{\varepsilon} \frac{1}{KN_{max}} \frac{1}{n_e} + \frac{1}{N_{max}} \tag{4.4}$$

Here N_e (g g^{-1}) is the steady state dye concentration on the packed bed and K is the steady state rate constant. The dye concentration leaving the bed is given by n_e, and N_{max} (g g^{-1}) is maximum packed bed capacity.

By using the RTD function from inert tracers and the plug flow adsorption BTCs, the amount captured per unit time is obtained by integrating the area between the two curves [44, 51] (*Equation 4.5*). Subsequently, the rate of attachment (dye adsorption) per unit time, is determined by fitting the individual BTCs to a pseudo-first order kinetics model (*Equation 4.6*) [52].

$$N_e = Qn_o \int_0^{t_c} \left(1 - \frac{n_{(t)}}{n_o}\right) dt \tag{4.5}$$

$$\ln(N_e - N_t) = \ln N_e - k_{ads} t \tag{4.6}$$

Here N_e, N_t, n_o, n_t, t and Q are amount adsorbed at equilibrium, amount adsorbed at specified time, initial concentration, concentration at time t, time and flow rate, respectively.

4.3 Materials and Methods

4.3.1 Materials

Bleached soft wood kraft pulp (Q-90) was used as a cellulose raw material to synthesize DAC. The pulp sheets were obtained from Domtar, Canada, and then mechanically ground into a powder using a GlenMills Retsch™ SM300 grinder, fitted with 0.5 mm screen. Reaction grade sodium meta-periodate ($NaIO_4$), ethylene glycol and sodium chloride were supplied by Sigma-Aldrich, Ontario Canada. Basic fuchsine was supplied by Santa Cruz Biotechnology Inc, Texas USA. Analytical reagent grade sucrose, sodium hydroxide solution (0.01 *N*), hydrochloric acid (0.5 M), and hydroxylamine hydrochloride ($NH_2OH{\cdot}HCl$) were acquired from Sigma-Aldrich, Ontario Canada. All reagents were used without modification, unless otherwise stated.

4.3.2 Periodate oxidation of Q-90 cellulose pulp

The periodate oxidation reaction conditions were adopted according to Sabzalian *et al* (2014) and Conley *et al* (2014) [30, 53], with minor modifications on reactant quantities. Cellulose kraft pulp (100 g) was dispersed in distilled water making a 7% w/w solution, to which NaCl was dissolved to make a 1 M NaCl solution. The solution was homogenized for 10 minutes before adding excess $NaIO_4$ (130 mol% based on cellulose anhydroglucose units) to produce a theoretical maximum of 12.5 mmol of aldehyde groups per gram of cellulose (12.5 mmol g^{-1}). While stirring, the reaction proceeded for 7 days in the dark, after which a few drops of ethylene glycol were added to quench the reaction. The product was washed in distilled water and then filtered with a 20 µm nylon cloth. The modified pulp was stored at 4 °C without drying.

4.3.3 Schiff base reaction with basic fuchsine in the packed bed

A 1.5 g DAC packed bed (1 cm height) reactor was used to graft basic fuchsine onto the fibres, at pHs of 2, 4, 6, 8 and 10, to determine the optimal conditions for the highest mass transfer. Initially, the packed bed was conditioned [11] with aqueous solvent to ensure beds are well solvated, and remove fines and bubbles in the tubing. Basic fuchsine influent was then pumped in a continuous flow process at 50 mL min^{-1} and a valve is used to switch between water, dye and salt solutions

(**Scheme 4.1**). A dilution line was installed to ensure that the UV-Visible data acquired is within the dynamic range of calibration.

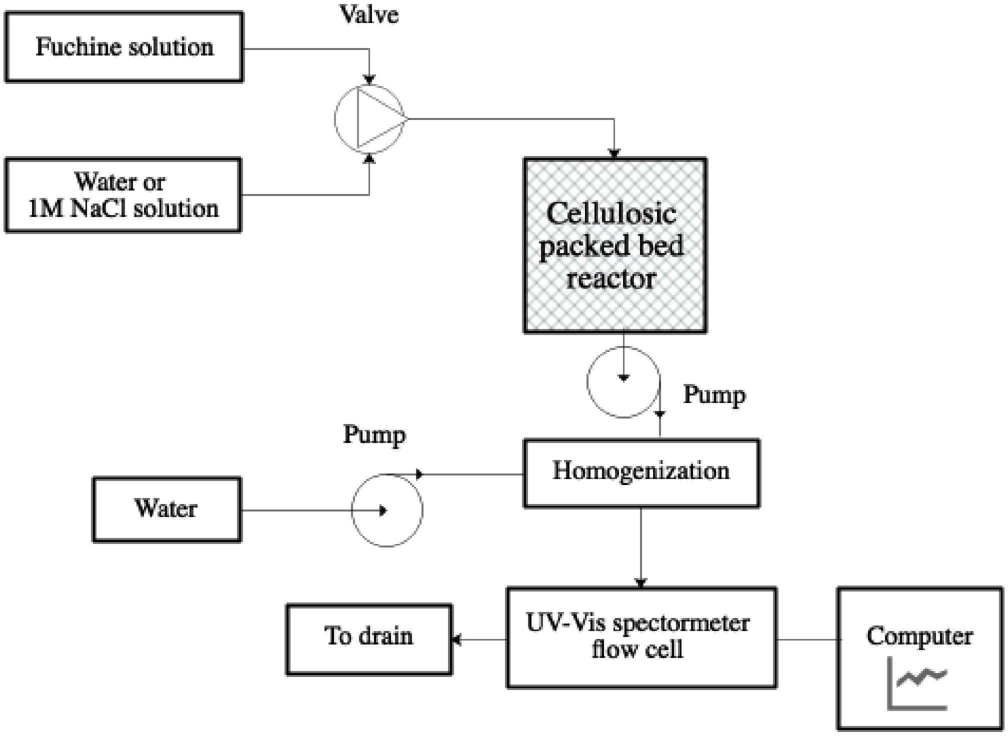

Scheme 4.1: Flow diagram for the experimental set-up of basic fuchsine adsorption onto cellulosic fibres to obtain BTCs

4.3.4 Qualitative and quantitative sample analysis

Quantitative determination of aldehyde groups (–CHO) was achieved using an oxime titration method [54, 55]. A 1% w/w sample of DAC was solubilized at 80 °C for 6 hours, then cooled to room temperature and non-fibrillated fibres were separated using a 20 μm pore size nylon filter. An aliquot was obtained to determine the dry mass percent, after drying to a constant weight at 50 °C. Another aliquot was used for a titration to measure –CHO content on the fibres. The pH of the aliquot and 5% w/w $NH_2OH{\cdot}HCl$ solutions were adjusted to 3.5, independently. The oxime reaction (**Figure 4.2**) was initiated by mixing the solutions and the HCl produced was titrated against 10 mM NaOH by maintaining the pH at 3.5. The endpoint was established when there was no change in pH and –CHO content was calculated from *Equation 4.7* [56]:

$$A_{CHO} = V_{NaOH} \cdot N/m_{cel} \tag{4.7}$$

Here A_{CHO} is the aldehyde content (mmol g^{-1}), V_{NaOH} is volume of NaOH consumed during titration, N being the normality concentration of NaOH (eq. L^{-1}) and m_{cel} is the dry mass of cellulose.

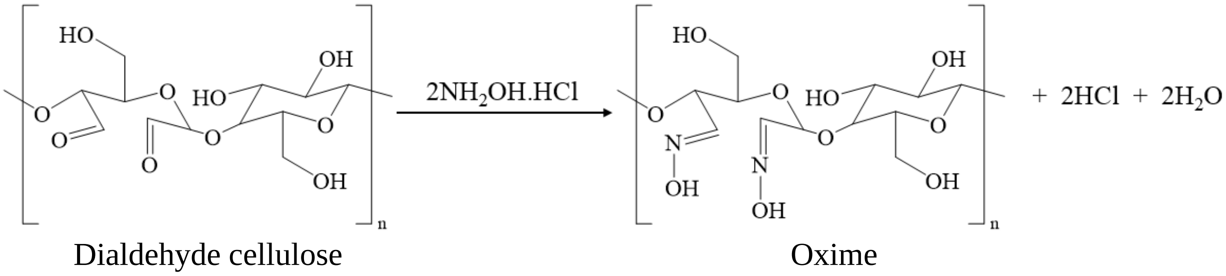

Figure 4.2: Oxime formation in titration of aldehydes with $NH_2OH \cdot HCl$ to release HCl [30].

Qualitative and quantitative analysis of basic fuchsine was conducted on a Varian TCA-Cary 300 UV-visible spectrometer. To obtain the absorption spectra for basic fuchsine, the instrument was operated in scan mode at a scan rate of 600 nm min^{-1} in a double beam mode with a slit band width of 1.5 nm. The determined maximum absorption wavelength (λ_{max}) for basic fuchsine was 544 nm (**Figure S4.1**) for all pH values and salt concentrations. This single point λ_{max} was used in quantifying basic fuchsine during the packed bed adsorption experiments. A five-point calibration curve (0 – 20 mg L^{-1}) was used and all statistical analysis performed using OriginPro® 2018 graphing software.

A 30% w/w sucrose solution inert tracer was used as a non-reactive and non-adsorbing component of the packed bed, according to the axial dispersion plug flow model, to determine the residence time distribution [44, 50]. This was done under the same conditions described in **Section 4.3.3** above and quantified using the refractive index at 589 nm and using a previously obtained calibration curve (0 – 50% w/w at 22.5 °C). The acquired fuchsine BTCs were subjected to a Langmuir type adsorption isotherm to obtain kinetics of adsorption.

4.3.5 Surface chemical properties

Cellulose, DAC and fuchsine-DAC samples were dried to a constant weight at 50 °C and used to acquire Fourier transform infrared (FTIR) and nuclear magnetic resonance (NMR) spectra for chemical characterization. Attenuated Total Reflectance (ATR)-FTIR vibrational measurements were conducted on a Bruker IR instrument equipped with a single bounce diamond ATR accessory and Opus software for peak analysis. After background noise subtraction, FTIR spectra were obtained by applying maximum force on solid samples positioned on an ATR crystal, by collecting and averaging 32 scans in a wavenumber range of 400 – 4000 cm^{-1} and 4 cm^{-1} resolution.

A Varian/Agilent VNMRS-400 Wide-bore spectrometer operated at a frequency of 100.5 MHz was used to acquire solid-state ^{13}C NMR spectra. Finely ground samples were packed in a 7.5 mm zirconium rotor and then spun at 14 kHz and acquired 48,000 transients using a contact time and recycle delay of 1 ms and 2 s, respectively. Spinning sidebands were suppressed using the TOSS sequence [57].

4.4 Results and discussion

4.4.1 Determination of aldehyde content via oxime titration

In DAC synthesis, the theoretical maximum –CHO content is 12.5 mmol g^{-1} of cellulose. The average –CHO determined was 10.8 mmol g^{-1}, representing an 86% conversion. It has been observed that increased conversion results in decreased fibre yield, due to dissolution of hemicellulose [30, 58]. Therefore, a 10.8 mmol g^{-1} oxidation provided a good balance between fibre yield and aldehyde functionalization. This DAC batch was subsequently used in basic fuchsine adsorption experiments on a PBR.

4.4.2 Packed bed reactor operation and data acquisition conditions

A sucrose seven-point linear calibration curve ($R^2 = 0.9967$), **Figure S4.2**, was used to establish the RTD for a non-adsorbing material (sucrose). The residence time was 1.0 minutes for cellulose and 1.1 minutes for DAC at a flow rate of 50 mL min^{-1}. Based on the total data acquisition time, this difference is insignificant. The Peclet numbers for cellulose and DAC were 40 and 43, respectively, with literature reporting Peclet numbers ranging between 30-50 for packed beds of cellulosic materials [43, 50].

A five-point calibration curve ($R^2 = 0.9999$), **Figure S4.2**, was used in quantifying basic fuchsine concentration before and during the adsorption process. The effect of pH, sodium chloride and fuchsine concentration on adsorption was studied and normalized BTCs are shown in **Figure 4.3**, **Figure** S4.3 and**Figure** S4.4, respectively. For cellulose, the adsorption observed can be attributed to ion exchange due to the presence of negative charge groups on hemicellulose and their corresponding counterions, to physisorption and to dye diffusion into the fibre wall and lumen. For DAC, adsorption at pH 4 (150 ppm dye concentration) had the longest breakthrough time (t_b), hence the highest amount adsorbed at t_b and dynamic equilibrium time (t_∞) (**Table 4.1**). This is attributed to the efficiency of the Schiff-base reaction, which is optimal at a pH range of 4-5 [59]. Consequently, the chemical adsorption process enhances the relationship between ion exchange, physisorption and chemical reactivity, thus improving dye fixation onto cellulosic fibres [60]. The adsorption of fuchsine depends strongly on pH: A Schiff base reaction is acid catalyzed, however, at pH values < 4, the amine is protonated rendering it unable to perform a nucleophilic attack on the carbonyl carbon and at pH > 6, there are insufficient protons.

Using the integral in *Equation 4.5*, the area between inert tracer and basic fuchsine BTCs represents the amount of particles deposited, or dye molecules adsorbed, on the packed bed (**Table 4.1**). For all adsorption values reported here, the residence time from the inert tracer is subtracted. The S-shape curve of the inert tracer is similar to an ideal plug flow which is represented by a vertical step-change wavefront. It has been observed that cellulose adsorbs basic fuchsine, commonly used as a staining agent [37]. The increased adsorption capacity in DAC, compared to cellulose (~3× more), is due to the presence of aldehyde functionality that provides active sites for chemical adsorption via imine formation.

The amount of dye adsorbed can be evaluated at any specified time. As the length of unutilized bed reduces, the number of active sites also reduces, this result in decreased capture efficiency, herein defined as the amount of dye deposited on the packed bed relative to the amount pumped per unit time. In this study, we determine the amount of dye adsorbed and removal percentage at breakthrough (t_b), midpoint (t_m) and dynamic equilibrium times (t_∞); an example of these times is shown in **Figure 4.3,** for the DAC pH 4 system. At time t_b there is a change in effluent concentration, t_∞ is the time to reach a plateau and t_m is intermediate of t_∞ and t_m. The BTCs indicate that the adsorption on cellulose has a steeper gradient (10.6 ppm min^{-1}) after t_b compared to the DAC packed bed (3.2 ppm min^{-1}). This suggest that since rates of chemisorption are lower (see **Section 4.4.5** below) in DAC, the initial ion exchange and physisorption attachments are necessary to increase the dye particles residence time to allow for chemisorption. Once the chemisorption takes places, a physisorption site becomes available again and the process repeats.

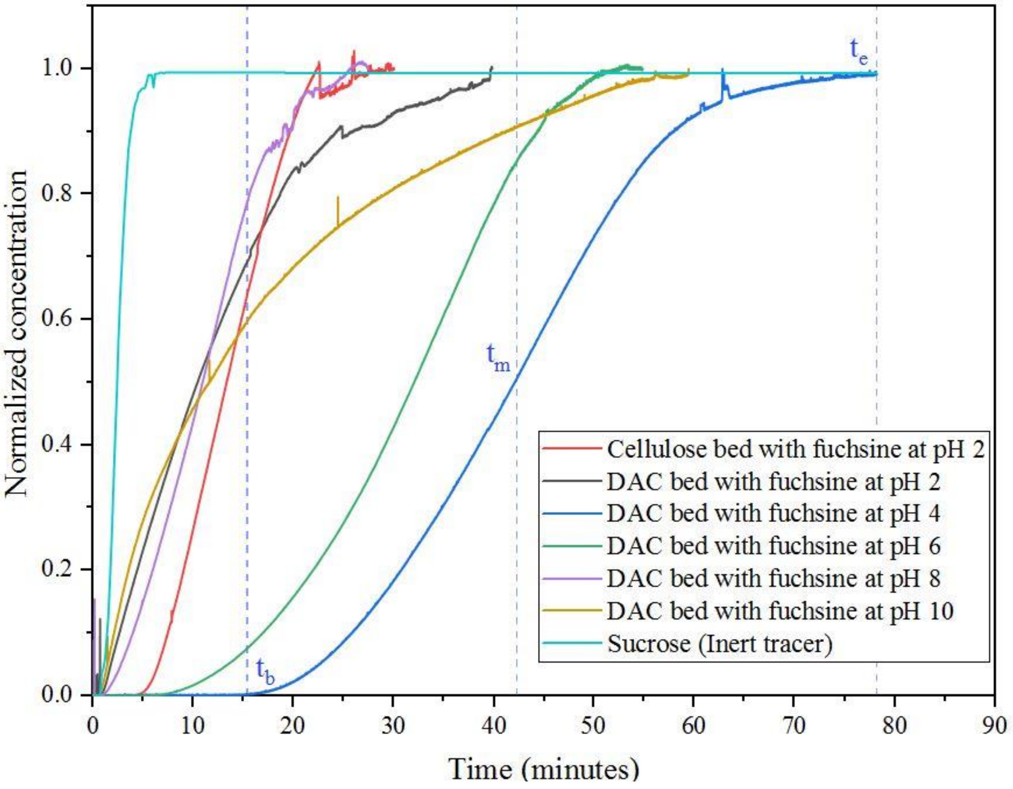

Figure 4.3: Normalized concentration BTCs for sucrose and basic fuchsine adsorption on cellulose and DAC (H = 1 cm and Q = 50 mL min^{-1}).

The kraft cellulose pulp used in these experiments, has about 12% hemicellulose [24] which contains carboxylic acid functional groups that provide the negative charge. The charge content of pulp was determined to be 0.07 mmol g^{-1} (**Figure S4.5**) using a conductometric titration method described by Yang *et al* (2012) [61]. A cationic dye ion exchange model has been developed using methylene blue and carboxyl groups in alginate gels containing carboxylated nanocrystalline cellulose [20], which led to an enhanced adsorption capacity [62]. Adsorption of fuchsine on kraft cellulose pulp and DAC is expected to follow this model as well. The maximum fuchsine adsorption capacity of 61 mg g^{-1} (**Table 4.1**) on cellulose is equivalent to a dye charge content of 0.18 mmol g^{-1}, indicating that about 40% of the dye is electrostatically bound via an ion exchange mechanism. The packed bed void volume of 0.87 accounts for about 0.002 mmol g^{-1} of dye resident in the bed. The charge content available on cellulose (0.07 mmol g^{-1}) indicates an excess of about 37 mg (0.11 mmol g^{-1}) of dye is physisorbed.

Table 4.1: Basic fuchsine adsorption on 1.5 g of cellulose and DAC using PBRs at t_b, t_s and t_e.

Material (pH)	**Cellulose (4)**	**DAC (2)**	**DAC (4)**	**DAC (6)**	**DAC (8)**	**DAC (10)**
Adsorption at t_b (mg)	27	0.5	124	49	2	1
Removal (%)	100	-	100	100	100	95
Adsorption at t_m (mg)	77	55	268	206	56	88
Removal (%)	84	72	87	88	77	49
Amount adsorbed at t_∞ (mg)	91	83	306	224	73	114
Adsorption capacity(mg/g)	61	56	204	150	49	76
Removal (%)	56	25	54	56	37	26

The ion exchange adsorption mechanism on cellulose was confirmed by displacing the unbound dye resident in the packed bed inter-fibre void volume with distilled water, followed by a 1M NaCl solution shown in **Figure 4.4**. The fuchsine displacement S-shape curves are similar to the mirror image of a sucrose (a non-adsorbing inert tracer) BTC. After displacing the dye in the void volume of cellulose, there is a linear dye desorption rate of 0.1 ppm min^{-1} (5×10^{-3} mg min^{-1}). Upon addition of 1M NaCl solution, a rapid release of the dye was observed. The baseline approaches zero quicker for DAC packed bed relative to the baseline for cellulose, taking about 1 hour. Additionally, dye is not released upon replacing water with a 1M NaCl solution in the DAC packed bed. These observations strongly suggest that the dye initially adsorbed physically and by ion exchange eventually becomes chemisorbed.

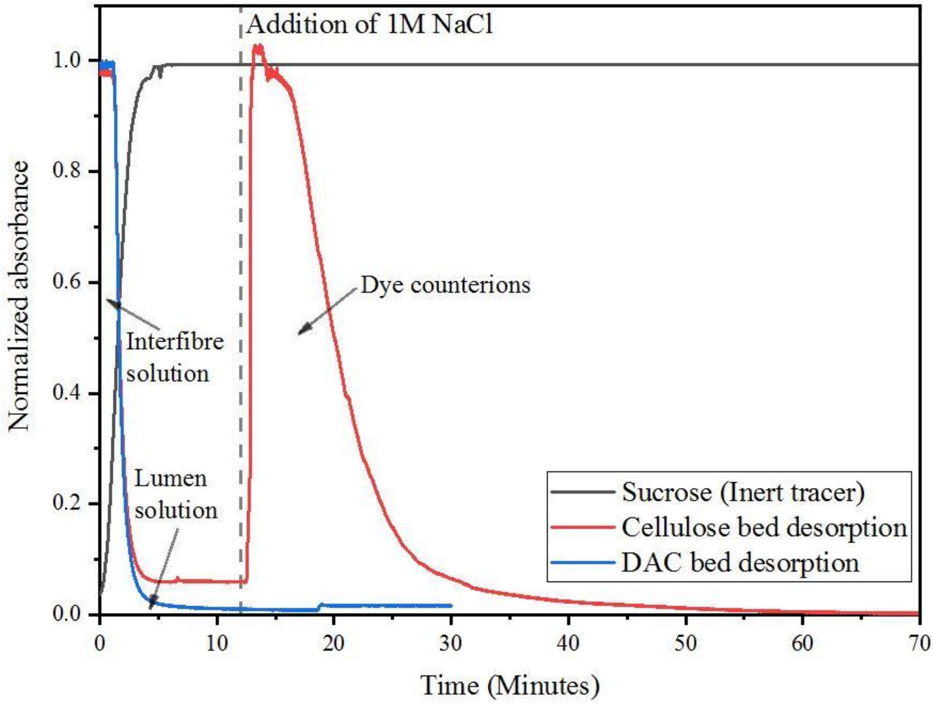

Figure 4.4: Basic fuchsine desorption. At time = 0 minutes, distilled water is added to displace unbound dye resident in packed bed, which is completed in about 4 minutes, after which physisorbed ions very slowly are being released. At t = 12 min, 1M NaCl is added, which triggers

the release of dye counterions. Physisorbed ions continue to be released up to about 1 hour. For comparison, a sucrose breakthrough curve is shown as well.

On cellulose beds, once distilled water is displaced by a NaCl solution, there is a sharp increase in fuchsine concentration in the effluent followed by a gradual decrease. The area below the curve was used to determine the amount of dye desorbed by a salt solution. Increasing the time between distilled water and 1M salt solution addition (**Figure S4.6** and **Figure S4.7**) results in a lower amount of salt-induced dye release. The highest and lowest amounts of dye desorbed by salt solution were 51 mg g^{-1} (0.15 mmol g^{-1}) and 21 mg g^{-1} (0.06 mmol g^{-1}) for shorter and longer times, respectively. Salt increases the desorption rate constant for the physisorbed dye and a large excess of Na^+ triggers a quick release of the counter ions, approaching charge stoichiometry at longer times. Therefore, the order of dye removal from cellulose packed beds is void volume dye displacement, followed by the release of physisorbed dye. Dye counterions are only released upon the addition of salt, which also accelerates the desorption of physisorbed ions. In DAC packed beds, no dye is released upon NaCl addition, because at the time of salt addition all ions are chemisorbed on the DAC fibres.

After the adsorption process, the packed beds (cellulose and DAC) were dried at room temperature and atmospheric pressure without washing nor purification. It was observed that the dye adsorbed on cellulose is released upon dispersion in distilled water or acetone and stains the glassware and materials it encounters. However, upon dispersion in water or acetone, the DAC-based packed beds do not release the dye and therefore work as an anti-stain. Dry basic fuchsine dye crystals are dark green and turn red in aqueous solution. It was also observed that the cellulose-dye product retains the red color in both dry and wet forms, while the chemisorbed DAC-dye imine becomes purple. Photographic images are shown in **Figure S4.8**. This change, also reflected in UV-Vis spectra (**Figure S4.9**), can be attributed to extension in conjugation due to the formation of a chemical bond, which affects the π-π and σ-π energy transitions, similarly observed by Heinemann (1970) [40].

4.4.3 Effect of sodium chloride in fuchsine dye solution

Adsorption of fuchsine solution (150 ppm) at pH 4 and salt concentrations of 0.0, 0.5 and 1.0 M was examined and shown in **Figure S4.3**. In the presence of both the Na^+ and fuchsine, dye adsorption is reduced because Na^+ replaces fuchsine dye as counterions, hence lower adsorbed amounts are observed at 0.5 M NaCl concentration for both cellulose and DAC. The steeper slope (10.5 ppm min^{-1}) at breakthrough for DAC at 0.5 M NaCl, relative to DAC (3.2 ppm min^{-1}) at 0 M NaCl, strongly indicates the significance of the initial ion exchange attachment prior to covalent bond formation, in achieving higher adsorption amounts.

The 1 M NaCl dye solution adsorption on DAC outperforms the other packed beds (**Table 4.2**), however, it was observed that the dye coagulates at the packed bed/dye solution interface. At 1M NaCl concentration, fuchsine is flocculated although the flocs are broken up during stirring of the dye solution. The salt leads to bed contraction in DAC, resulting in a layer of unstirred salt/fuchsine solution on top of the bed leading to fuchsine aggregation. This in turn leads to the deposition of a layer of aggregated dye on top of the bed. This is not seen in beds of cellulose, which were slightly compressed when forming a 1 cm high bed, which explains the small difference in Peclet numbers for cellulose and DAC beds. When cellulose beds shrink due to salt, the shrinking compensates for the initial compression and the cellulose continues to fill the whole bed and no aqueous layer of dye is formed on top of the bed.

Table 4.2: Adsorption of fuchsine with concentration of 150 ppm at pH 4 and varying NaCl concentration on 1.5 g cellulose and DAC.

Material **[NaCl] M**	**Cellulose [0]**	**Cellulose [0.5]**	**Cellulose [1.0]**	**DAC [0]**	**DAC [0.5]**	**DAC* [1.0]**
Amount adsorbed at t_∞ (mg)	91	66	264	306	243	733
Adsorption capacity at t_∞ (mg/g)	61	44	176	204	162	489
Removal (%)	56	46	29	54	72	98

*The DAC [1.0] adsorption and efficiency is determined at the time experiment was terminated (100 minutes) since the plateau could not be reached.

Upon drying DAC fibers containing aggregated fuchsine on top of the bed, the dye retains its dark green color. In contrast, the bed interior was purple, an indication that Schiff base reaction happens even under saline conditions. This demonstrates that salt allows the recovery of the dye non-destructively and in a more concentrated form, therefore, the DAC packed bed reactor can potentially be used as a water purification method.

4.4.4 Effect of basic fuchsine concentration

Adsorption of fuchsine solution at 50, 100, 150, 250 and 500 ppm, at pH 4 and without salt addition on DAC packed beds was studied (**Figure 4.5**). Adsorbed dye amounts increased up to 204 mg g^{-1} at 150 ppm because of a balanced contribution of all active sites involved in ion exchange, physi- and chemisorption. Above 150 ppm, a decreasing trend was observed. Since the adsorption driving force relies on ion exchange, physi- and chemisorption with a higher ion exchange adsorption rate

(See **Section 4.4.5** below), a longer residence time is required for chemical attachment. Therefore, at concentrations above 150 ppm, an apparent plateau in the BTCs is quickly reached since there was insufficient time for chemisorption to occur. This results in an apparent reduction of adsorption capacity at higher concentrations, although chemisorption eventually happens at longer residence times. This effect manifests itself in the decreased breakthrough time as the dye concentration increases, as shown in **Figure S4.4**.

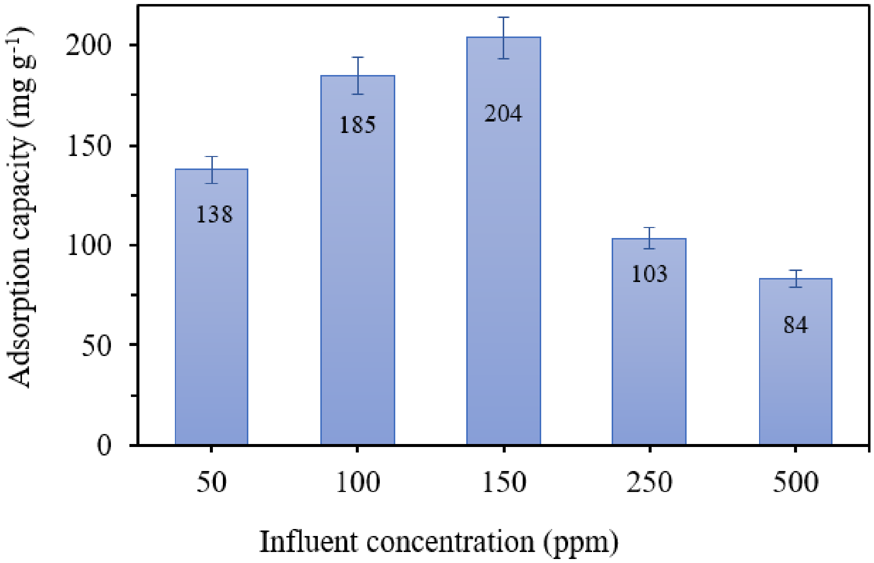

Figure 4.5: Effect of feedstock concentration on adsorption capacity of basic fuchsine on DAC.

A wide range of dye adsorption studies on cellulose fibres and nanocellulose have reported removal capacities in the range of 1.7 – 683.0 mg g^{-1} [60, 63] and 101 – 2,200 mg g^{-1} [20, 64], respectively. Our value for cellulose fibres, 61 mg g^{-1}, is within this range. Higher removal capacities are due to dye flocculation. There are limited studies on basic fuchsine adsorption on modified cellulose which had a range of 2.2 – 458.8 mg g^{-1} [60, 65, 66]. The highest dye removal of 489 mg g^{-1} (for flocculated dye) is comparable with previous studies, while chemisorption capacity of 204 mg g^{-1} falls within that range. However, incorporating chemisorption is advantageous in preventing desorption. Leaching of dyes from materials in textiles and water treatment is of great environmental concern. A high adsorption capacity is achieved when cellulose nanomaterials are used due to increased surface area and multi-functionalization [67], which is desirable in environmental applications. Therefore, nano-dialdehyde cellulose could potentially have a higher adsorption capacity for amine-functionalized dyes than DAC fibres. However, DAC fibers' lower cost would be advantageous in textile applications since a lower amount of adsorbed dye is needed for coloring.

The highest chemisorbed dye (204 mg g^{-1}) corresponds to about 6% of the aldehyde groups available. The low adsorption capacity could be due the blockage and inaccessibility of the smaller fiber pores which might prevent fuchsine dye diffusion into pores < 4 nm, due to blocking of pores at the entrance. Fuchsine dye has a diameter of about 1.2 nm [68] and can only freely enter pores > 4 nm. Alince and van de Ven (1997) [69] have shown that the pore size distribution in kraft fibres is bimodal with small nano-size pores and large pores of about 75 nm. The total internal surface area is about 300 m^2 g^{-1}, whereas the surface area of the large pores is about 15 m^2 g^{-1}, representing about 5% of the total surface area. Therefore, adsorption likely takes place mainly in the larger pores and the nanopores are blocked.

4.4.5 Adsorption kinetics

The equilibrium constant (K) estimated for individual BTCs is determined from Langmuir kinetics using *Equation 4.4* above, in which ρ_c is 1.5 kg dm^{-3}, obtained from Al-Jabari *et al.* (1994) [44], and ε is 0.87 ± 0.05, experimentally determined by the displacement method [70]. At steady-state, K is the ratio of adsorption and desorption coefficients (= $k_{adsorption}/k_{desorption}$). Therefore, an increase in K is due to particle accumulation in the packed bed and/or a reduced rate of desorption (**Table 4.3**). For cellulose fibres relying on ion exchange and physisorption only, the equilibrium constant is lower and is of a similar order of magnitude as observed for other cellulosic materials [44, 49].

Table 4.3: Equilibrium constants for deposition of fuchsine dye on cellulosic fibres at various packed bed operating conditions.

System	**pH**	**[NaCl] (M)**	**Fuchsine [n$_o$] (ppm)**	**N$_{max}$ (mg/g)**	**K ($g_{fuchsine}/g_{fibre}$)**	**k_{ads} (min^{-1})**	**k_{des} (min^{-1})**	**R^2**
Cellulose	4	0	150	61	51	0.17	0.0034	0.9884
DAC#	2	0	150	56	42	-	-	-
DAC	4	0	150	204	570	0.05	9×10^{-5}	0.9738
DAC	6	0	150	150	306	0.08	3×10^{-4}	0.9905
DAC#	8	0	150	49	33	-	-	-
DAC#	10	0	150	76	79	-	-	-
Cellulose#	4	0.5	150	44	26	-	-	-
Cellulose*#	4	1.0	150	176	425	-	-	-
DAC#	4	0.5	150	162	359	-	-	-
DAC*#	4	1.0	150	489	3271	-	-	-
DAC	4	0	50	138	87	0.02	2×10^{-4}	0.9897
DAC	4	0	100	185	312	0.03	1×10^{-4}	0.9779
DAC#	4	0	250	104	244	-	-	-
DAC#	4	0	500	84	318	-	-	-

*For cellulose and DAC systems at 1 M NaCl concentration, the high equilibrium K value is due to coagulation of the dye, and as noted above, the DAC system plateau could not be reached.

#In many cases, the BTCs could not be fit to pseudo-first order kinetics, and hence no k_{ads} and k_{des} values are reported for them.

The 10-fold increase in the equilibrium constant for DAC can be attributed to chemisorption due to the formation of an imine which is not easily susceptible to detachment at the experimental pH. This also follows from observing the product after drying, without washing or purification: the ability of the dye to detach and stain was eliminated when DAC was redispersed in distilled water. This observation suggests that dye molecules initially attached by ion exchange and physisorption become chemisorbed with time. This is further confirmed by the change in UV-vis spectra of the free and bound dye (**Figure S4.9**), also indicating that the dye initially bound by ion exchange and physically eventually becomes covalently attached. The red shift of the peak at 544 to 568 nm and the appearance of a major peak at 253 nm, after formation of a Schiff base, has also been reported by Heinemann (1970) [40].

Pseudo-first order kinetics (*Equation 4.6 above*) was used to determine the rates of adsorption (k_{ads}) under the packed bed operating conditions (**Figure S4.10**). It was observed that charge primarily influenced the dye adsorption, hence a high k_{ads} value for cellulose was observed. This results in shorter breakthrough times and a quicker rate to reach the plateau, as the ion exchange binding sites deplete. For DAC packed beds, exhibiting longer breakthrough times, covalent binding becomes the major driving force, in addition to ion exchange and physisorption. Ion exchange and physisorption on DAC occur first and thereafter the attached molecules become chemisorbed; therefore, chemisorption is the rate determining step. This proposed mechanism is shown and discussed in Section 3.7, **Scheme 4.2** below. Although the covalent attachment has lower k_{ads}, the rate of k_{des} is significantly reduced, which is important for materials with a dye-containing product, such as textiles. Therefore, considering that the rates of chemical adsorption are low, it would be better for DAC fibres to apply the dye prior to spinning of textile filaments. This would maximize dye fixation, thereby minimizing pollution due to dye release.

Yang *et al.* (2016) [70] observed that increasing the ionic strength results in dye aggregation, and Wu and Andrews (2020) [71] concluded that by increasing the Na^+ concentration, Na^+ ions compete with dye ions for binding sites. This combined effect was observed in fuchsine adsorption on cellulose and DAC as it resulted in altering the shape of the adsorption BTCs. Therefore, in the case of high salt concentrations causing dye aggregation, the major mechanism of dye removal is via filtration, resulting in longer breakthrough times. At low salt concentrations without aggregation, Na^+ ions are competing counterions. The displacement of fuchsine with salt results in short breakthrough times (**Figure S4.3**). Hence, the data could not be fitted to a pseudo-first order kinetic model as the kinetics is much more complex than pseudo- first or -second order [72].

4.4.6 Surface chemical and physical properties

4.4.6.1 Characterization by infrared spectroscopy

Qualitative determination for oxidative functionalization was performed on unmodified cellulose, DAC and fuchsine-DAC using FTIR spectroscopy and variations in spectra are shown in **Figure 4.6**. The broad peak at about 3300 cm^{-1} is due to –OH stretching affected by hydrogen bonding, with corresponding bending modes at 1328 cm^{-1}. C–H stretching, scissoring and CH_2–CH_2 stretching vibrational modes are observed around 2925, 1428 and 1018 cm^{-1}, respectively. The characteristic C=O stretch is located at 1728 cm^{-1} with the associated asymmetric stretching for hydrated –CHO and hemiacetal groups at 877 cm^{-1}, similar to peak interpretations by Conley *et al.* (2016) [53], Zeng *et al.* (2017) [31], and Koshani *et al.* (2018) [57].

The fuchsine-DAC spectrum shows the disappearance of the C=O stretch (1728 cm^{-1}), with a small residue peak left, indicating that aldehyde groups have reacted with fuchsine. The residual peak implies that not all the -CHO groups are reacted, due to inaccessibility of the smaller pores (see **Section 4.4.4** above) and/or steric hinderance after addition of rigid aromatic rings. The peak at 877 cm^{-1} indicates that the residual -CHO still form hemiacetals upon drying of the samples. Formation of a Schiff base with diamines results in broadening of the peak between 3000 – 3680 cm^{-1} due to additional hydrogen bonding. In addition, the peak at 1586 cm^{-1} is for C=N stretch in conjugated systems which is complemented by C=C at 1515 cm^{-1} due to aromatic rings vibrations. The primary amine (N–H) out of plane bending modes are expected around 800 – 650 cm^{-1} [73], and the spectra shows no evidence of residual primary amines. From the various assignments of the FTIR peaks, we can conclude that fuchsine dye was successfully chemisorbed on DAC fibres.

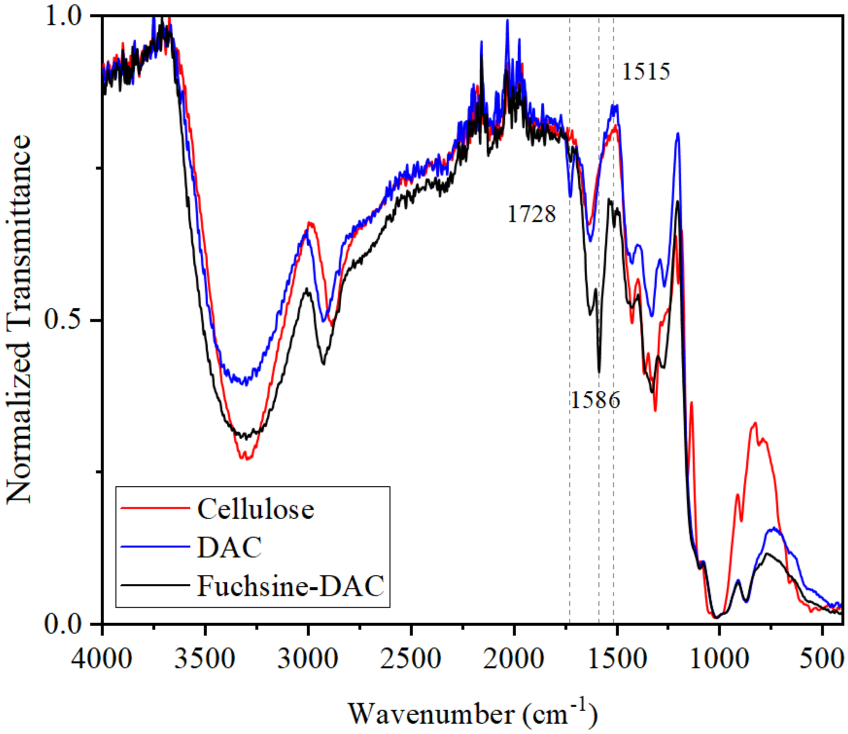

Figure 4.6: FTIR spectra of unmodified and modified cellulose. Fuchsine-DAC spectrum obtained after breakthrough experiment with fuchsine concentration of 150 ppm at pH 4.

4.4.6.2 Characterization by NMR spectroscopy

The solid-state ^{13}C NMR spectra for unmodified cellulose, DAC and the packed bed product of fuchsine-DAC (150 ppm at pH 4) are shown in **Figure 4.7**. The cellulose spectrum shows the characteristic chemical shifts of D-glucopyranoside unit in the range 60 – 110 ppm and peaks distinctively assigned according to Koshani *et al*. (2018) [57]. D-glucopyranose ring-opening due to periodate oxidation results in peak shape changes within the same region. The –CHO shift is expected to be in the range 185 – 220 ppm [73], and the absence of this peak has been attributed to self-assembly of DAC into hemiacetals [30, 74], or may not have been observed since measurements are typically done up to 200 ppm.

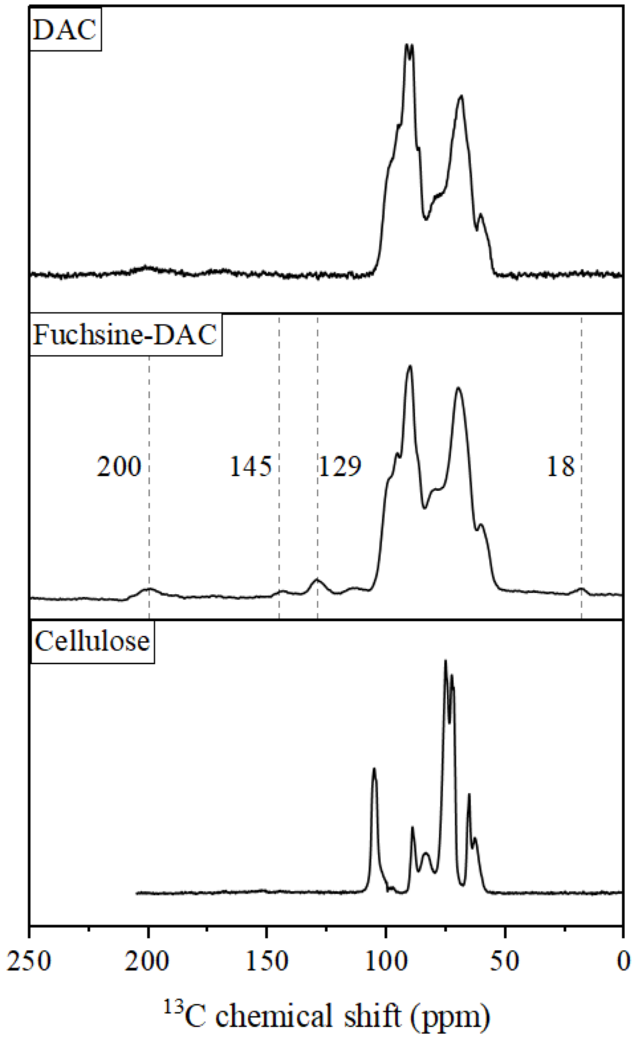

Figure 4.7: ^{13}C solid-state NMR spectra of unmodified cellulose, DAC and fuchsine-DAC product from packed bed experiment.

A minor peak at 200 ppm was observed, confirmed by computational calculations, which predict a peak at 202 ppm [75, 76] in both the DAC and fuchsine-DAC spectra, which can be attributed to

–CHO functionalization. The presence of the peak at 200 ppm demonstrates that the Schiff base reaction does not go to completion which could be due to blocking of nanopores and/or steric hinderance, as discussed above. The –C=N, –C=C on conjugated ring and $–CH_3$ appear at 145 <149>, 129 <132> and 18 <17> ppm, respectively, with values in <brackets> representing theoretical predictions.

4.4.6.3 Solubility of DAC and fuchsine-DAC product at 80 °C

Cellulose is insoluble in H_2O, even at elevated temperatures. However, DAC is > 99% soluble at 80 °C, forming a thermodynamically stable solution, which does not precipitate upon cooling. This is attributed to hydrogen bonding disruption and formation of a more flexible polymeric chain, due to the D-glucopyranose ring-opening. After the reaction between fuchsine and DAC on packed beds, the product was heated at 80 °C for 6 hours and the solubility was only ~30%. The reduction in solubility is due to crosslinking of DAC fibres by the triamine dye. Furthermore, the heat does not break the Schiff base bond, as observed in the UV-vis spectrum of the supernatant of the solubilized fuchsine-DAC solution (**Figure S4.9**). The supernatant had a faint purple colour and does not stain glassware; therefore, its anti-stain properties could be explored further.

4.5 Proposed fuchsine adsorption mechanism on dialdehyde cellulose

Overall, considering the chemical composition of kraft cellulose as the starting material and the fuchsine as a cationic dye, it was observed that adsorption happened via ion exchange due to carboxylic acid groups present in hemicellulose and physically onto the walls of the pores and lumen due to van der Waals forces and/or hydrogen bonding. Upon aldehyde functionalisation of cellulose, adsorption is achieved via imine bond (–C=N) formation, in addition to ion exchange and physisorption, although at long resident times ion exchanged and physisorbed dye eventually chemisorbs. Therefore, the initial attachment is fast and critical in ensuring a longer resident time to form an imine in a continuous flow experiment. Hence the proposed mechanism, schematically shown in **Scheme 4.2**, is such that ion exchange and physisorption are occurring first followed by chemisorption. This resulted in a reduction of adsorption rates from which we can conclude that chemisorption is the rate determining step. Additionally, since the Schiff base reaction is irreversible under these conditions, the desorption rates are significantly reduced.

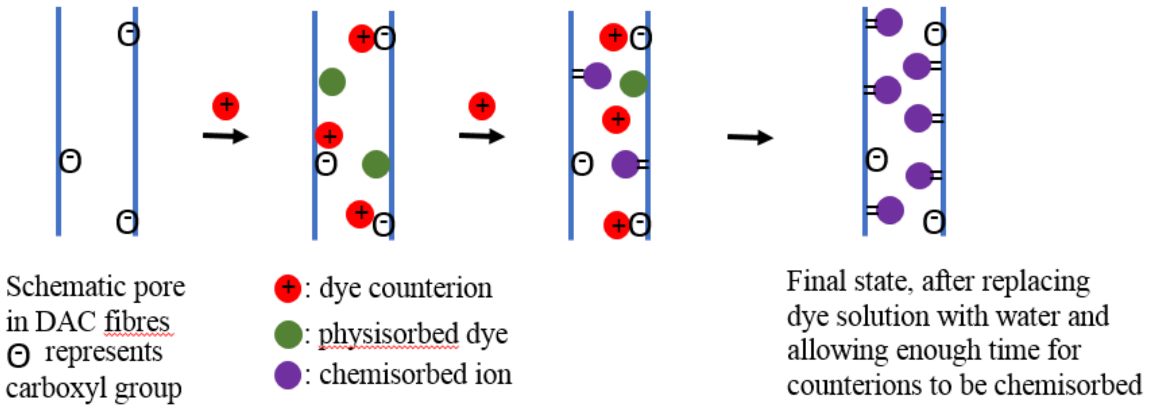

Scheme 4.2: Proposed mechanism of chemisorption of basic fuchsine dye on dialdehyde cellulose fibres, via ion exchange and physisorption, followed by a Schiff base reaction.

4.6 Conclusions

Dialdehyde cellulose (DAC), with aldehyde content of 10.8 mmol g^{-1}, was used to prepare packed beds with a height of 1 cm and a Peclet number of 43. The packed beds were used in basic fuchsine dye adsorption and breakthrough curves were measured. The adsorption study was conducted at various dye influent conditions while maintaining the flow rate at 50 mL min^{-1}. The formation of a Schiff base was confirmed by FTIR and ^{13}C-NMR spectrometry with characteristic peaks at 1586 nm and 145 ppm, respectively.

Using Kraft pulp cellulose as a control, it was observed that ion exchange and physical adsorption has the highest rates of adsorption (0.17 min^{-1}) whereas desorption was slow (0.0034 min^{-1}), resulting in an adsorption capacity of 61 mg g^{-1}. Dye adsorption and removal mechanisms on DAC included ion exchange, chemical and physical adsorption. Dye influent at pH 4 had the highest average adsorption capacity of 204 mg g^{-1}, with adsorption and desorption rates of 0.05 and 9×10^{-5} min^{-1}, respectively. The DAC-fuchsine, produced by chemisorption, prevents the dye from leaching; therefore, it is best suited for application in textiles or anti-stain materials. The highest dye removal capacity was ~ 490 mg g^{-1} when the dye concentration is 150 ppm at pH 4 with a salt concentration of 1M. The mechanism of dye removal in this case was filtration due to aggregation of the dye upon contact with the packed bed, therefore, these operating conditions would be best suited for dye reclamation or water purification.

4.7 Acknowledgements

The authors acknowledge funding support by a NSERC SRN on Green Fibers and a NSERC SPG (506303-17), supported by FPInnovations. User fees were partly covered by the FRQNT Centre for Advanced Materials (QCAM/CQMF).

4.8 Supplementary information for Deposition of basic fuchsine on packed beds of dialdehyde cellulose (DAC) fibres

*Martin Sichinga, Roya Koshani and Theo G. M. van de Ven**

Department of Chemistry, Pulp and Paper Research Centre, McGill University, 3420 Rue University, Montreal, Quebec, H3A 2A7, Canada

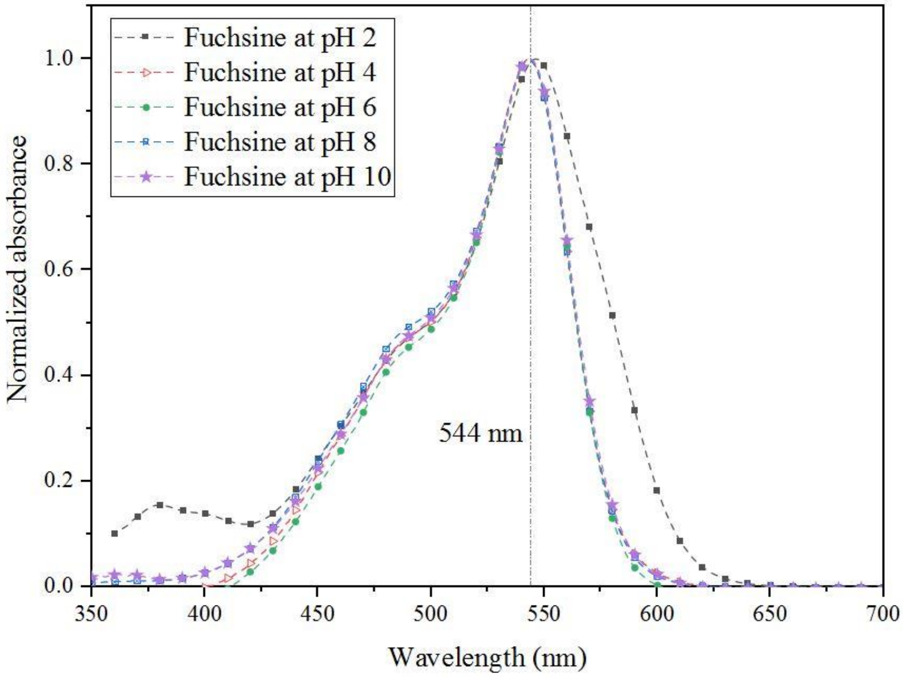

Figure S4.1: UV-visible absorption spectra of basic fuchsine as a function of wavelength at various pHs.

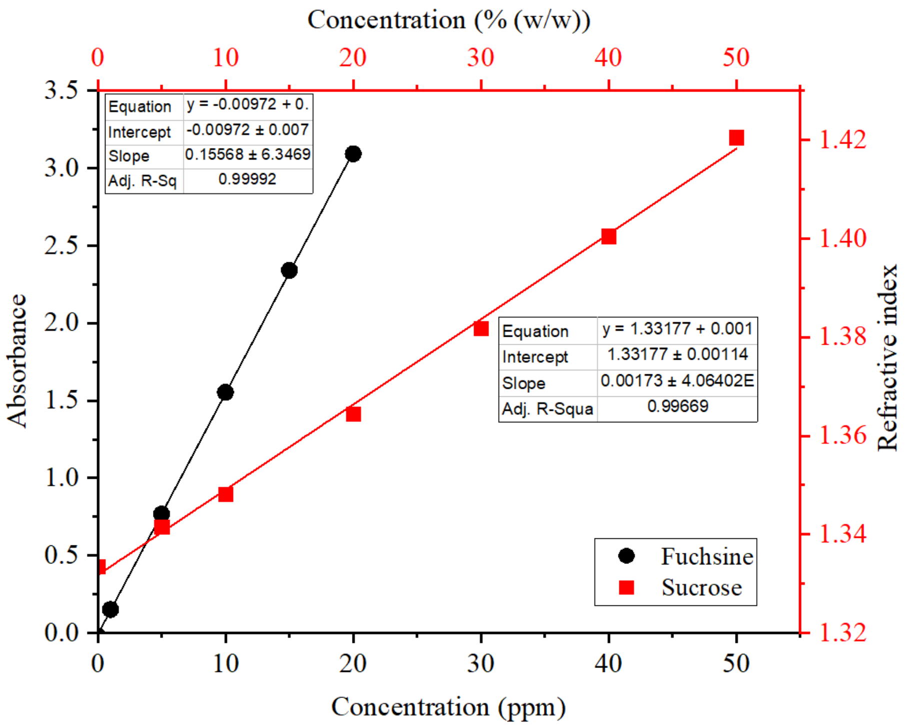

Figure S4.2: UV-Vis (544 nm) calibration curve for basic fuchsine and refractive index (589 nm at 22.5 °C) calibration curve for sucrose.

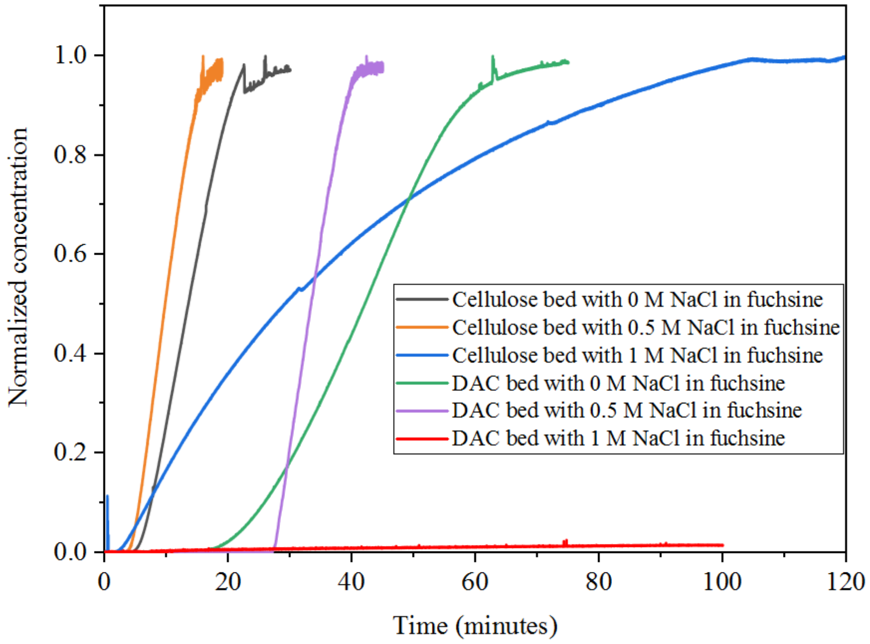

Figure S4.3: Effect of NaCl concentration on adsorption of basic fuchsine (150 ppm) on cellulose and DAC packed bed reactors.

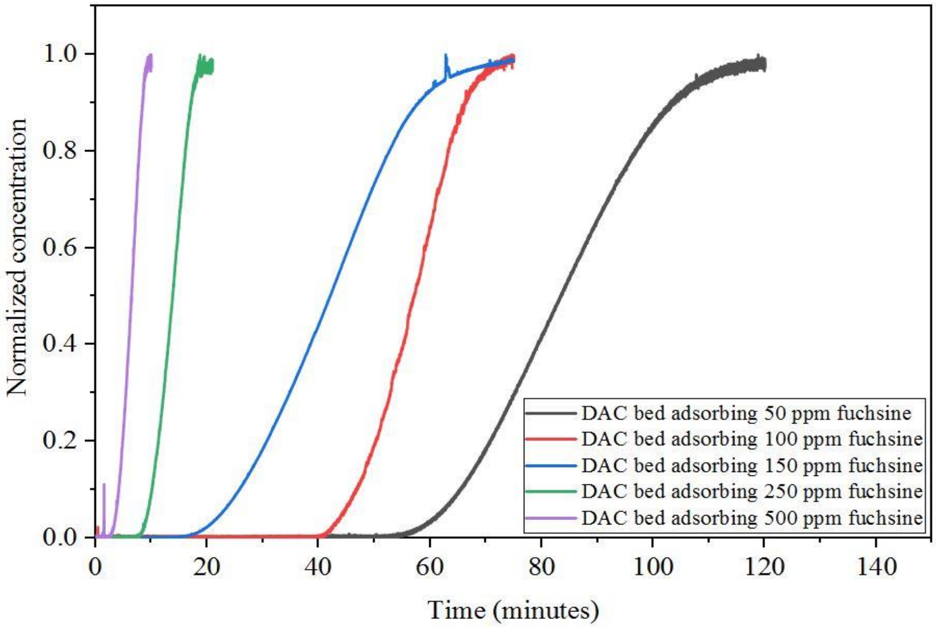

Figure S4.4:Effect of basic fuchsine concentration on adsorption on DAC packed beds.

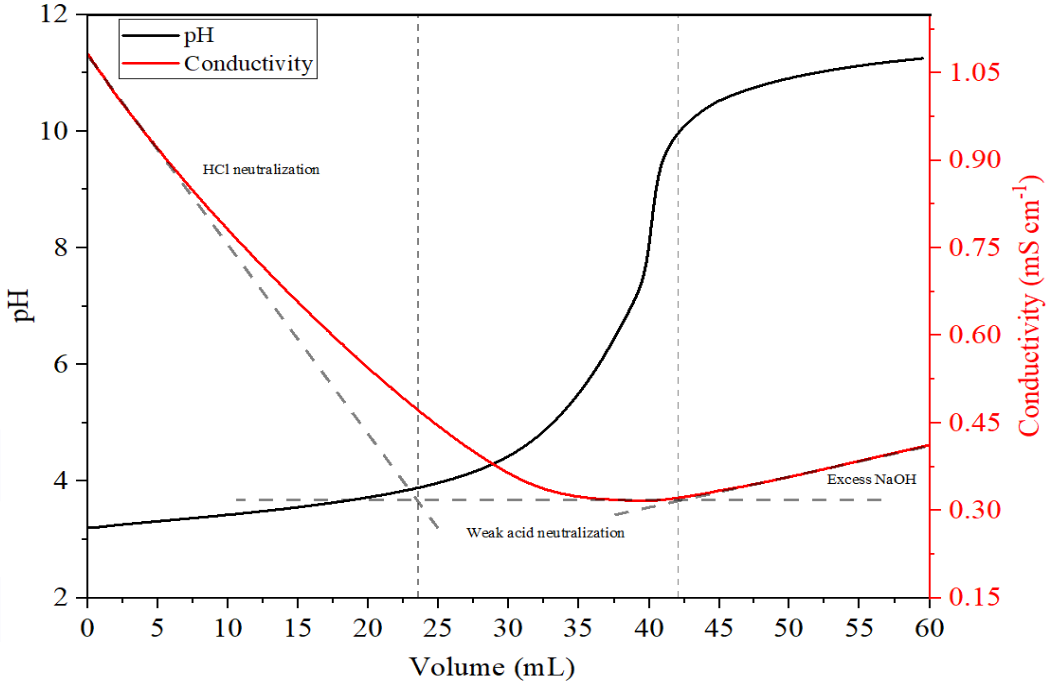

Figure S4.5: Conductivity and pH titration curves of 2.83 g of unmodified kraft cellulose pulp for the determination of carboxylic acid charge content due to hemicellulose using 10 mM NaOH.

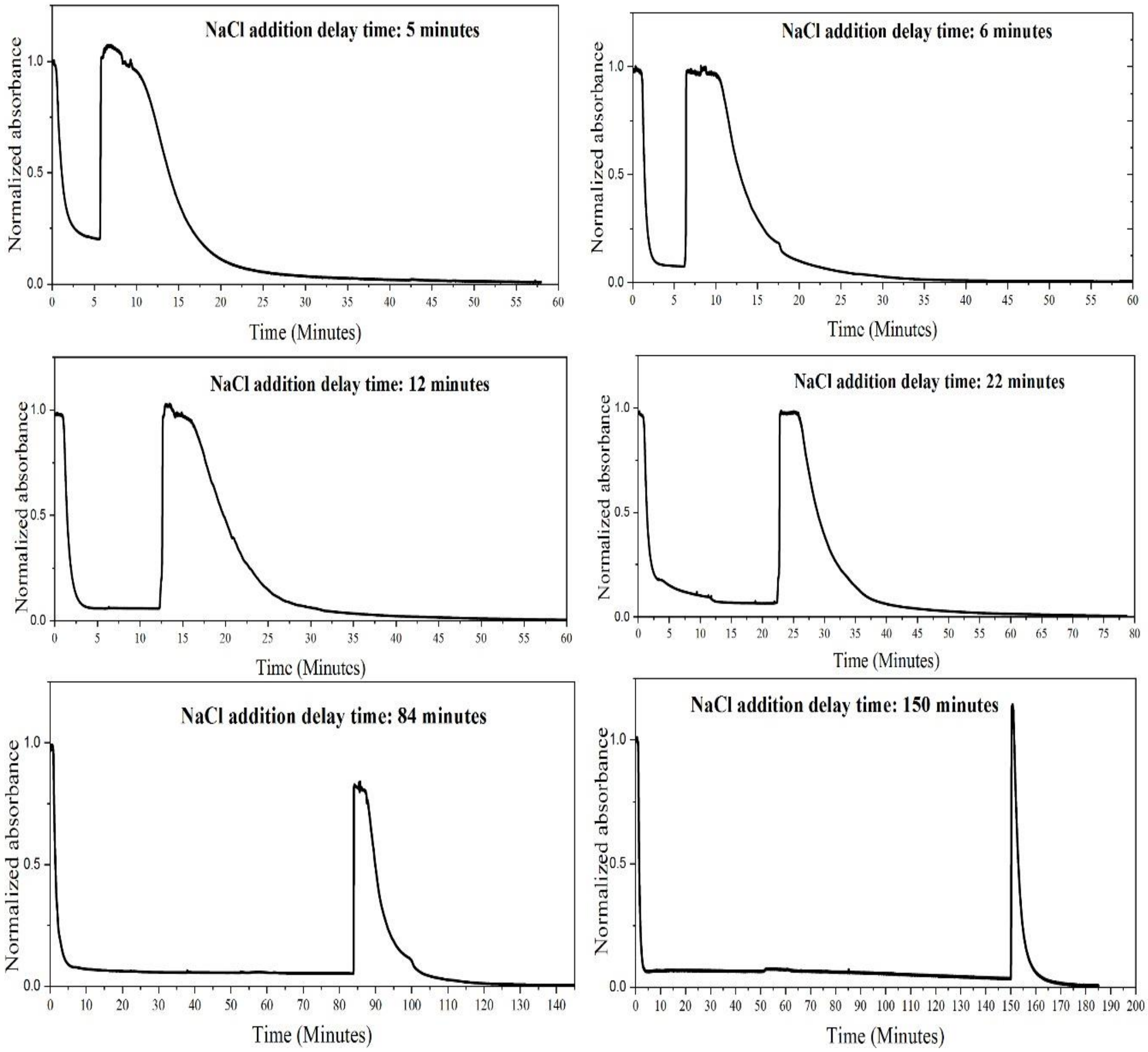

Figure S4.6: Basic fuchsine desorption from cellulose packed beds using distilled water, followed by a 1M NaCl solution after various delay times.

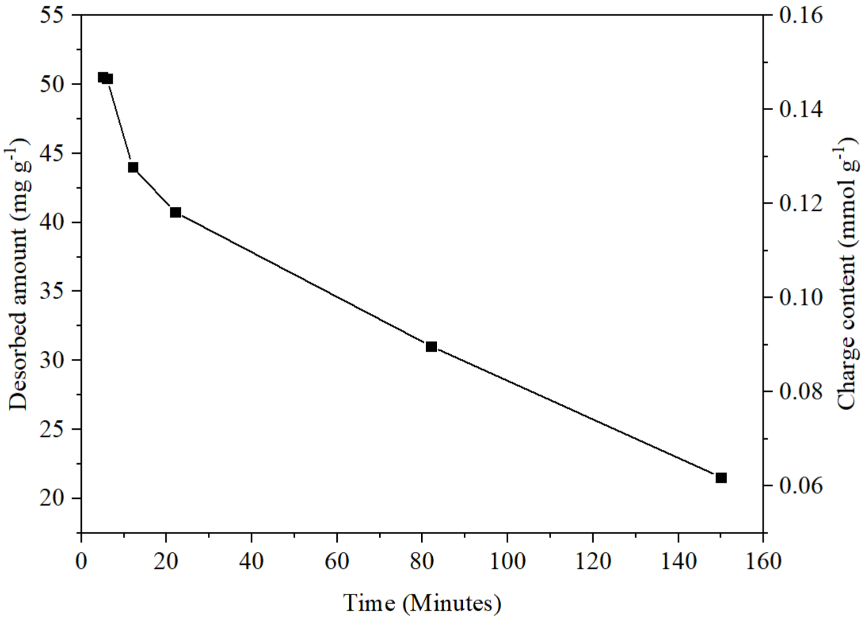

Figure S4.7: Fuchsine amounts desorbed from cellulose packed beds after various delay times between distilled water and 1M NaCl solution addition. Also shown is the charge content of the fibers, assuming all released ions were charge stoichiometrically adsorbed counterions.

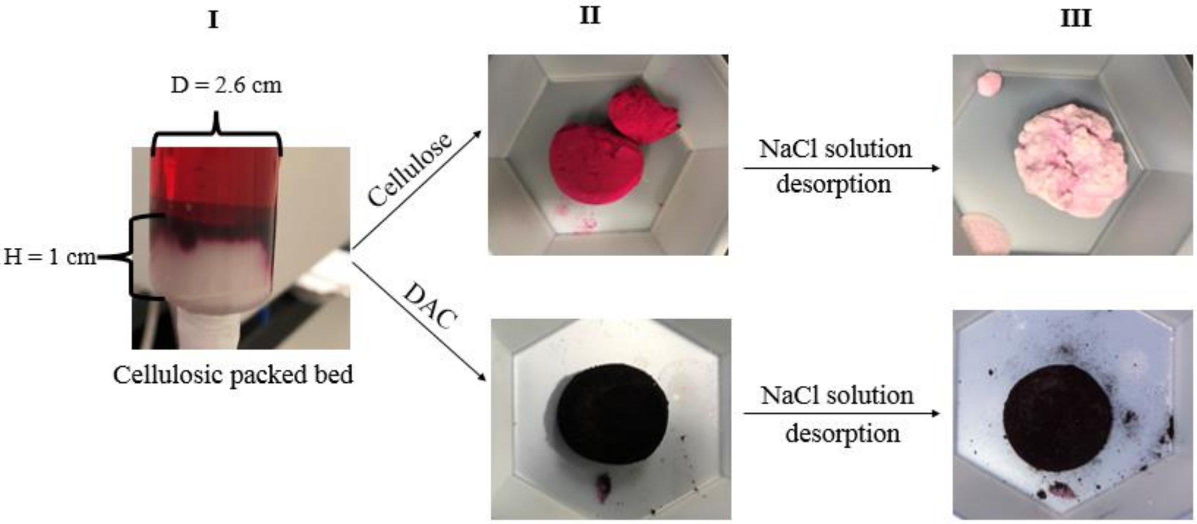

Figure S4.8: Photographic images of the physical appearance of cellulose and DAC packed beds during and after fuchsine dye adsorption. I: Cellulose and DAC fibers are white in color and shows the solution front during dye adsorption. II: The samples were air dried without purification, cellulose retains the red color whereas DAC forms a dark purple product. III: Using 1M NaCl solution, the dye is desorbed from cellulose due to physisorption and ion exchange mechanisms, while there is no change in the DAC product due to chemisorption.

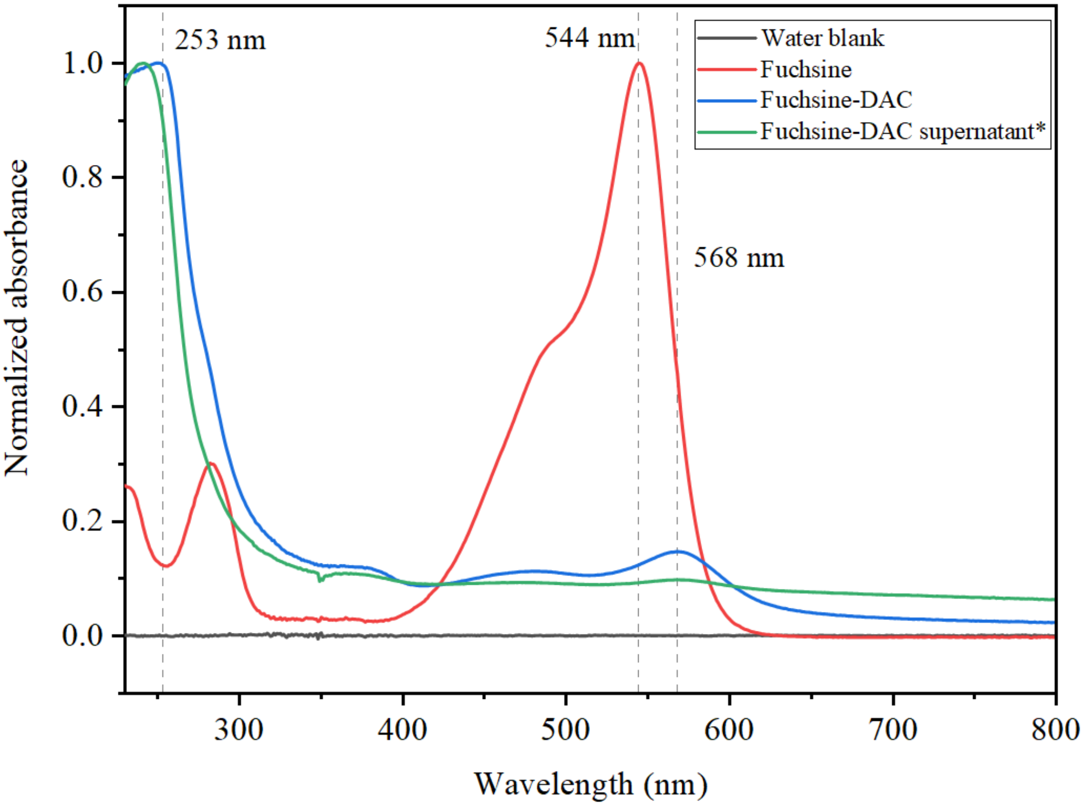

Figure S4.9: UV-vis scan of re-dispersed fuchsine-DAC product of packed bed reaction, without sample purification. *Fuchsine-DAC supernatant measured after heating the product at 80 °C for 6 hours.

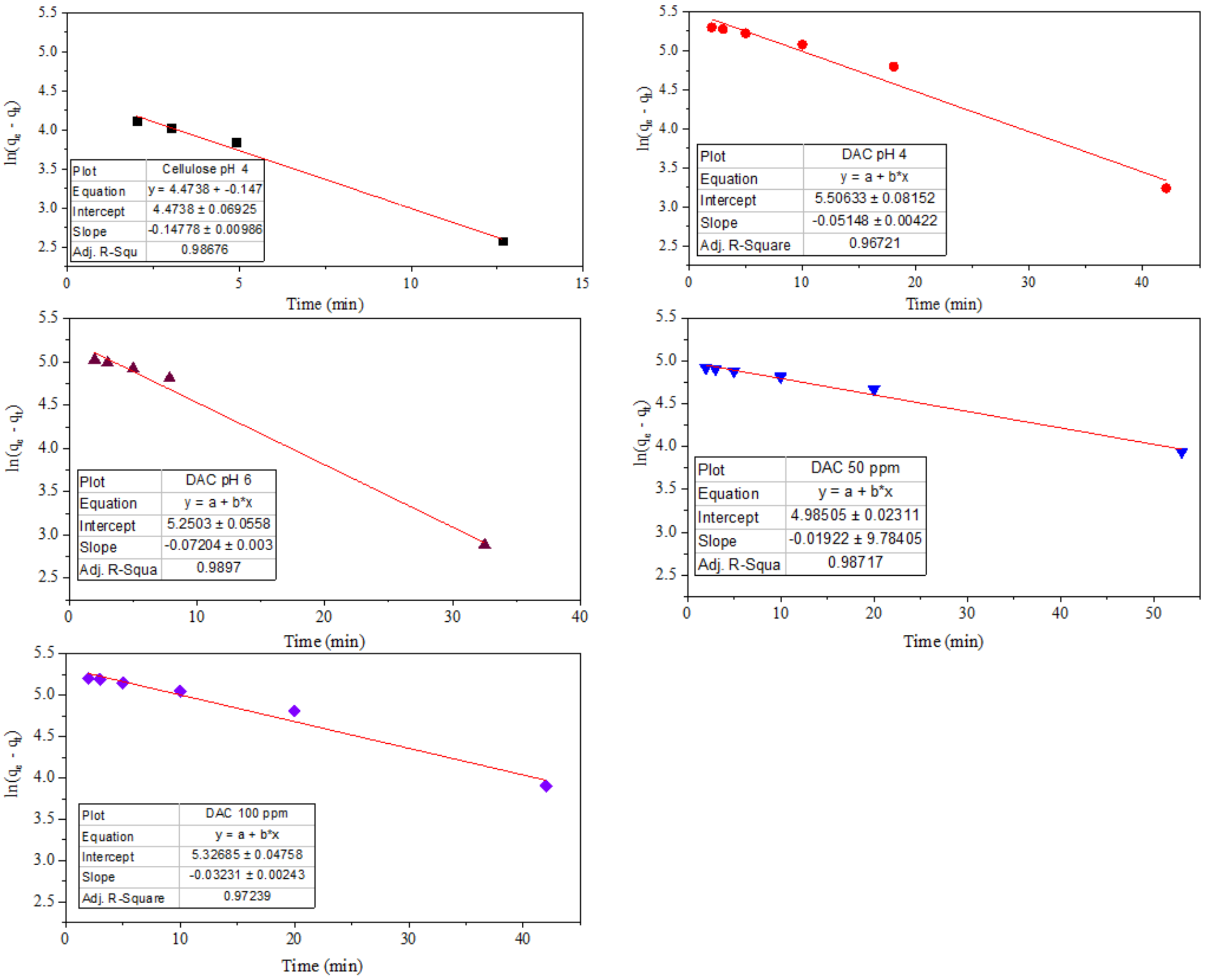

Figure S4.10: Fitted pseudo-first order kinetics for adsoprtion of basic fuchsine on cellulosic fibres.

References

[1] P. Earth, World's pollution problems: The toxics beneath our feet, New York, USA, 2016.

[2] H. Ali, Biodegradation of Synthetic Dyes—A Review, Water, Air, & Soil Pollution 213 (2010) 251-273.

[3] B. Padhi, Pollution due to synthetic dyes toxicity & carcinogenicity studies and remediation, International Journal of Environmental Sciences 3 (2012) 940-955.

[4] I. Gonçalves, A. Gomes, R. Brás, M. Ferra, M.T. Amorim, R. Porter, Biological treatment of effluent containing textile dyes, Coloration Technology 116 (2006) 393-397.

[5] C. O'Neill, F.R. Hawkes, D.L. Hawkes, N.D. Lourenco, H.M. Pinheiro, W. Delee, Colour in textile effluents - sources, measurement, discharge consents and simulation: a review, J. Chem. Technol. Biotechnol. 74 (1999) 1009-1018.

[6] A. Ghaly, R. Ananthashankar, M. Alhattab, V. Ramakrishnan, Production, characterization and treatment of textile effluents: a critical review, J Chem Eng Process Technol 5 (2014) 1-18.

[7] B.K. Nandi, A. Goswami, M.K. Purkait, Removal of cationic dyes from aqueous solutions by kaolin: Kinetic and equilibrium studies, Applied Clay Science 42 (2009) 583-590.

[8] F.E. Titchou, R.A. Akbour, A. Assabbane, M. Hamdani, Removal of cationic dye from aqueous solution using Moroccan pozzolana as adsorbent: Isotherms, kinetic studies, and application on real textile wastewater treatment, Groundwater for Sustainable Development 11 (2020) 100405.

[9] S. Rodríguez Couto, Dye removal by immobilised fungi, Biotechnology Advances 27 (2009) 227-235.

[10] R.-J. Lan, J.-T. Li, B.-H. Chen, Ultrasonic Degradation of Fuchsin Basic in Aqueous Solution: Effects of Operating Parameters and Additives, International Journal of Photoenergy 2013 (2013).

[11] M. Sichinga, J. Frazee, A. Tong, Efficiency and kinetics in treatment of wastewater from garages and residential oil spills using membrane bioreactor technology, International Journal of Environmental Science and Technology 13 (2015).

[12] A.J. Ghoshdastidar, J.E. Saunders, K.H. Brown, A.Z. Tong, Membrane bioreactor treatment of commonly used organophosphate pesticides, Journal of Environmental Science and Health, Part B 47 (2012) 742-750.

[13] A. Spagni, S. Casu, S. Grilli, Decolourisation of textile wastewater in a submerged anaerobic membrane bioreactor, Bioresource technology 117 (2012) 180-185.

[14] C.-H. Liu, J.-J. Li, H.-L. Zhang, B.-R. Li, Y. Guo, Structure dependent interaction between organic dyes and carbon nanotubes, Colloids and Surfaces A: Physicochemical and Engineering Aspects 313-314 (2008) 9-12.

[15] S. Chowdhury, S. Chakraborty, P. Saha, Biosorption of Basic Green 4 from aqueous solution by Ananas comosus (pineapple) leaf powder, Colloids and Surfaces B: Biointerfaces 84 (2011) 520-527.

[16] B.H. Hameed, M.I. El-Khaiary, Malachite green adsorption by rattan sawdust: Isotherm, kinetic and mechanism modeling, Journal of Hazardous Materials 159 (2008) 574-579.

[17] E.E. Baldez, N.F. Robaina, R.J. Cassella, Employment of polyurethane foam for the adsorption of Methylene Blue in aqueous medium, Journal of Hazardous Materials 159 (2008) 580-586.

[18] G. Annadurai, R.-S. Juang, D.-J. Lee, Use of cellulose-based wastes for adsorption of dyes from aqueous solutions, Journal of Hazardous Materials 92 (2002) 263-274.

[19] G. Zhang, L. Yi, H. Deng, P. Sun, Dyes adsorption using a synthetic carboxymethyl cellulose-acrylic acid adsorbent, Journal of Environmental Sciences 26 (2014) 1203-1211.

[20] M. Tavakolian, H. Wiebe, M.A. Sadeghi, T.G.M. van de Ven, Dye Removal Using Hairy Nanocellulose: Experimental and Theoretical Investigations, ACS Applied Materials & Interfaces 12 (2020) 5040-5049.

[21] T.G.M. van de Ven, K. Saint-Cyr, M. Allix, Adsorption of toluidine blue on pulp fibers, Colloids and Surfaces A: Physicochemical and Engineering Aspects 294 (2007) 1-7.

[22] E. Lizundia, E. Meaurio, J.L. Vilas, Chapter 3 - Grafting of Cellulose Nanocrystals, in: D. Puglia, E. Fortunati, J.M. Kenny (Eds.), Multifunctional Polymeric Nanocomposites Based on Cellulosic Reinforcements, William Andrew Publishing2016, pp. 61-113.

[23] F. Rol, M.N. Belgacem, A. Gandini, J. Bras, Recent advances in surface-modified cellulose nanofibrils, Progress in Polymer Science 88 (2019) 241-264.

[24] M. Moradian, M.S. Islam, T.G.M. van de Ven, Insoluble Regenerated Cellulose Films Made from Mildly Carboxylated Dissolving and Kraft Pulps, Industrial & Engineering Chemistry Research 60 (2021) 5385-5393.

[25] B. Alince, T.G.M. van de Ven, Porosity of swollen pulp fibers evaluated by polymer adsorption, in: C.F. Baker (Ed.) Proceedings of the Trans. of 11th Fundamental Research Symposium, Pira International, Surrey, Cambirdge U.K, 1997, pp. 771 - 788.

[26] J. Krishnan, S. Sunil Kumar, R. Krishna Prasad, Characterization of kraft pulp delignification using sodium dithionite as bleaching agent, Chemical Engineering Communications 207 (2020) 837-846.

[27] T. Exchanges, Preferred fiber & materials market report 2020 welcome to the 2020 Preferred fiber & materials market report, 2020.

[28] C. Felgueiras, N.G. Azoia, C. Gonçalves, M. Gama, F. Dourado, Trends on the Cellulose-Based Textiles: Raw Materials and Technologies, Frontiers in Bioengineering and Biotechnology 9 (2021).

[29] R. Koshani, M. Tavakolian, T.G.M. van de Ven, Natural Emulgel from Dialdehyde Cellulose for Lipophilic Drug Delivery, ACS Sustainable Chemistry & Engineering 9 (2021) 4487-4497.

[30] Z. Sabzalian, M.N. Alam, T.G.M. van de Ven, Hydrophobization and characterization of internally crosslink-reinforced cellulose fibers, Cellulose 21 (2014) 1381-1393.

[31] T. Zheng, X. Yu, S. Pilla, Mechanical and moisture sensitivity of fully bio-based dialdehyde carboxymethyl cellulose cross-linked soy protein isolate films, Carbohydrate Polymers 157 (2017) 1333-1340.

[32] A.A. Adeyi, S.N.A.M. Jamil, L.C. Abdullah, T.S.Y. Choong, K.L. Lau, M. Abdullah, Simultaneous Adsorption of Cationic Dyes from Binary Solutions by Thiourea-Modified Poly(acrylonitrile-co-acrylic acid): Detailed Isotherm and Kinetic Studies, Materials (Basel) 12 (2019) 2903.

[33] K.B. Tan, M. Vakili, B.A. Horri, P.E. Poh, A.Z. Abdullah, B. Salamatinia, Adsorption of dyes by nanomaterials: Recent developments and adsorption mechanisms, Separation and Purification Technology 150 (2015) 229-242.

[34] D. Li, Q. Li, N. Bai, H. Dong, D. Mao, One-Step Synthesis of Cationic Hydrogel for Efficient Dye Adsorption and Its Second Use for Emulsified Oil Separation, ACS Sustainable Chemistry & Engineering 5 (2017) 5598-5607.

[35] B. Fugetsu, S. Satoh, T. Shiba, T. Mizutani, Y.-B. Lin, N. Terui, Y. Nodasaka, K. Sasa, K. Shimizu, T. Akasaka, M. Shindoh, K.-i. Shibata, A. Yokoyama, M. Mori, K. Tanaka, Y. Sato, K. Tohji, S. Tanaka, N. Nishi, F. Watari, Caged Multiwalled Carbon Nanotubes as the Adsorbents for Affinity-Based Elimination of Ionic Dyes, Environmental Science & Technology 38 (2004) 6890-6896.

[36] N. Mohammed, H. Lian, M.S. Islam, M. Strong, Z. Shi, R.M. Berry, H.-Y. Yu, K.C. Tam, Selective adsorption and separation of organic dyes using functionalized cellulose nanocrystals, Chemical Engineering Journal 417 (2021) 129237.

[37] L. Luna, AFIP manual of histologic staining methods, New York, EUA (1986).

[38] V.K. Gupta, A. Mittal, V. Gajbe, J. Mittal, Adsorption of basic fuchsin using waste materials—bottom ash and deoiled soya—as adsorbents, Journal of Colloid and Interface Science 319 (2008) 30-39.

[39] M. El Haddad, Removal of Basic Fuchsin dye from water using mussel shell biomass waste as an adsorbent: Equilibrium, kinetics, and thermodynamics, Journal of Taibah University for Science 10 (2016) 664-674.

[40] R.L. Heinemann, Comparative Spectroscopy of Basic Fuchsin, Schiff Reagent, and a Formalin-Schiff Derivative in Relation to Dye Structure and Staining, Stain Technology 45 (1970) 165-172.

[41] H.A. Jakobsen, Packed Bed Reactors, in: H.A. Jakobsen (Ed.), Chemical Reactor Modeling: Multiphase Reactive Flows, Springer Berlin Heidelberg, Berlin, Heidelberg, 2008, pp. 953-984.

[42] A.N. Colli, J.M. Bisang, Evaluation of the hydrodynamic behaviour of turbulence promoters in parallel plate electrochemical reactors by means of the dispersion model, Electrochimica Acta 56 (2011) 7312-7318.

[43] M. Al-Jabari, A.R.P. van Heiningen, T.G.M. van de Ven, Modeling the flow and the deposition of fillers in packed beds of pulp fibres, Journal of pulp and paper science 20 (1994) J249-J253.

[44] M. Al-Jabari, A. van Heiningen, T. van de Ven, Experimental study of deposition of clay particles in packed beds of pulp fibres, Journal of Pulp and Paper Science 20 (1994) J289-J295.

[45] P.V. Danckwerts, Continuous flow systems: distribution of residence times, Chemical engineering science 2 (1953) 1-13.

[46] A. Poursaeidesfahani, E. Andres-Garcia, M. de Lange, A. Torres-Knoop, M. Rigutto, N. Nair, F. Kapteijn, J. Gascon, D. Dubbeldam, T.J.H. Vlugt, Prediction of adsorption isotherms from breakthrough curves, Microporous and Mesoporous Materials 277 (2019) 237-244.

[47] H. Brenner, The diffusion model of longitudinal mixing in beds of finite length. Numerical values, Chemical Engineering Science 17 (1962) 229-243.

[48] S. Vitthal, M.M. Sharma, A Stokesian dynamics model for particle deposition and bridging in granular media, Journal of colloid and interface science 153 (1992) 314-336.

[49] R. Koshani, T.G.M. van de Ven, Carboxylated Cellulose Nanocrystals Developed by Cu-Assisted H2O2 Oxidation as Green Nanocarriers for Efficient Lysozyme Immobilization, Journal of Agricultural and Food Chemistry 68 (2020) 5938-5950.

[50] S. Arora, F. Potucek, Modelling of displacement washing of packed bed of fibers, Brazilian Journal of Chemical Engineering 26 (2009) 385-393.

[51] Z. Aksu, F. Gönen, Biosorption of phenol by immobilized activated sludge in a continuous packed bed: prediction of breakthrough curves, Process Biochemistry 39 (2004) 599-613.

[52] D. Robati, Pseudo-second-order kinetic equations for modeling adsorption systems for removal of lead ions using multi-walled carbon nanotube, Journal of Nanostructure in Chemistry 3 (2013) 55.

[53] K. Conley, M. Whitehead, T.G.M. van de Ven, Chemically peeling layers of cellulose nanocrystals by periodate and chlorite oxidation, Cellulose 23 (2016) 1553-1563.

[54] E.S. Madivoli, P.G. Kareru, A.N. Gachanja, S.M. Mugo, D.S. Makhanu, Synthesis and characterization of dialdehyde cellulose nanofibers from O. sativa husks, SN Applied Sciences 1 (2019) 723.

[55] H. Yang, D. Chen, T.G.M. van de Ven, Preparation and characterization of sterically stabilized nanocrystalline cellulose obtained by periodate oxidation of cellulose fibers, Cellulose 22 (2015) 1743-1752.

[56] A. Tejado, M. Alam, M. Antal, H. Yang, T.G.M. van de Ven, Energy requirements for the disintegration of cellulose fibers into cellulose nanofibers, Cellulose 19 (2012) 831-842.

[57] R. Koshani, T.G.M. van de Ven, A. Madadlou, Characterization of Carboxylated Cellulose Nanocrytals Isolated through Catalyst-Assisted H2O2 Oxidation in a One-Step Procedure, Journal of Agricultural and Food Chemistry 66 (2018) 7692-7700.

[58] J. Sirvio, U. Hyvakko, H. Liimatainen, J. Niinimaki, O. Hormi, Periodate oxidation of cellulose at elevated temperatures using metal salts as cellulose activators, Carbohydrate Polymers 83 (2011) 1293-1297.

[59] J. MacMurry, Organic chemistry, Brooks/Cole Publishing Company, Pacific Grove, California, 1992.

[60] F.C. Silva, L.C. Lima, R.D. Bezerra, J.A. Osajima, E.C. Silva Filho, Use of cellulosic materials as dye adsorbents—a prospective study, Cellulose (2015) 115-132.

[61] H. Yang, A. Tejado, N. Alam, M. Antal, T.G.M. van de Ven, Films Prepared from Electrosterically Stabilized Nanocrystalline Cellulose, Langmuir 28 (2012) 7834-7842.

[62] X.-M. Fan, H.-Y. Yu, D.-C. Wang, Z.-H. Mao, J. Yao, K.C. Tam, Facile and Green Synthesis of Carboxylated Cellulose Nanocrystals as Efficient Adsorbents in Wastewater Treatments, ACS Sustainable Chemistry & Engineering 7 (2019) 18067-18075.

[63] C.-Q. Ruan, M. Strømme, J. Lindh, Preparation of porous 2,3-dialdehyde cellulose beads crosslinked with chitosan and their application in adsorption of Congo red dye, Carbohydrate Polymers 181 (2018) 200-207.

[64] X. He, K.B. Male, P.N. Nesterenko, D. Brabazon, B. Paull, J.H.T. Luong, Adsorption and Desorption of Methylene Blue on Porous Carbon Monoliths and Nanocrystalline Cellulose, ACS Applied Materials & Interfaces 5 (2013) 8796-8804.

[65] J. Yuan, F. Qiu, P. Li, Synthesis and characterization of β-cyclodextrin–carboxymethyl cellulose–graphene oxide composite materials and its application for removal of basic fuchsin, Journal of the Iranian Chemical Society 14 (2017) 1827-1837.

[66] J. Xing, B. Yang, Y. Shen, Z. Wang, F. Wang, X. Shi, Z. Zhang, Selective Removal of Acid Fuchsin from Aqueous Solutions by Rapid Adsorption onto Polypyrrole Crosslinked Cellulose/Gelatin Hydrogels, Journal of Dispersion Science and Technology 40 (2019) 1591-1599.

[67] F. Tang, H. Yu, S. Yassin Hussain Abdalkarim, J. Sun, X. Fan, Y. Li, Y. Zhou, K. Chiu Tam, Green acid-free hydrolysis of wasted pomelo peel to produce carboxylated cellulose nanofibers with super absorption/flocculation ability for environmental remediation materials, Chemical Engineering Journal 395 (2020) 125070.

[68] S. Loera-Serna, E. Ortiz, H.I. Beltrán, First trial and physicochemical studies on the loading of basic fuchsin, crystal violet and Black Eriochrome T on HKUST-1, New Journal of Chemistry 41 (2017) 3097-3105.

[69] B. Alince, T. Van de Ven, Porosity of swollen pulp fibers evaluated by polymer adsorption, The Fundamentals of Papermaking Materials 2 (1997) 771-788.

[70] H. Yang, A. Sheikhi, T.G.M. van de Ven, Reusable Green Aerogels from Cross-Linked Hairy Nanocrystalline Cellulose and Modified Chitosan for Dye Removal, Langmuir 32 (2016) 11771-11779.

[71] J. Wu, M.P. Andrews, Carboxylated Cellulose Nanocrystal Microbeads for Removal of Organic Dyes from Wastewater: Effects of Kinetics and Diffusion on Binding and Release, ACS Applied Nano Materials 3 (2020) 11217-11228.

[72] Y. Xiao, J. Azaiez, J.M. Hill, Erroneous Application of Pseudo-Second-Order Adsorption Kinetics Model: Ignored Assumptions and Spurious Correlations, Industrial & Engineering Chemistry Research 57 (2018) 2705-2709.

[73] L.D. Pavia, M.G. Lampman, S.G. Kriz, R.J. Vyvyan, Introduction to Spectroscopy, 4 ed., Brooks/Cole Cengage Learning, United States of America, 2009.

[74] J. Lindh, D.O. Carlsson, M. Strømme, A. Mihranyan, Convenient One-Pot Formation of 2,3-Dialdehyde Cellulose Beads via Periodate Oxidation of Cellulose in Water, Biomacromolecules 15 (2014) 1928-1932.

[75] D. Banfi, L. Patiny, www.nmrdb.org: Resurrecting and Processing NMR Spectra On-line, CHIMIA International Journal for Chemistry 62 (2008) 280-281.

[76] A.M. Castillo, L. Patiny, J. Wist, Fast and accurate algorithm for the simulation of NMR spectra of large spin systems, Journal of Magnetic Resonance 209 (2011) 123-130.

Preface to Chapter 5

Chapter 3 investigated the use of CMF as the base material in producing environmentally friendly aqueous-based textile filaments. Mechanosynthesis improves the energy efficiency and atom economy by eliminating use of organic solvents and obtaining a higher charge content in comparison to the conventional method. Chapter 4 examined chemisorption of amine dyes in a Schiff base reaction for eventual application in textiles. It was observed that chemisorption significantly reduces dye fastness, which is desired for end-product lifetime use. However, the rates of chemisorption are lower than physisorption and ion exchange, making it challenging to chemically adsorb the dyes in a continuous flow process as a post-treatment, without having dye waste runoff. Therefore, this study focuses on efficiently chemically adsorbing the dyes, by using limited quantities, to minimize dye waste and then functionalize the fibers with carboxyl groups to be able to continuously extrude the fibers into textile filaments. To minimize the filament productions steps, a one-pot multi-functionalization is explored and the product subjected to an aqueous based extrusion process. This research has been published in the following paper:

Martin Chewe Sichinga, Timothy Kline, M.A (Tony) Whitehead, Theo G. M. van de Ven. `One-pot eco-friendly oxidative synthesis of imine carboxymethyl dialdehyde cellulosic fibers`, *Cellulose* (2022): 29:799-815: DOI: https://doi.org/10.1007/s10570-021-04352-1

5 One pot eco-friendly oxidative synthesis of Imine carboxymethyl dialdehyde cellulosic (ICDAC) fibres

5.1 Abstract

The quest to efficiently produce renewable and sustainable functional cellulosic products has prompted the development of an environmentally sensitive and cost-effective method to produce multi-functionalized cellulose fibers, which can further be molded or spun to functional products. Here we report on imine carboxymethyl dialdehyde modified cellulose fibers (ICDAMF). Its synthesis is achieved by optimizing a sequential one-pot consisting of (i) partial modification of Kraft cellulose pulp using carboxymethylation (0.92 ± 0.21 mmol/g), (ii) periodate oxidation (3.0 ± 0.4 mmol/g) and (iii) Schiff base (~0.1 mmol/g) reactions. Multi-functionalization allows integration of desirable functional groups, in this case, carboxyl groups (0.9 ± 0.2 mmol/g) for gel formation and aldehyde groups (3.0 ± 0.4 mmol/g) for covalent adsorption of diamine dyes. Periodate oxidation stereospecifically cleaves the C2-C3 bonds of glucose units to form aldehydes, locally disturbing the crystalline structure which leads to high temperature solubility. Diamine dyes can act as crosslinkers thereby reducing fiber disintegration and high temperature solubility. ICDAMF has potential use in textiles, via waste-free covalent addition of dyes, critical in preventing leaching of dyes which can cause serious environmental pollution. The reaction progress was monitored by conductometric titrations and UV-visible spectroscopy. Product characterization was done by Fourier transform infrared, nuclear magnetic resonance, UV-visible and X-ray diffraction spectroscopies.

Keywords: · Cellulose pulp · Cellulose dying · Dialdehyde cellulose · Carboxymethyl cellulose · Periodate oxidation · Schiff base

5.2 Introduction

Cellulosic products continue to advance the replacement of non-renewable polymeric products and provide a source of biobased materials. This is mainly due to advantageous characteristics such as high abundance, renewability, low cost, non-toxicity, biodegradability, biocompatibility, reaction versatility and recyclability [1-4]. Surface modification of cellulose is necessary to obtain desired properties for specific domestic and industrial applications [5].

Utilizing the hydroxyl groups present on cellulose (C2, C3 and C6), a variety of derivatives have been explored [6]. Surface modifications involve grafting substituents; covalently, electrostatically, through hydrophobic interactions or hydrogen bonding. Such modifications enhance properties and utility of polymers [4, 7, 8]. Cellulose can also be modified via anhydro D-glucopyranose ring-opening using a stereospecific 1,2-diol reaction to form 2,3-dialdehyde cellulose (DAC). In addition to hydroxyl groups, aldehyde functionalization enhances reactivity that can be explored further, i.e., by hydrophobizing cellulose using long-chain alkylation [9-12].

By taking advantage of carboxylic acid grafting and glucose ring-opening reactions, this study aims to develop an efficient one-pot multifunctional synthetic route to produce mildly modified cellulosic fibers. The multifunctional product can be solubilized and regenerated by extrusion into filaments. One-pot synthesis eliminates isolation and purification of intermediate products, thereby creating a condensed and efficient process. The product has potential applications in eco-friendly and smart-textile, food, and pharmaceutical industries. The reactions explored are carboxymethylation, periodate oxidation and Schiff base reactions. The desired characteristics for covalently dyed modified cellulose are; (i) gelation in an appropriate solvent for wet spinning and/or molding, which is provided by carboxymethylation functionalization [13, 14]; (ii) prevention of leaching of dye by forming Schiff bases [11], prior to extrusion.

Carboxymethyl cellulose (CMC) is a commercially available, non-toxic and the most used cellulose ether, with applications in textile, food, pharmaceutical, paint and paper industries [15]. CMC is produced by an alkali-catalyzed etherification of cellulose by monochloroacetic acid with varying degrees of substitution (DS = 0 – 3 or equivalently 0 – 18.5 mmol –COOH/g of cellulose), shown in **Figure 5.1**. The DS regulates its functional properties; CMC with low DS is insoluble in water and is commonly referred to as carboxymethyl cellulose fibers (CMF) [15-18]. Under basic conditions, CMF is soluble and forms an ideal gel for wet spinning and/or molding by regenerating in acid [19]. It has been observed that carboxymethyl cellulose fibers do not rapidly degrade in 10% H_2SO_4 [17, 20].

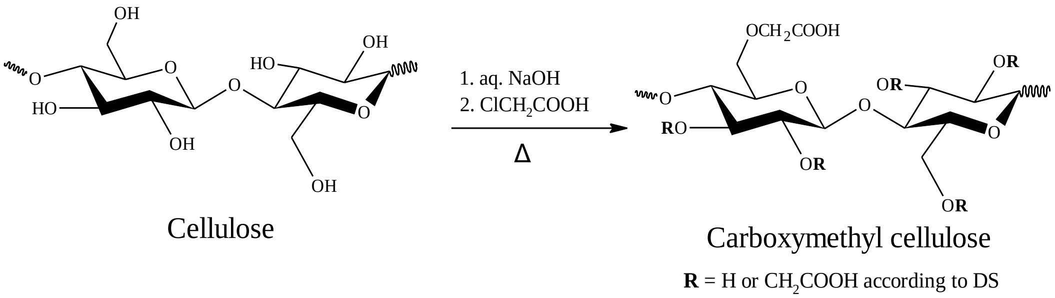

Figure 5.1: Reaction scheme for carboxymethylation of cellulose to form CMC or CMF

Anhydro D-glucopyranose ring-opening via periodate oxidation (**Figure 5.2**) adds flexibility to a rigid cellulose polymeric ring structure [21], in addition to the added aldehyde functionality.

Aldehyde groups can be converted further to di-alcohols, imines and 2,3-dicarboxyl cellulose [22]. The degree of oxidation (DO) range is 0 – 2 or equivalently 0 – 12.5 mmol –CHO/g of cellulose, with 12.5 mmol/g (DO = 2) corresponding to DAC and with low DO corresponding to dialdehyde modified fibers (DAMF). The DO greatly affects the chemical and physical properties, as periodate oxidation occurs on both the amorphous and crystalline regions, proceeding faster in the amorphous regions [22].

Therefore, high DO reduces crystallinity, increases polymer amorphous chain flexibility in solution, induces formation of nanofibers and reduces decomposition temperatures. These properties can be advantageous or disadvantageous depending on application [22-24]. Cellulose dissolution or mercerization mechanisms have been explored under varying conditions such as temperature, solvents and solution combinations, with pros and cons of various systems discussed by [25]. DAMF and DAC are soluble in water above 60 °C or by reducing them di-alcohols. Solubility reduces with decreased DO [26]. The solution formed is thermodynamically stable and the process is irreversible upon cooling. Therefore, using DAMF ensures preservation of some physical and chemical properties, such as insolubility in water and tensile strength, of unmodified cellulose.

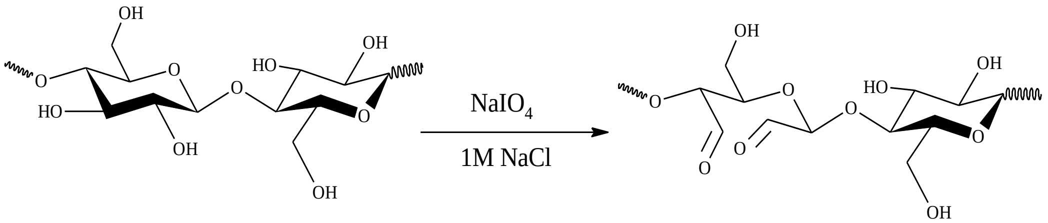

Cellulose

DAMF

Figure 5.2: Reaction scheme for partial periodate oxidation of cellulose forming dialdehyde modified fibers (DAMF), achieved via ring opening of the glucopyranose ring on the 2-3 positions

Imines, also known as Schiff bases, are nitrogen analogues of aldehydes or ketones which are formed by reacting primary amines with aldehydes or ketones (**Figure 5.3**). Imines are commonly used as dyes, organic reaction intermediates, polymer stabilizers and biological agents due to antifungal, antibacterial, anti-inflammatory and antiviral properties [27]. Grafting Schiff bases on DAC has been demonstrated to have a structural reinforcement effect when crosslinked with di-amine alkyl chains. High structural stability and fiber recovery were achieved when initial DAC had a low DO and lower reaction time, and vice-versa [11]. It was also observed that anhydro D-glucopyranose ring-opening resulted in reduced viscosity. Highly charged dialdehyde carboxymethyl cellulose can be precipitated from solution using an alcohol as a poor solvent [28].

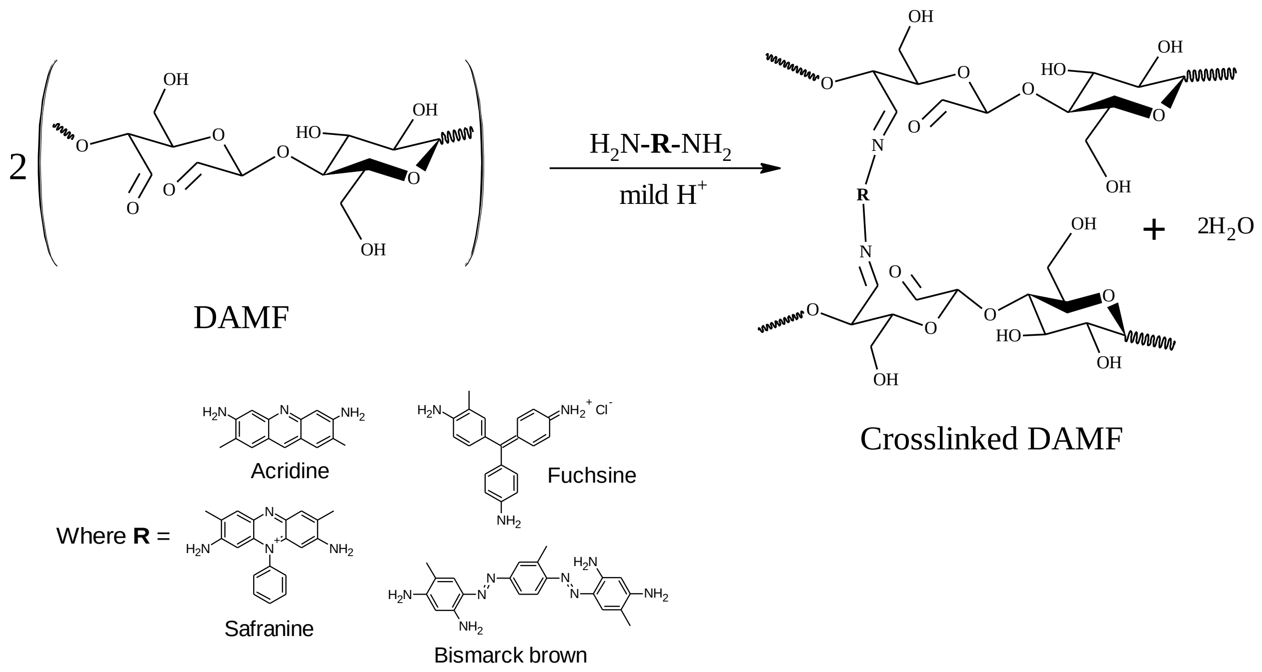

Figure 5.3: Scheme of crosslinking DAMFs via Schiff base reaction using multi-amine dyes under mild acidic conditions

Numerous scholars have studied one-pot cellulose modification synthesis routes. Overall, the majority of reactions are multistep reactions that lead to addition of a single functionality [29-31]. It has also been observed that these routes start with already modified cellulose as a precursor (cellulose acetate [29]) or modify, extract and then proceed to the next synthetic step (cellulose sulfuric acid [30] and CMC [32]). Bi-functional modification of cellulose has also been researched, mainly by using pre-functionalized precursors and then adding another functional group [11, 28, 33, 34], or modifying a grafted carboxylic acid group by reducing it to an alkene or alkyne in a one-pot reaction [35].

This study demonstrates the synthesis of multifunctional, mildly modified cellulose fibers using a sequential one-pot method, with each functional group providing a desired property. Carboxymethylation, periodate oxidation and Schiff base reactions are explored to sequentially add multi-functionality to cellulose, without extraction of intermediate products. Mild modification ensures only sufficient carboxyl groups are added for gel formation in alkaline media and minimal aldehydes to prevent fiber degradation but enough to consume the amines in a Schiff base reaction.

5.3 Materials and methods

5.3.1 Materials

Bleached soft wood kraft pulp (Q-90) was used as a cellulose starting raw material in the synthesis of imine carboxymethyl dialdehyde modified cellulose fibers (ICDAMF). The pulp sheets were supplied by Domtar, Canada, and mechanically ground into a powder using a Foss CT293 Cyclotec^{TM} grinder, fitted with 0.5 mm screen. Sodium periodate ($NaIO_4$), monochloroacetic acid

(MCA), ethylene glycol and sodium chloride were supplied by Sigma Aldrich, Ontario Canada. The diamine dyes (acridine yellow G, basic fuchsine, Bismarck brown R and safranine O) were supplied by Santa Cruz Biotechnology Inc, Texas USA. Sodium hydroxide (NaOH), methanol, ethanol (100%) and isopropanol were obtained from Fisher Scientific, Ontario Canada. All chemicals were used without modification, unless otherwise stated.

ICDAMF was purified via dialysis using regenerated cellulose dialysis tubing (MWCO: 6 – 8 kDa) obtained from Fisher Scientific. For quantitative analysis purposes, certified analytical grade sodium hydroxide solution (0.01 *N* and 0.5 M), hydrochloric acid (0.5 M), and hydroxylamine hydrochloride were acquired from Sigma Aldrich, Ontario Canada. These chemicals were used in the analysis of starting materials, intermediate and ICDAMF products.

5.3.2 Carboxymethylation of cellulose pulp

The carboxymethylation reaction was conducted according to [17, 36], with minor modifications on temperature, reactant amounts and time. A solution (8% w/w) of ground pulp in isopropanol was prepared and an aqueous NaOH solution (10 mmol equivalent per gram of cellulose) was added. The mixture was stirred for 1 hr at 40 ˚C. The temperature was increased to 60 ˚C and an aqueous solution of monochloroacetic acid (2.76 mmol equivalent per gram of cellulose) was added. The mixture was stirred for 2 hrs, then cooled down to room temperature before proceeding with periodate oxidation.

The control carboxymethylation product was washed twice in ethanol-water mixture (60:40, w/w) and finally with 100% ethanol and then air dried. The expected carboxyl content for the produced carboxymethyl cellulose fibers (CMF) was 1 mmol carboxylic acid per gram of cellulose (1 mmol/g), which is equivalent to degree of substitution (DS) of 0.16. The theoretical maximum charge content is 18.5 mmol/g (DS = 3). Excess monochloroacetic acid was used due to hydrolysis in water and under basic conditions forming glycolic acid [37].

5.3.3 Periodate oxidation and Schiff base reactions from CMF

About 70% of isopropanol was decanted from the CMF-isopropanol mixture and substituted with water to make an isopropanol-water mixture (30:70 w/w) at room temperature. The presence of isopropanol prevented the CMF from gelling, while ensuring fibers were well dispersed. As a control, previously purified and dried CMF was dispersed in an isopropanol-water mixture (30:70 w/w). NaCl was added to make a 1 M NaCl solution, to improve accessibility of the fibers' interior after swelling [10]. Partially periodate oxidized cellulose can be obtained by using a limited amount of periodate or using reaction rates and control of the reaction time [22].

In this study, a limited amount of $NaIO_4$ (0.3 g/g of cellulose) was added to produce 3 mmol of aldehyde groups per gram of CDAMF (3 mmol/g) and 20% excess to produce 10.4 mmol/g DAC. Under constant stirring, the reaction proceeded for 6 days in the dark, after which drops of ethylene glycol were added to quench the reaction. Ethylene glycol ensured that if there was residual periodate, it would get consumed and prevent interference with absorption spectra of the dyes (**Figure S5.1**), although the quenching product i.e., formaldehyde, can also form an imine with the dye. Therefore, it was critical to use a limited amount of periodate to ensure that it was all consumed prior to adding ethylene glycol.

Without isolating the product, a diamine (0.09 mmol eq. NH_2) (acridine yellow G, basic fuchsin, bismarck brown R or safranine O) was added and the pH adjusted to ~4.5. The reaction proceeded for 24 hrs and then flocculated with ethanol, as a poor solvent. It was subsequently filtered with a 20 µm nylon cloth. Sample washing was done with an ethanol-water mixture (70:30 w/w) twice and then washed with 100% ethanol. The product was then air dried. The ICDAMF samples used for characterization were further purified by dialysis for 48 hours. This ensured that the unreacted dyes, physically bound to the cellulose fibers, diffuses out in aqueous solution and were removed. The samples used to determine the dry mass recovery, were oven dried at 50 °C overnight and remeasured every 3 hours until a constant mass was reached.

5.3.4 Qualitative and quantitative characterization analysis

Qualitative analysis of solvents, reactants, reaction progress and products were conducted on a Varian TCA-Cary 300 UV-visible spectrometer. The instrument was operated at a scan rate of 600 nm/min in a double beam mode with a slit bandwidth of 2 nm. Additionally, UV-vis and infrared data were computationally simulated using Gaussian 16, and then analyzed utilizing GaussView 6.0. This was achieved by optimizing structural models of cellobiose using Semi-Empirical PM6 method. The optimized structures were then subjected to a time-dependent self-consistent field (TD-SCF) DFT B3LYP 6-311++(d,p) energy computational calculation to predict the UV-vis spectra, similar to studies conducted by [38] and [39]. Infrared spectra were acquired via a frequency calculation using DFT B3LYP 6-311++(d,p).

The charge density for CMF and ICDAMF was determined by conductometric titration using a Metrohm 836 Titrando titrator (Ontario, Canada). The titration was automatically operated with a starting pH of ~3.5 and 10 mM NaOH solution added at 0.1 mL/min until a final pH of ~11 was reached, allowing excess NaOH to determine the –COOH neutralization end point [40, 41]. Each statistical test and confidence intervals were determined at 95% confidence levels.

Quantitative determination of aldehyde (–CHO) groups was achieved using an oxime titration method [22, 40, 42]. A 1% solution of modified cellulose fibers was solubilized at 80 ˚C for 6 hours and unfibrilated fibers filtered using a 20 μm pore size nylon filter. An aliquot was obtained to determine dry mass percent, after drying to a constant weight at 50 ˚C. Another aliquot was titrated to determine –CHO content on the fibers. The pH of the aliquot and 5% hydroxyl amine-hydrochloride ($NH_2OH{\cdot}HCl$) solutions were adjusted to 3.5, independently. The oxime reaction, shown in **Figure 5.4**, was initiated by mixing the solutions. The HCl produced *in situ* was titrated against 10 mM NaOH by maintaining the pH at 3.5. The endpoint was established when there was no significant change in pH [43]:

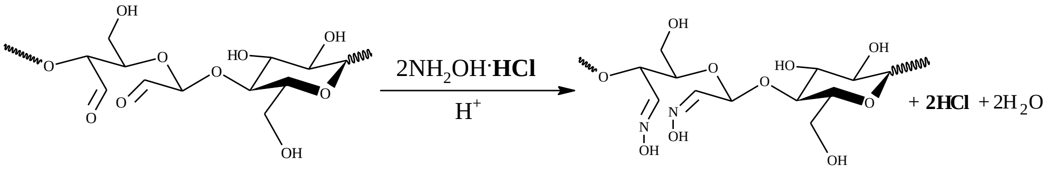

DAMF

Oxime

Figure 5.4: Oxime formation in titration of aldehydes with $NH_2OH{\cdot}HCl$ to release HCl [11]

5.3.5 Surface chemical properties

Attenuated Total Reflectance Fourier Transform Infrared (ATR-FTIR) vibrational measurements were conducted on a Bruker IR instrument equipped with a single bounce diamond ATR accessory and Opus software for peak analysis. After background noise subtraction, IR spectra were obtained by applying maximum force on solid samples positioned on an ATR crystal, by collecting and averaging 32 scans in a wavenumber range of 400 – 4000 cm^{-1} and 4 cm^{-1} resolution. Additionally, a DFT frequency calculation was used to predict vibrational frequencies by applying the b3lyp/6-311++g(d,p) basis set, as described in methods by [44] and [45].

A Varian/Agilent VNMRS-400 operated at 100.5 MHz was used to acquire solid-state ^{13}C NMR spectra. Finely ground samples were packed in a 7.5 mm zirconium rotor and then spun at 5,500 Hz and acquired 6,000 transients using a contact time and recycle delay of 2 ms and 2 s, respectively. Spinning sidebands were suppressed using the TOSS sequence [46].

The changes in crystallinity of modified cellulose were investigated using a Bruker Discover D8 two-dimensional diffractometer, equipped with CuKα radiation (λ= 1.54 Å) and VANTEC 2D detector. The X-ray diffractograms were acquired with a 2Θ angle range of 5 – 40°, at a scan rate of 0.005° s^{-1}. The crystalline (2 0 0 reflection plane) and amorphous (1 1 0 reflection plane) peaks were assigned according to [47].

5.4 Results and Discussion

5.4.1 ICDAMF optimized reaction procedure

The aim for developing an optimal one-pot reaction is to efficiently obtain mildly functionalized cellulose fibers that are insoluble in water but capable to form a gel in solution and chemically adsorb a dye to prevent leaching. The product is then solubilized and extruded to form filaments that can be used to produce textile yarn. The optimized reaction steps and conditions are summarized in **Scheme 5.1**.Carboxymethylation reaction grafts –COOH functional groups onto cellulose with a high reaction rate on the hydroxyl group of C6, and forms a gel under neutral or basic conditions [14]. At high charge content, CMC is highly soluble in water, therefore, a charge content sufficiently low for gelation is desired. CMC with a low degree of substitution (DS) between 0.1 and 0.4 is fibrous and insoluble in water, and is commonly referred to as carboxymethyl fiber (CMF) [48]. The CMF reaction is conducted at about 60 °C, prior to periodate oxidation, because DAMF is partially soluble at elevated temperatures [26] and periodate decomposes at 55 °C [49]. Therefore, to prevent fiber solubility and periodate decomposition during the synthesis, the CMF reaction at about 60 °C is an ideal and critical first step. The subsequent periodate oxidation and Schiff base reactions were conducted at room temperature.

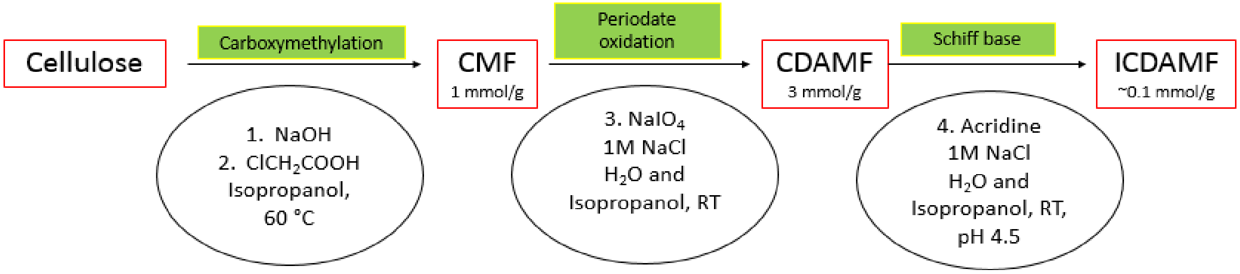

Scheme 5.1: Optimized reaction steps and conditions for one-pot synthesis of ICDAMF indicating the order of addition of active reagents

Periodate oxidation reactions are stereospecific to 1,2 diols [50]; therefore this reaction occurs on C2, C3 diols of cellulose forming –CHO. Independent solubility tests of DAMF in 0.5 M NaOH, discussed below, indicate that a lower degree of oxidation has lower solubility, hence, 3 mmol/g or less is ideal. This provides excess –CHO for conjugation with diamines. Overall, the proposed intermediate and final products are shown in reaction **Scheme 5.2**.The waste products generated are Na$^+$, Cl$^-$, IO$_3^-$ which are soluble in solution can all be collected and processed as halogenated waste, during chemical recycling.

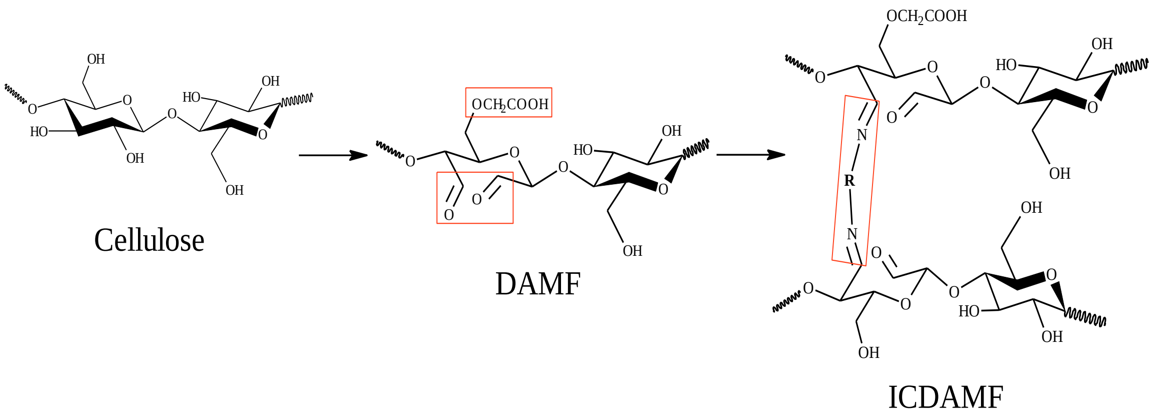

Scheme 5.2: Proposed partial carboxymethyl and aldehyde oxidative intermediates and ICDAMF final product, indicating modified sites. The R-groups for various diamine dyes are shown in Figure 5.3, crosslinking can either be intra or interchain on the fibers.

The UV-Vis spectra of cellulose, acridine yellow G and acridine-CDAMF are compared in **Figure 5.5**. The maximum absorption wavelength (λ_{max}) shifts from 436 to 295 nm, during the reaction. Acridine yellow G has a large absorption band of 430 – 444 nm depending on the concentration ratio between its monomeric form and dimers [51]. The observed major peak λ_{max} of 436 nm with a minor peak at ~280 nm is in agreement with literature and the TD-DFT computated λ_{max} at 433 and 269 nm for major and minor peaks, respectively. The normalized-DFT peaks at 269 nm (minor) and 433 nm (major) have oscillator strengths of 75% and 79%, respectively. The oscillator strengths indicate a high probability that the peaks are real, but does not show the difference in peak size relative to one another.

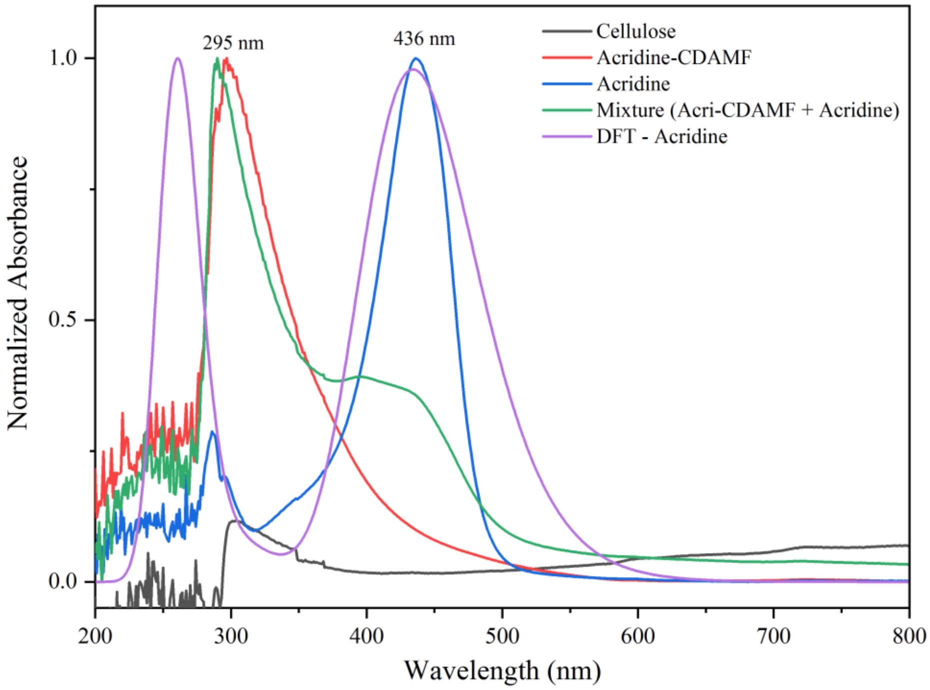

Figure 5.5: UV-Vis spectra of acridine and cellulose as controls with the product (acri-CDAMF) shift in λ_{max} and the physical adsorption-desorption in a mixture

In addition, UV-Vis absorption spectra of cellulose and its derivatives have been studied extensively [52]. Computational simulation and **Figure 5.5** confirm that cellulose, CMF and DAMF do not absorb in the UV-Vis region (200 – 800 nm). However, it is worth noting that the cellulose spectrum goes below zero absorbance below 300 nm, possibly due to imperfections in the cuvette. Therefore, the observed major absorption peaks are due to presence and influence of the dye. Hence, after reaction with DAMF, the acridine yellow G conjugation is extended, causing a change in absorption wavelength for acridine from 436 [51] to 295 nm.

5.4.2 Carboxymethyl cellulose quantification via conductometric titration

Carboxylic group content and degree of substitution (DS) of CMF were determined using conductometric titration. Approximately 50 mg of CMF is titrated against 10 mM NaOH to obtain pH titration and conductivity curves (**Figure 5.6**), from which the –COOH content is calculated. The average –COOH content was 0.99 ± 0.05 mmol/g or equivalently DS of 0.16 ± 0.01, representing fiber modification of 5.5%. ICDAMF average yield was 93 ± 9% and the average charge content was 0.92 ± 0.21 mmol/g or DS of 0.15 ± 0.03. The slight difference in the average charge content is likely due to a small reduction in yield, therefore, periodate oxidation does not significantly affect the cellulose –COOH groups.

Additionally, using the titration curves (**Figure 5.6**) and applying the Henderson-Hasselbalch equation ($pH = pK_a + \log_{10}[R\text{-}COO^-]/[R\text{-}COOH]$) at the point of neutralization, the pK_a values for CMF and ICDAMF were determined as 4.78 ± 0.06 and 4.72 ± 0.17, respectively. There is no significant difference between the mean pK_a values. Reported CMC pK_a values are in the range of 3.2 – 4.7 [53, 54], with the large spread attributed to CMC electric properties in solution. It has been observed that since CMC is a weak polyelectrolyte, the dissociation constant of carboxyl groups in CMC highly depends on the presence of vicinal carboxyl groups. Therefore, a single pK_a value cannot be assigned to CMC, but instead dissociation must be described by a distribution of intrinsic dissociation constants [54]. Even for low DS CMF and ICDAMF, this phenomenon is observed as the theoretical and experimental pH curves do not perfectly match, hence the reported pK_a values are at the point of intersection.

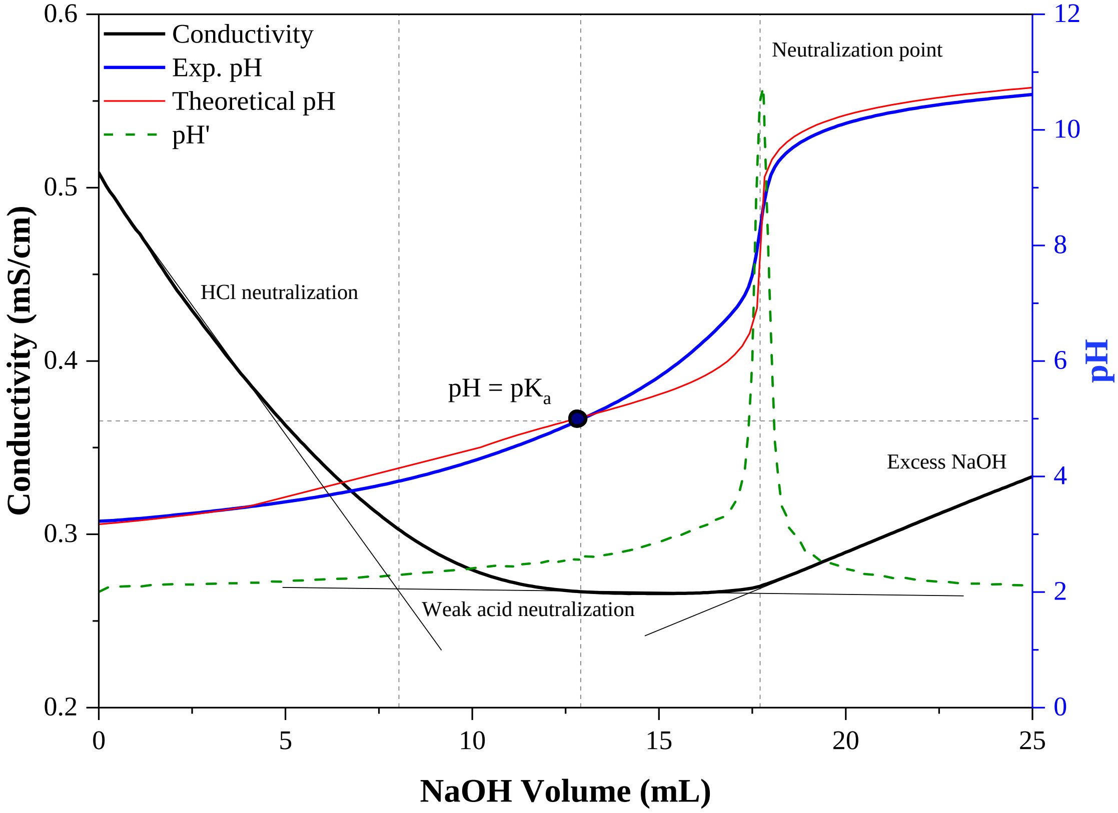

Figure 5.6: Modified cellulose titration curves (conductivity, experimental and the theoretical pH and the first derivative of pH) for the determination of -COOH content, DS and pK$_a$

5.4.3 Determination of aldehyde content via oxime titration

Using a 10.4 mmol/g DAC sample, a solubility profile using drops of 0.5 M NaOH was established, shown in **Figure 5.7**. Solubilization and fiber regeneration adhere to this profile regardless of the –CHO content. However, it was determined that increased –CHO content results in increased solubility and degradation, in 0.5 M NaOH when pH ≈ 13, shown in **Table 5.1**.Furthermore, upon regeneration only about 30% of fibers are recovered at pH ≈ 2. Additionally, regenerated fibers disperse in solution without gel formation.

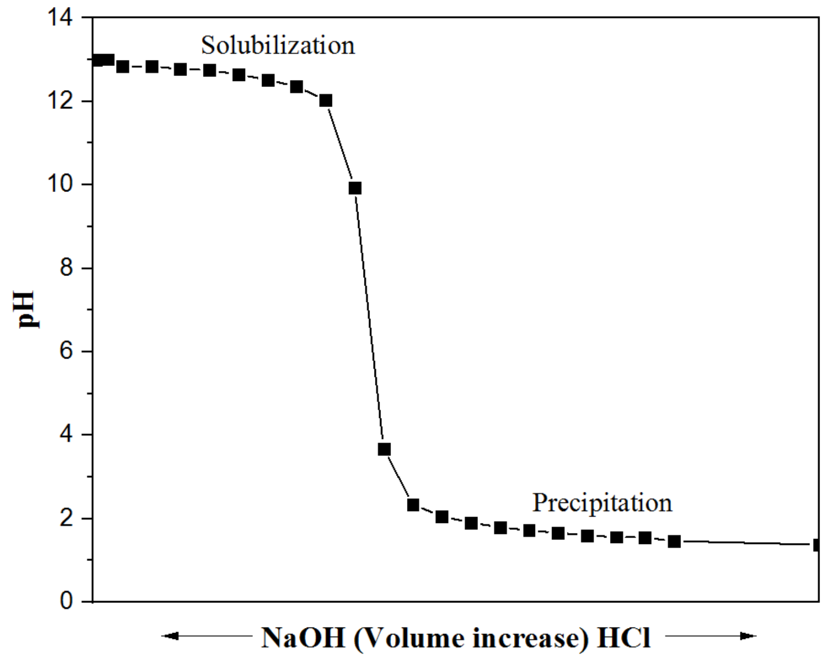

Figure 5.7: Solubility-precipitation profile for DAMF in 0.5 M NaOH and HCl

Table 5.1: Maximum solubility of DAMF in 0.5 M NaOH based on –CHO content.

Sample	**Aldehyde content (mmol/g)**	**Maximum Solubility (%)**
Cellulose (control)	0	Insoluble
DAMF 1	4	31
DAMF 2	8	97
DAMF 3	10	99

During ICDAMF synthesis, the target –CHO content was 3 mmol/g of cellulose. The average –CHO determined was 3.0 ± 0.4 mmol/g, prior to diamine dye addition. A concentration of 3 mmol/g is ideal for minimizing cellulose solubility and decomposition under alkaline conditions, at room temperature. A lower degree of oxidation ensures minimal cellulose chain fragmentation via the β-alkoxy mechanism which affect the degree of polymerization [21, 55]. After the reaction with diamine dyes to produce ICDAMF, the –CHO content was measured again. The average –CHO content was 2.8 ± 0.5 mmol/g. This reduction was due to aldehyde groups reacting with the dye (acridine yellow G, basic fuchsine, bismarck brown R and safranine O). The quantity of dye added was 0.09 mmol $–NH_2$ groups equivalent. Therefore, the reaction conditions were optimal for imine formation from the four diamine dyes utilized.

In addition, the protocol for measuring –CHO content requires sample solubilization at 80 °C [40] and solubility increases with high degree of oxidation (DO). An independent test on high temperature solubilization was conducted using DAC (10.8 mmol/g) and an imine made of basic fuchsine (6% mole equivalence) and DAC. It was observed that the solubility after 6 hours was >99% and ~30% for DAC and fuchsine-DAC, respectively. The reduction in solubility could be attributed to crosslinking and/or the presence of a chemically bound dye. The fuchsine-DAC supernatant UV-Vis spectra (**Figure S5.2**) indicated that heat did not break the imine bond. Therefore, diamines would be advantageous to products that would be exposed to high temperature liquids, such as washers.

Qualitative reaction monitoring via UV-visible spectroscopy

The acridine-CDAMF reaction progress is followed by UV-Vis using scan kinetics mode to obtain spectra (200 – 800 nm) at a rate of 600 nm per minute. As the reaction progresses, a peak at 295 nm emerges and continue to increase over time, **Figure 5.8** *(a)* and *(b)*. An absorbance change is observed at 295 nm, an indication that the product formed (acridine-CDAMF) absorbs at that wavelength. The UVB absorption range for the formation of Schiff bases is 243 – 295 nm [56].

Acridine yellow G is used as a control for dye and instrument stability under the reaction conditions. Overlay spectra (42 graphs), **Figure S5.3**, show the stability of the dye solution, instrument stability and reproducibility. The change in background noise noticed in **Figure 5.8** and **Figure S5.4** is signal interference due to sedimentation characteristics of cellulose, as it is insoluble in the solvent. It is observed that there is broadening at the apex of the peak at 436 nm during the reaction (**Figure 5.8**), in comparison with the controls (**Figure S5.3** and **Figure S5.4**) and no significant change in intensity. This is an indication that the reaction conditions do not chemically degrade the dye and the product red shifts the peak, *i.e.* towards longer wavelengths, from 436 nm to 458 nm (**Table 5.2** and **Figure S5.5**), a phenomenon also observed by Heinemann (1970) [56]. The peak apex broadening is due to overlap of peaks between unreacted dye and product formation, which is not observed in the controls. The red shift and peak apex narrowing are observed in purified acridine-CDAMF (**Figure S5.5**).

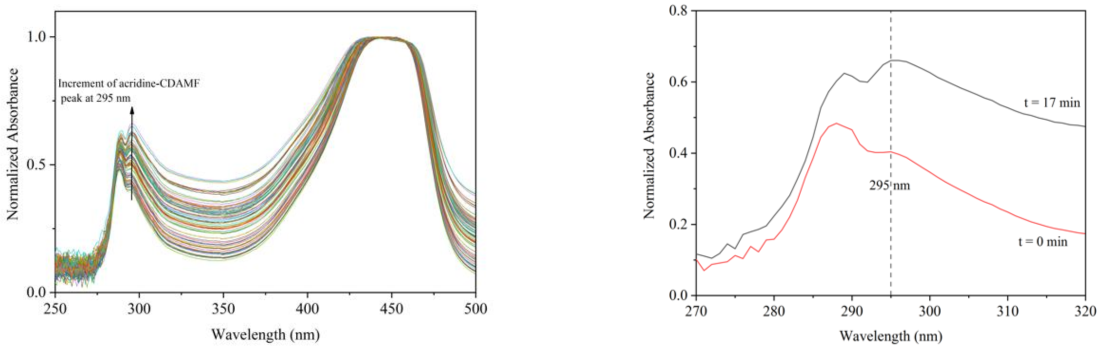

[A] [B]

Figure 5.8: [A]Acridine-CDAMF reaction monitoring and product formation at 295 nm (81 overlayed spectra) [B] Change in Acridine-CDAMF absorbance peak during the reaction

In Addition, under the same reaction conditions as for the reaction between unmodified cellulose and acridine yellow G, the peak at 295 nm is not observed even though the dye is adsorbed, shown in **Figure S5.4**. This indicates that aldehyde groups and optimal reaction conditions are necessary to covalently bind the dye to cellulose, otherwise, physical adsorption is obtained. Hence, when physical adsorption occurs, a desorption-absorption equilibrium is established and peaks are observed at about 295 and 436 nm, observed in **Figure 5.5** above for a mixture.

The developed one-pot synthetic reaction protocol for oxidatively modified cellulose is applied to four different diamine dyes (acridine yellow G, basic fuchsin, bismarck brown R and safranine O). The UV-Vis maximum absorption wavelengths of ICDAMF after dialysis purification are shown in **Table 5.2**.The shift in absorbance between the dye and grafted dye strongly indicate that this procedure is applicable to a variety of primary diamines, additionally, the major peak appears in the UV region (**Figure S5.5**).

Table 5.2: Maximum absorption wavelengths (λ_{max}) for diamine dyes and modified cellulose

Compound	**Mass recovered (%)**	**Observed λ_{max} (nm)**	**Literature λ_{max} (nm)**
Cellulose	-	0	0
CDAMF	85	0	0
Acridine yellow G	-	436	430 - 444
Acri-CDAMF	86	242 and 458	-
Basic fuchsine	-	252 and 561	544
Fuc-CDAMF	98	240 and 566	-
Bismarck brown R	-	458	459
Bis-CDAMF	96	251 and 450	-
Safranine O	-	518	520
Saf-CDAMF	88	243 and 535	-

Using ethanol as a poor solvent for cellulosic materials allowed for easy filtration of the flocculated products with relatively high recoveries. The high recoveries can be attributed to possible fiber crosslinking, as it was observed that tri- (fuchsine) and quad- (Bismarck brown) amines had the highest recoveries. Upon flocculation, fuchsine-CDAMF has a gummy appearance and did not disperse in solution. Additionally, fiber disintegration could have been minimized by charge stoichiometry between the pulp and the dyes. Cellulose pulp has a negative charge due to carboxyl groups while dyes have a positive charge which allow the attraction via an ion exchange process [57]. This is further supported by the low recoveries of CDAMF which was not subjected to a Schiff base reaction.

5.4.4 Surface chemical properties

5.4.4.1 Characterization by infrared spectroscopy

The unmodified softwood pulp, CMF, DAMF and ICDAMF FTIR spectra were obtained for qualitative comparison of chemical functionalization (**Figure 5.9**). The changes in the chemical structure due to oxidation reactions confirm the multi-functionalization of cellulose fibers. The broad peak at about 3300 cm^{-1} is due to –OH stretching influenced by hydrogen bonding, with corresponding bending modes at 1325 cm^{-1}. C–H stretching, scissoring and CH_2–CH_2 stretching vibrational modes are observed at 2920, 1425 and 1009 cm^{-1}, respectively. The peaks at 1640 and 877 cm^{-1} observed are assigned to asymmetric stretching for hydrated –CHO groups and the characteristic C=O stretch is observed at 1724 cm^{-1}. Our results are consistent with interpretations and peak assignments in previous cellulose modification studies [22, 28, 46].

Formation of a Schiff base with diamines results in broadening of the peak between 2980 – 3665 cm^{-1}, a peak shoulder at 1642 cm^{-1} for C=N stretch and 1500 – 1400 cm^{-1} due to the presence of aromatic rings vibrations [58]. The Schiff base peaks are masked resulting in broadening of the peak between 1501 – 1697 cm^{-1}, where the characteristic C=N stretches, N–H bend modes, aromatic ring vibrations, and C–N bends are expected around 1650, 1600, 1550 – 1450 and 888 cm^{-1}, respectively. This is also confirmed by DFT vibrational frequency calculations (**Figure 5.9**) and consistent with Schiff base FTIR literature [11, 58, 59].

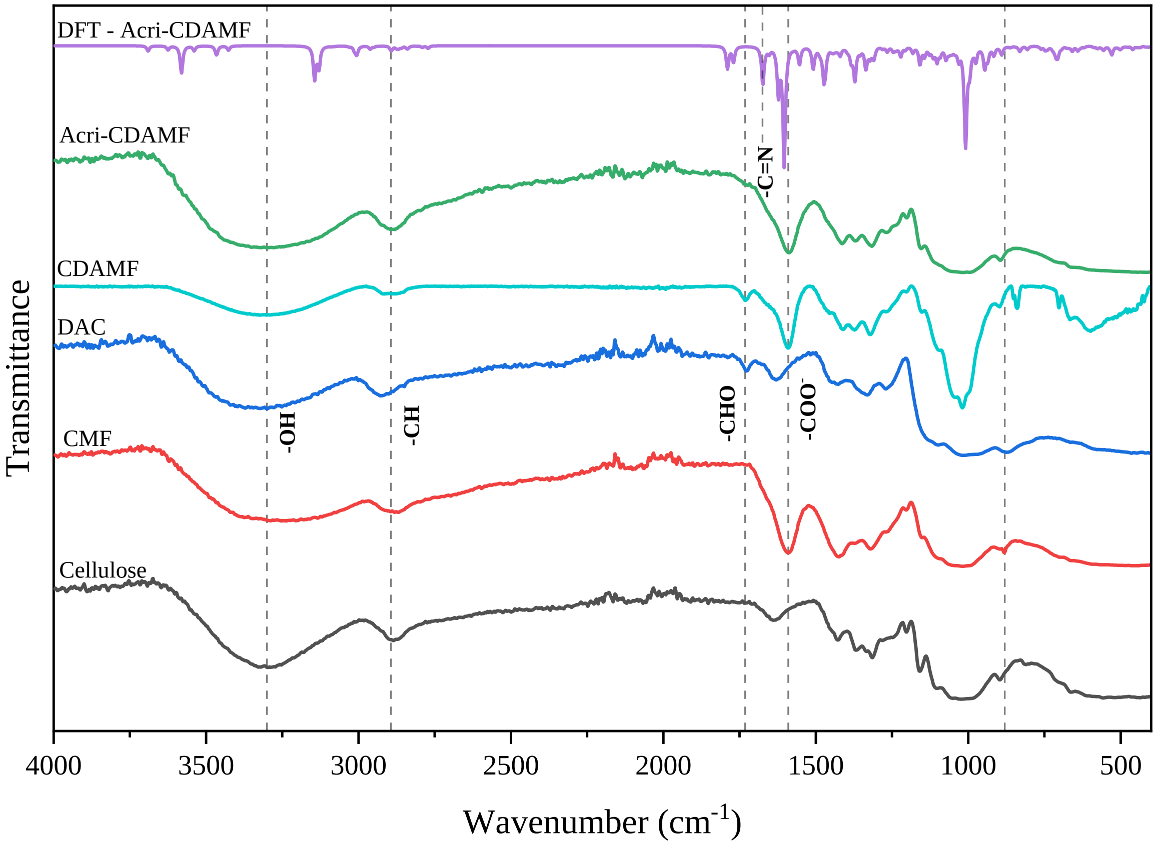

Figure 5.9: FTIR spectra of carboxymethyl cellulose fibers, dialdehyde cellulose, carboxymethyl dialdehyde cellulose and imine carboxymethyl-dialdehyde cellulose functionalized fibers.

5.4.4.2 Characterization by solid-state NMR spectroscopy

The ^{13}C NMR spectra for Cellulose, carboxymethyl cellulose (CMF), dialdehyde modified fibers (DAMF) and ICDAMF are shown in **Figure. 5.10**. The ICDAMF spectrum shows chemical shift peaks at 178 and 158 ppm, due to –COOH and aromatic ring =C–N, respectively. The –COOH peak is also observed in CMF. These characteristic peaks for carbonyl carbons in organic acids are expected in the range of 155 – 185 [58] and observed in carboxymethyl cellulose at 177 – 178 ppm [16].

The aldehyde (–CHO) chemical shift is expected in the range of 185 – 220 ppm [58]. The absence of this peak has been attributed to the formation of hemiacetals [9, 11, 23] or the peak may not have been observed in the reported range of chemical shifts (0 – 200 ppm). The weak peak at 202 ppm in fully oxidized DAC (**Figure S5.6***)* strongly suggest that there are –CHO groups that did not form hemiacetals.

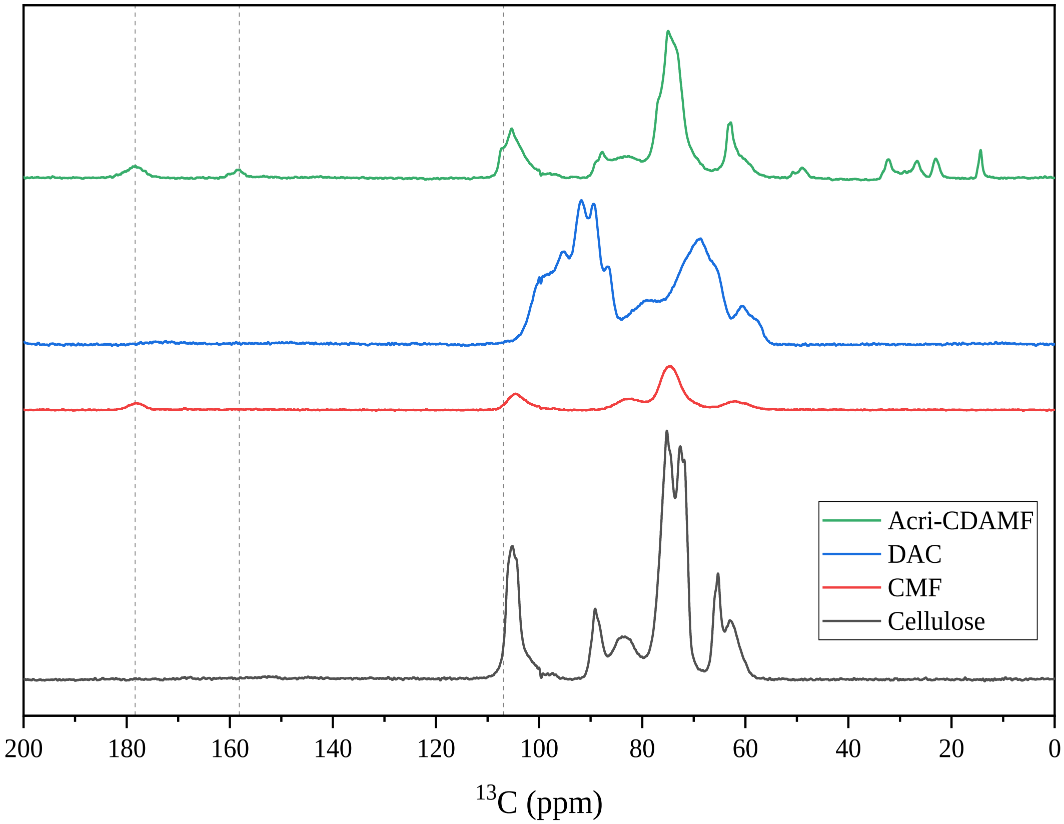

Figure. 5.10: Solid-state ^{13}C NMR spectra for cellulose carboxymethyl cellulose fibers, dialdehyde cellulose and imine carboxymethyl-dialdehyde cellulose functionalized fibers.

The peaks at 60 – 110 ppm are due to the glucopyranoside unit as assigned by [46] and the slight shape variations observed in ICDAMF are due to the partial oxidation reactions. These variations occur due to loss of crystallinity with increasing degree of oxidation [9, 23]. The peaks in ICDAMF at about 15 – 50 ppm are due to alkyl groups [11] attached to aromatic rings in the dye. Carbon-13 NMR correlation charts [58] predict that peaks due to aromatic rings are expected in the range 110 – 175. There is a broad peak in the ICDAMF spectrum ~110 ppm, which could be aromatic ring peaks overlapped with cellulose ring moieties.

5.4.4.3 Characterization by X-ray diffraction

Cellulose, dialdehyde cellulose, acridine yellow G and acridine-CDAMF X-ray diffractograms are presented in **Figure 5.11**. Reduction of the peak intensity at the 2 0 0 plane in acridine-CDAMF indicates a considerable reduction in crystallinity relative to cellulose, whereas the amorphous scatter is retained at the Bragg's 2θ angle of ~15°. Kraft cellulose pulp has two prominent peaks at 15.6° and 22.5°, in agreement with observations by Sabzalian (2014) [11]. Anhydro D-glucopyranose ring-opening, via periodate oxidation, is the major contributor to the loss in crystallinity. This is observed in the diffraction pattern between highly oxidized DAC and partially oxidized acridine-CDAMF. Therefore, partial oxidation results in retention of some crystallinity, similarly observed by Lindh (2014) [9] and Conley (2016) [22]. In addition, cellulosic-product crystallinity can be affected by solvents through interruption of intra- and inter-fibre hydrogen bonds resulting in reconfiguration during self-assembly [60]. Furthermore, the highly crystalline acridine dye sharp peaks observed are absent in an acridine-CDAMF diffractogram. This is attributed to the covalent binding of the dye onto the cellulose fibers, thereby preventing crystallization upon drying. Therefore, dangling Schiff base product may also contribute to the loss in crystallinity and a marginal shift in the amorphous and crystalline peak positions.

Additionally, a change in crystallinity due to partial oxidation affects the NMR peak shape and sharpness at about 65 and 90 ppm. Loss of crystallinity leads to broadness of the two peaks as observed between unmodified cellulose and acridine-CDAMF in **Figure. 5.10**. These two peaks shape variations have been assigned due to contributions by amorphous and crystalline regions of cellulose when C4 and C6 are affected [61].

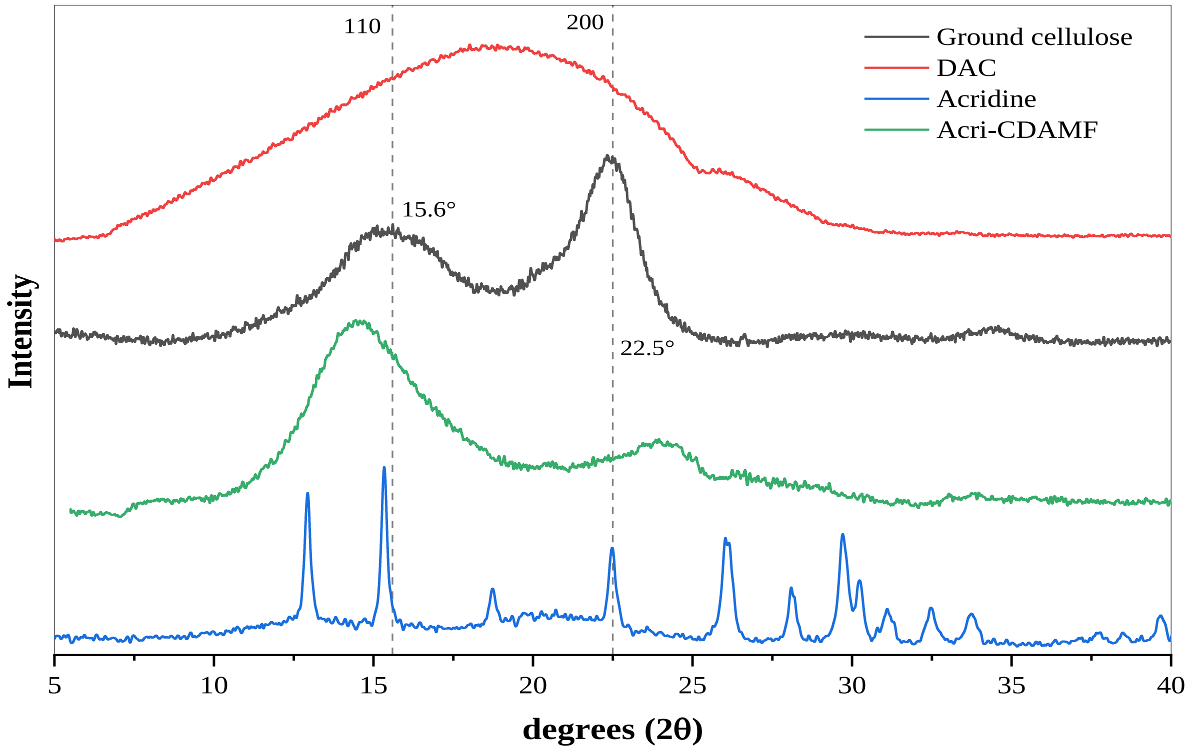

Figure 5.11: XRD patterns for cellulose, dialdehyde cellulose and imine carboxymethyl-dialdehyde cellulose functionalized fibers.

Dispersion in water, ethanol, sodium hydroxide (0.5 N), sulphuric acid (0.5 N) and hydrochloric acid (0.5 N)

Dispersion in 1% solutions indicates that the cellulose fiber modification increases solubility and/or mercerization under alkaline conditions and can be regenerated in acid, as shown pictorially by optical polarized micrographs in water, ethanol, sodium hydroxide (0.5 N), sulphuric acid (0.5 N) and hydrochloric acid (0.5 N) used as solvents in **Figure 5.12**. The ICDAMF was solubilized and extruded according to a method described by [19] and a video provided in supplemental material. Additionally, ethanol had a tendency to bundle the fibres together, and it has been recommended as a good solvent for cellulose regeneration [62]. It was observed that decolorization does not occur in all solvents except hydrochloric acid. Under strong alkali conditions, irreversible swelling of cellulose I crystalline structure transforms to cellulose II via the Na-Cellulose intermediate crystalline species [25].

Material **Solvent**	**Cellulose**	**Acridine-CDMAF**
H_2O	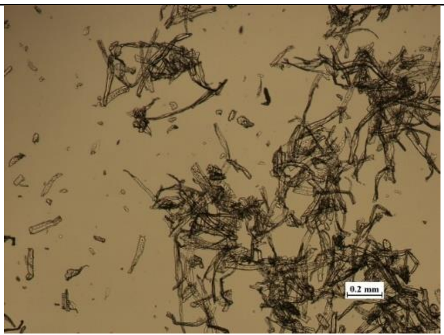	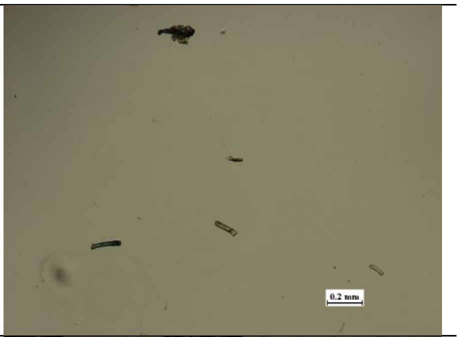
Ethanol		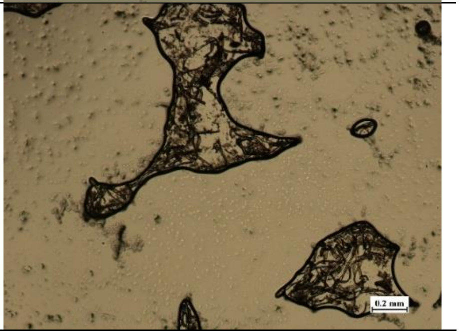

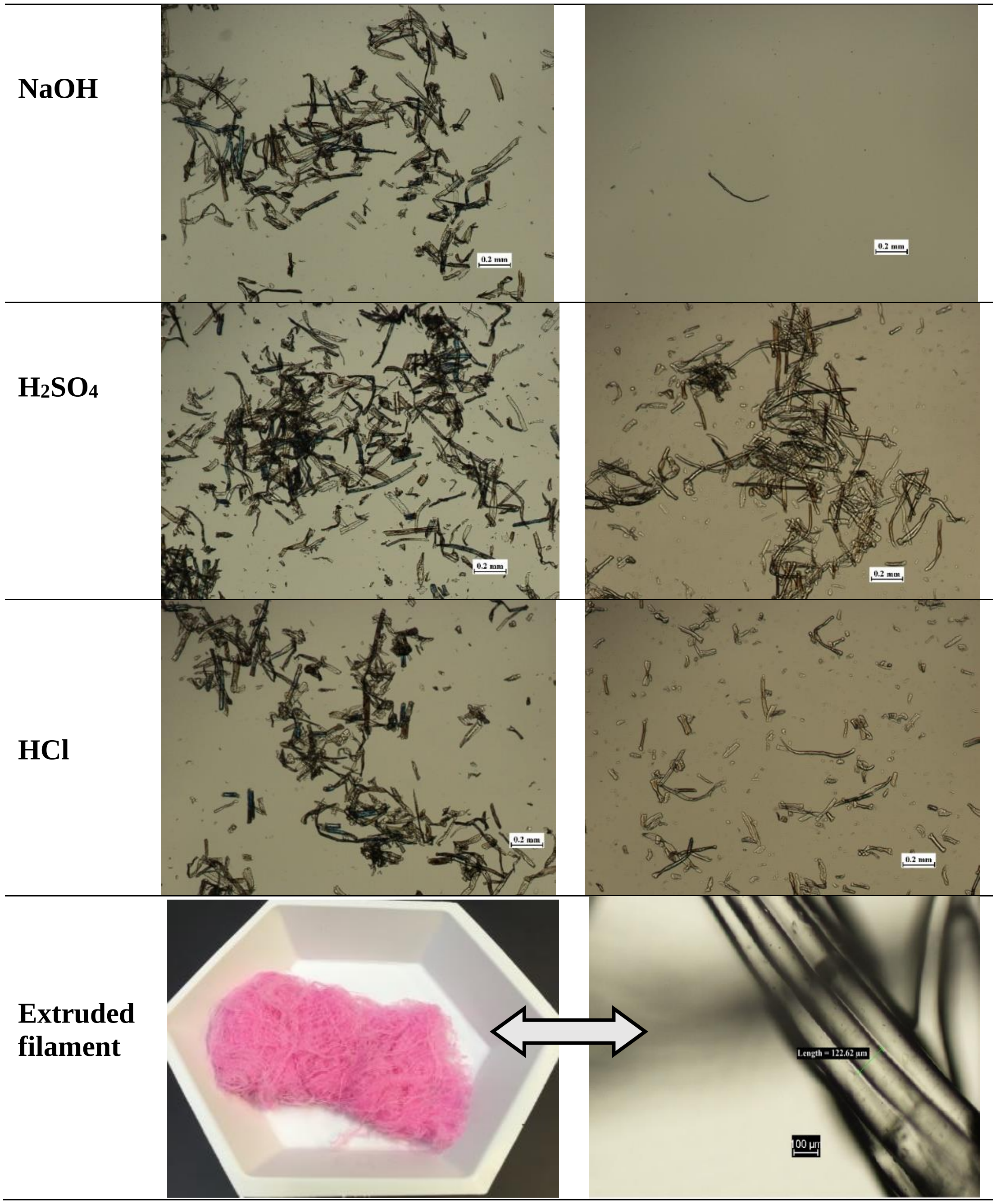

Figure 5.12: Optical and polarized microscopy images on effect of solvent on solubility. A photographic and microscopy image of the physical appearance of a wet extruded filament fibre from modified cellulose.

5.5 Conclusions

Cellulose fibers were 30% chemically modified to develop a one-pot synthetic pathway to produce multi-functionalized fibers by carboxymethylation (0.92 ± 0.21 mmol/g), periodate oxidation (3.0 ± 0.4 mmol/g) and Schiff base reactions (~0.1 mmol/g). Sequential addition of reagents, without isolating and purifying intermediate products, is time and cost saving. This is achieved by minimizing competing reactions and optimize the conditions that best suit each reaction step. The established order of reaction is starting with carboxymethylation because it requires elevated temperatures and isopropanol solvent. This is followed by periodate oxidation, under aqueous conditions, to obtain aldehyde groups. Diamine dyes were used to further functionalize aldehydes to Schiff bases at pH 4.5. Diamines are preferred due to the ability to crosslink and reinforce the fiber structure, in addition to the self-assembly of DAMF.

The protocol was applied to four different amine-based dyes and imine carboxymethyl dialdehyde modified cellulose fibers (ICDAMF) were produced. ICDAMF was characterized and dispersion tests were conducted in aqueous and organic solvents, and no leaching of dye was detected. In aqueous solution, ICDAMF was able to form a gel and was insoluble under acidic conditions. This shows the product has great potential for wet spinning and/or molding into textile or other functional products.

5.6 Acknowledgements

The authors acknowledge funding support by a NSERC SRN on Green Fibers and a NSERC SPG, supported by FPInnovations.

5.7 Supplementary information for One-pot eco-friendly oxidative synthesis of imine carboxymethyl dialdehyde cellulosic fibers

Martin Sichinga, Timothy Kline, M.A (Tony) Whitehead, Theo G. M. van de Ven*

Department of Chemistry, Pulp and Paper Research Centre, McGill University, 3420 Rue University, Montreal, Quebec, H3A 2A7, Canada

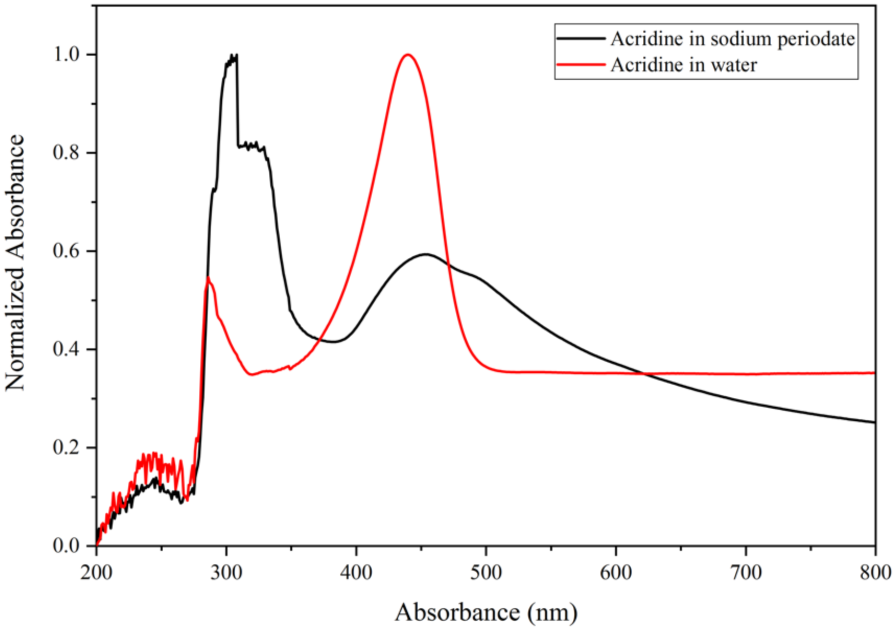

Figure S5.1: Effect of sodium periodate on absorption wavelength of acridine yellow G

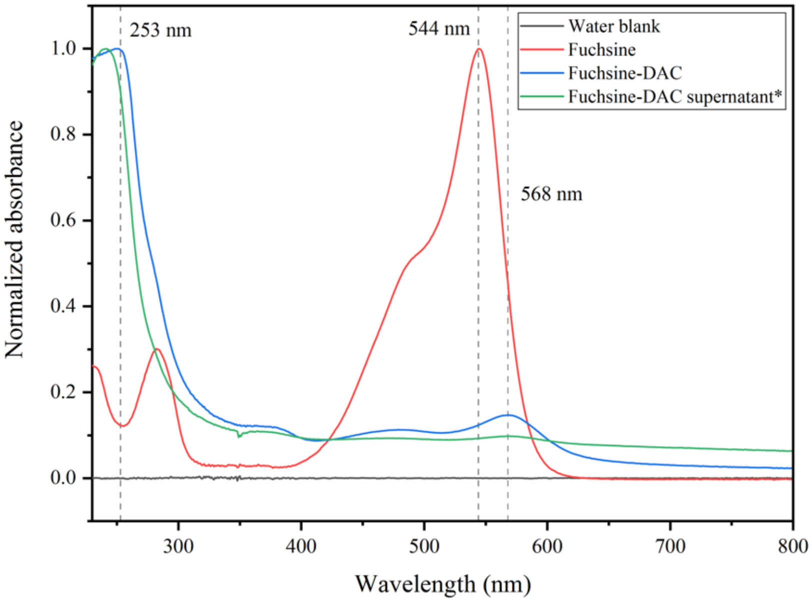

Figure S5.2: UV-vis spectra of basic fuchsine dye before and after Schiff base reaction with dialdehyde cellulose. *Fuchsine-DAC supernatant measured after heating the product at 80 °C for 6 hours

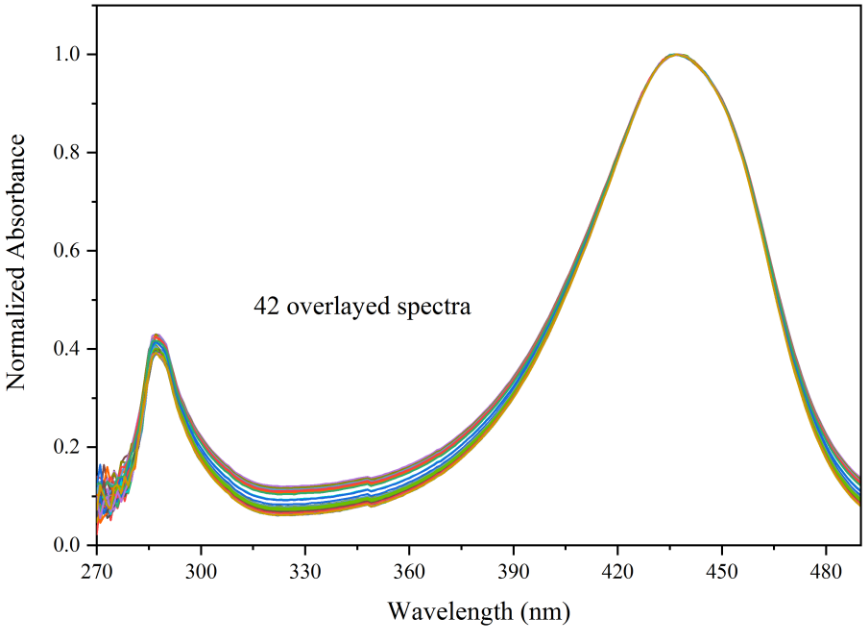

Figure S5.3: Acridine dye solution and UV-Vis instrument stability

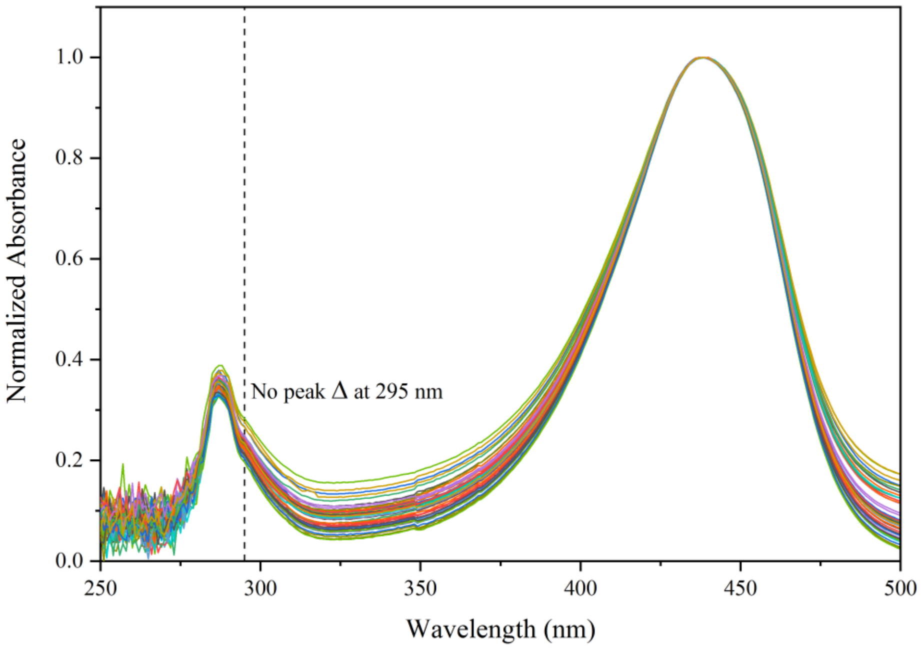

Figure S5.4: Cellulose and acridine yellow G reaction kinetics

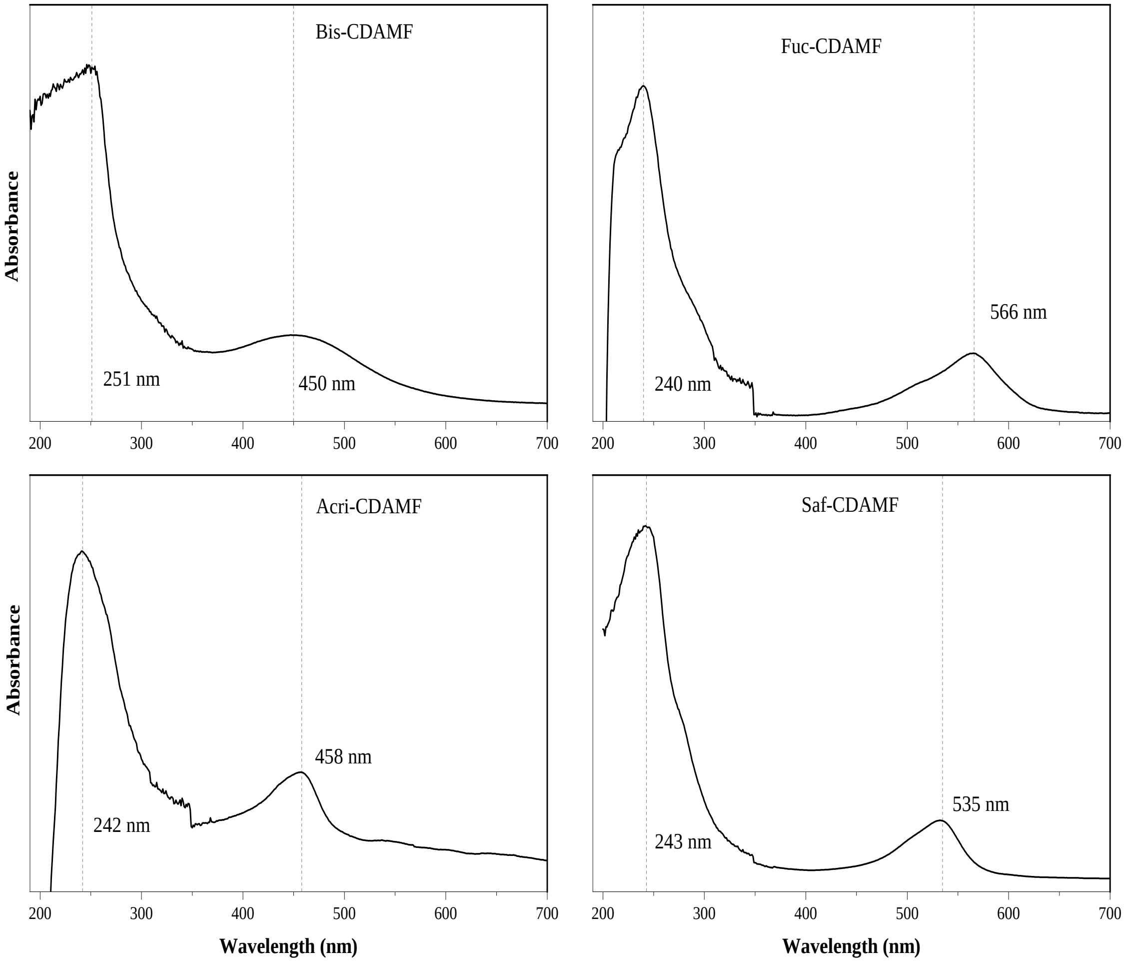

Figure S5.5: UV-Vis spectra of purified ICDAMFs

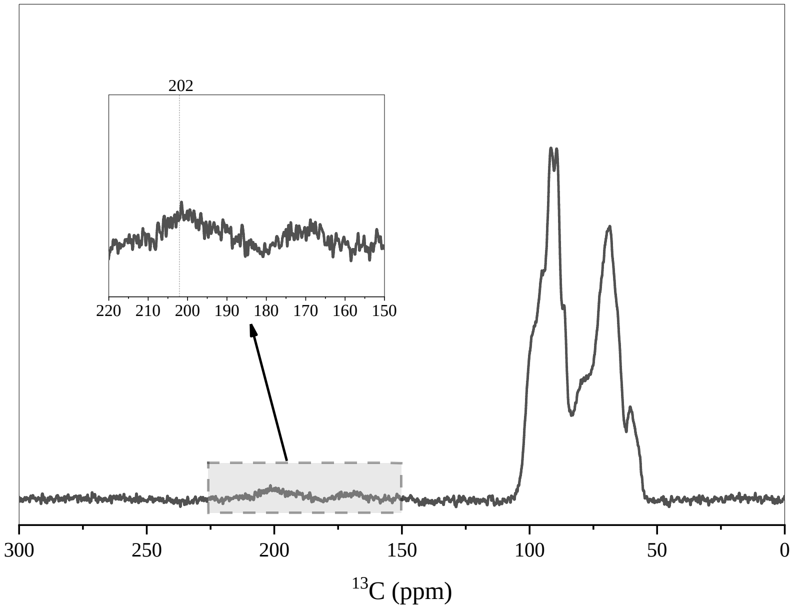

Figure S5.6: Residual aldehyde carbon on DAC

References

[1] L. Goetz, A. Mathew, K. Oksman, P. Gatenholm, A.J. Ragauskas, A novel nanocomposite film prepared from crosslinked cellulosic whiskers, Carbohydrate Polymers 75 (2009) 85-89.

[2] V. Nessi, X. Falourd, J.-E. Maigret, K. Cahier, A. D'Orlando, N. Descamps, V. Gaucher, C. Chevigny, D. Lourdin, Cellulose nanocrystals-starch nanocomposites produced by extrusion: Structure and behavior in physiological conditions, Carbohydrate Polymers 225 (2019) 115123.

[3] F. Rol, M.N. Belgacem, A. Gandini, J. Bras, Recent advances in surface-modified cellulose nanofibrils, Progress in Polymer Science 88 (2019) 241-264.

[4] E. Lizundia, E. Meaurio, J.L. Vilas, Chapter 3 - Grafting of Cellulose Nanocrystals, in: D. Puglia, E. Fortunati, J.M. Kenny (Eds.), Multifunctional Polymeric Nanocomposites Based on Cellulosic Reinforcements, William Andrew Publishing2016, pp. 61-113.

[5] S. Ramesh, P. Radhakrishnan, Cellulose nanoparticles from agro-industrial waste for the development of active packaging, Applied Surface Science 484 (2019) 1274-1281.

[6] R. Kumar, R.K. Sharma, A.P. Singh, Grafted cellulose: a bio-based polymer for durable applications, Polymer Bulletin 75 (2018) 2213-2242.

[7] M. Tavakolian, J. Lerner, F. Medina Tovar, J. Frances, T.G.M. van de Ven, A. Kakkar, Dendrimer directed assembly of dicarboxylated hairy nanocellulose, Journal of Colloid and Interface Science 541 (2019) 444-453.

[8] B.V. Basheer, J.J. George, S. Siengchin, J. Parameswaranpillai, Polymer grafted carbon nanotubes—Synthesis, properties, and applications: A review, Nano-Structures & Nano-Objects 22 (2020) 100429.

[9] J. Lindh, D.O. Carlsson, M. Strømme, A. Mihranyan, Convenient One-Pot Formation of 2,3-Dialdehyde Cellulose Beads via Periodate Oxidation of Cellulose in Water, Biomacromolecules 15 (2014) 1928-1932.

[10] M.N. Alam, M. Antal, A. Tejado, T.G.M. van de Ven, Salt-induced acceleration of chemical reactions in cellulose nanopores, Cellulose 19 (2012) 517-522.

[11] Z. Sabzalian, M.N. Alam, T.G.M. van de Ven, Hydrophobization and characterization of internally crosslink-reinforced cellulose fibers, Cellulose 21 (2014) 1381-1393.

[12] C.-Q. Ruan, M. Strømme, J. Lindh, Preparation of porous 2,3-dialdehyde cellulose beads crosslinked with chitosan and their application in adsorption of Congo red dye, Carbohydrate Polymers 181 (2018) 200-207.

[13] A. Benchabane, K. Bekkour, Rheological properties of carboxymethyl cellulose (CMC) solutions, Colloid and Polymer Science 286 (2008) 1173.

[14] P. Liu, M. Zhai, J. Li, J. Peng, J. Wu, Radiation preparation and swelling behavior of sodium carboxymethyl cellulose hydrogels, Radiation Physics and Chemistry 63 (2002) 525-528.

[15] V. Pushpamalar, S.J. Langford, M. Ahmad, Y.Y. Lim, Optimization of reaction conditions for preparing carboxymethyl cellulose from sago waste, Carbohydrate Polymers 64 (2006) 312-318.

[16] G. Joshi, S. Naithani, V.K. Varshney, S.S. Bisht, V. Rana, P.K. Gupta, Synthesis and characterization of carboxymethyl cellulose from office waste paper: A greener approach towards waste management, Waste Management 38 (2015) 33-40.

[17] N. Haleem, M. Arshad, M. Shahid, M.A. Tahir, Synthesis of carboxymethyl cellulose from waste of cotton ginning industry, Carbohydrate Polymers 113 (2014) 249-255.

[18] G. Sim, Y. Liu, T.G.M. van de Ven, Transparent composite films prepared from chemically modified cellulose fibers, Cellulose 23 (2016) 2011-2024.

[19] M.S. Islam, M.N. Alam, T.G.M. van de Ven, Production of textile filaments from carboxymethylated cellulosic pulps, Cellulose 28 (2021) 9475-9488.

[20] R. Barbucci, A. Magnani, M. Consumi, Swelling Behavior of Carboxymethylcellulose Hydrogels in Relation to Cross-Linking, pH, and Charge Density, Macromolecules 33 (2000) 7475-7480.

[21] P. Calvini, G. Conio, M. Lorenzoni, E. Pedemonte, Viscometric determination of dialdehyde content in periodate oxycellulose. Part I. Methodology, Cellulose 11 (2004) 99-107.

[22] K. Conley, M. Whitehead, T.G.M. van de Ven, Chemically peeling layers of cellulose nanocrystals by periodate and chlorite oxidation, Cellulose 23 (2016) 1553-1563.

[23] U.-J. Kim, S. Kuga, M. Wada, T. Okano, T. Kondo, Periodate Oxidation of Crystalline Cellulose, Biomacromolecules 1 (2000) 488-492.

[24] U.-J. Kim, S. Kuga, Thermal decomposition of dialdehyde cellulose and its nitrogen-containing derivatives, Thermochimica Acta 369 (2001) 79-85.

[25] T. Budtova, P. Navard, Cellulose in NaOH–water based solvents: a review, Cellulose 23 (2016) 5-55.

[26] H. Yang, D. Chen, T.G.M. van de Ven, Preparation and characterization of sterically stabilized nanocrystalline cellulose obtained by periodate oxidation of cellulose fibers, Cellulose 22 (2015) 1743-1752.

[27] C.M. da Silva, D.L. da Silva, L.V. Modolo, R.B. Alves, M.A. de Resende, C.V.B. Martins, Â. de Fátima, Schiff bases: A short review of their antimicrobial activities, Journal of Advanced Research 2 (2011) 1-8.

[28] T. Zheng, X. Yu, S. Pilla, Mechanical and moisture sensitivity of fully bio-based dialdehyde carboxymethyl cellulose cross-linked soy protein isolate films, Carbohydrate Polymers 157 (2017) 1333-1340.

[29] L. Dubrovina, O. Naboka, V. Ogenko, P. Gatenholm, P. Enoksson, One-pot synthesis of carbon nanotubes from renewable resource: cellulose acetate, Journal of Materials Science 49 (2014) 1144-1149.

[30] A. Shaabani, A. Maleki, J. Moghimi Rad, E. Soleimani, Cellulose Sulfuric Acid Catalyzed One-Pot Three-Component Synthesis of Imidazoazines, Chemical and Pharmaceutical Bulletin 55 (2007) 957-958.

[31] L. Jasmani, S. Eyley, C. Schütz, H. Van Gorp, S. De Feyter, W. Thielemans, One-pot functionalization of cellulose nanocrystals with various cationic groups, Cellulose 23 (2016) 3569-3576.

[32] A. Pettignano, A. Charlot, E. Fleury, Solvent-Free Synthesis of Amidated Carboxymethyl Cellulose Derivatives: Effect on the Thermal Properties, Polymers (Basel) 11 (2019) 1227.

[33] A. Sheikhi, S. Safari, H. Yang, T.G.M. van de Ven, Copper Removal Using Electrosterically Stabilized Nanocrystalline Cellulose, ACS Applied Materials & Interfaces 7 (2015) 11301-11308.

[34] H. Yang, A. Sheikhi, T.G.M. van de Ven, Reusable Green Aerogels from Cross-Linked Hairy Nanocrystalline Cellulose and Modified Chitosan for Dye Removal, Langmuir 32 (2016) 11771-11779.

[35] T. Kaldéus, P.T. Larsson, A. Boujemaoui, E. Malmström, One-pot preparation of bi-functional cellulose nanofibrils, Cellulose 25 (2018) 7031-7042.

[36] M.P. Adinugraha, D.W. Marseno, Haryadi, Synthesis and characterization of sodium carboxymethylcellulose from cavendish banana pseudo stem (Musa cavendishii LAMBERT), Carbohydrate Polymers 62 (2005) 164-169.

[37] L.F. Berhenke, E.C. Britton, Effect of pH on Hydrolysis Rate of Chloroacetic Acid, Industrial & Engineering Chemistry 38 (1946) 544-546.

[38] M.C. Nunes, F. dos Santos Carlos, O. Fuganti, L.A. da Silva, H.T. Ribas, S.M.B. Winnischofer, F.S. Nunes, A Facile Preparation of a New Water-Soluble Acridine Derivative and Application as a Turn-off Fluorescence Chemosensor for Selective Detection of Hg2+, Journal of Fluorescence 30 (2020) 235-247.

[39] C.F. Matta, M. Sichinga, P.W. Ayers, Information theoretic properties from the quantum theory of atoms in molecules, Chemical Physics Letters 514 (2011) 379-383.

[40] H. Yang, A. Tejado, N. Alam, M. Antal, T.G.M. van de Ven, Films Prepared from Electrosterically Stabilized Nanocrystalline Cellulose, Langmuir 28 (2012) 7834-7842.

[41] J. Araki, M. Wada, S. Kuga, Steric Stabilization of a Cellulose Microcrystal Suspension by Poly(ethylene glycol) Grafting, Langmuir 17 (2001) 21-27.

[42] E.S. Madivoli, P.G. Kareru, A.N. Gachanja, S.M. Mugo, D.S. Makhanu, Synthesis and characterization of dialdehyde cellulose nanofibers from O. sativa husks, SN Applied Sciences 1 (2019) 723.

[43] A. Tejado, M. Alam, M. Antal, H. Yang, T.G.M. van de Ven, Energy requirements for the disintegration of cellulose fibers into cellulose nanofibers, Cellulose 19 (2012) 831-842.

[44] E.G. Lewars, Computational Chemistry, Introduction to the theory and applications of molecular and quantum mechanics, Springer International Publishing, Switzerland, 2016, pp. 387-388.

[45] J.D. Kubicki, H.D. Watts, Quantum mechanical modeling of the vibrational spectra of minerals with a focus on clays, Minerals 9 (2019) 141.

[46] R. Koshani, T.G.M. van de Ven, A. Madadlou, Characterization of Carboxylated Cellulose Nanocrytals Isolated through Catalyst-Assisted H2O2 Oxidation in a One-Step Procedure, Journal of Agricultural and Food Chemistry 66 (2018) 7692-7700.

[47] L. Segal, J.J. Creely, A.E. Martin, C.M. Conrad, An Empirical Method for Estimating the Degree of Crystallinity of Native Cellulose Using the X-Ray Diffractometer, Textile Research Journal 29 (1959) 786-794.

[48] M. Moradian, M.S. Islam, T.G.M. van de Ven, Insoluble Regenerated Cellulose Films Made from Mildly Carboxylated Dissolving and Kraft Pulps, Industrial & Engineering Chemistry Research 60 (2021) 5385-5393.

[49] J. Sirvio, U. Hyvakko, H. Liimatainen, J. Niinimaki, O. Hormi, Periodate oxidation of cellulose at elevated temperatures using metal salts as cellulose activators, Carbohydrate Polymers 83 (2011) 1293-1297.

[50] G.J. Buist, C.A. Bunton, J.H. Miles, 149. The mechanism of oxidation of α-glycols by periodic acid. Part V. Cyclohexane-1 : 2-diols, Journal of the Chemical Society (Resumed) (1959) 743-748.

[51] N.P. Smirnova, N.I. Surovtseva, T.V. Fesenko, E.M. Demianenko, A.G. Grebenyuk, A.M. Eremenko, Photodegradation of dye acridine yellow on the surface of mesoporous TiO2, SiO2/TiO2 and SiO2 films: spectroscopic and theoretical studies, Journal of Nanostructure in Chemistry 5 (2015) 333-346.

[52] J.W. Rowen, C.M. Hunt, E.K. Plyler, Absorption Spectra in the Detection of Chemical Changes in Cellulose and Cellulose Derivatives, Textile Research Journal 17 (1947) 504-511.

[53] L.F.W. Vleugels, S. Ricois, I.K. Voets, R. Tuinier, Determination of the ‘apparent pKa’ of selected food hydrocolloids using ortho-toluidine blue, Food Hydrocolloids 81 (2018) 273-283.

[54] A.M. Zhivkov, Electric Properties of Carboxymethyl Cellulose, Cellulose - Fundamental Aspects2013, pp. 197-226.

[55] P. Calvini, The Influence of Levelling-off Degree of Polymerisation on the Kinetics of Cellulose Degradation, Cellulose 12 (2005) 445-447.

[56] R.L. Heinemann, Comparative Spectroscopy of Basic Fuchsin, Schiff Reagent, and a Formalin-Schiff Derivative in Relation to Dye Structure and Staining, Stain Technology 45 (1970) 165-172.

[57] M.C. Sichinga, R. Koshani, T.G.M. van de Ven, Chemisorption of basic fuchsine in packed beds of dialdehyde cellulose fibres, Colloids and Surfaces A: Physicochemical and Engineering Aspects 632 (2022) 127726.

[58] L.D. Pavia, M.G. Lampman, S.G. Kriz, R.J. Vyvyan, Introduction to Spectroscopy, 4 ed., Brooks/Cole Cengage Learning, United States of America, 2009.

[59] A. Cinarli, D. Gürbüz, A. Tavman, A.S. Birteksöz, Synthesis, spectral characterizations and antimicrobial activity of some Schiff bases of 4-chloro-2-aminophenol, Bulletin of the Chemical Society of Ethiopia 25 (2011) 407 - 417.

[60] N. Pircher, L. Carbajal, C. Schimper, M. Bacher, H. Rennhofer, J.-M. Nedelec, H.C. Lichtenegger, T. Rosenau, F. Liebner, Impact of selected solvent systems on the pore and solid structure of cellulose aerogels, Cellulose 23 (2016) 1949-1966.

[61] S. Park, J.O. Baker, M.E. Himmel, P.A. Parilla, D.K. Johnson, Cellulose crystallinity index: measurement techniques and their impact on interpreting cellulase performance, Biotechnology for Biofuels 3 (2010) 10.

[62] F. Liebner, A. Potthast, T. Rosenau, E. Haimer, M. Wendland, Cellulose aerogels: Highly porous, ultra-lightweight materials, 62 (2008) 129-135.

6 Conclusions and future work

6.1 Conclusions

In this thesis, cellulose derivates were synthesized and evaluated for suitability in textile manufacturing applications, by addressing the shortcomings of the rayon and lyocell processes. The major concerns in rayon processing are the release of carbon disulfide from cellulose xanthate and poor dye fastness which is mainly physisorbed. The lyocell process is energy intensive and requires the use of stabilizers leading to formation of by-products and high operation costs.

A mildly modified carboxymethyl cellulose fibers (CMF), with a charge content of 1.3 - 1.7 mmol g^{-1}, wet extrusion method was developed and optimized by dissolving the fibers in NaOH and extruded continuously in H_2SO_4, with salt as the only bi-product. Hence, the novel method attempts to address the technological, health and environmental drawbacks. Chapter 3 of this thesis builds on the method by performing the carboxymethylation reaction under solvent-free conditions using mechanical action. The conventional CMF synthesis method uses 2-propanol and ethanol solvents. These organic solvents prevent gelation in aqueous media, as a result, the CMF must be thoroughly washed and dried prior to making dope. Additionally, in an industrial setup, the alcohol recovery via distillation is energetically demanding. In the solvent-free process, the wash step is eliminated as alcohols are not utilized, thereby preparing the dope solutions following carboxymethylation. Furthermore, it was observed that mechanical milling minimizes monochloroacetic acid hydrolysis giving higher yields at a higher rate of reaction. Thus, mechanical milling provides a green alternative to conventional carboxymethylation, in combination with elimination of alcohol usage and reduction of filament processing steps has the potential to be more efficient, environmentally friendly and cost effective. These benefits make it viable for industrial adaptation.

In Chapter 4, the kinetics of fuchsine dye chemisorption on dialdehyde cellulose (DAC) fibers, in relation to physisorption on unmodified cellulose fibers, was evaluated. This was achieved in a continuous flow experiment using packed beds and a fixed flow rate. It was observed that physisorption had significantly higher adsorption/desorption rates than the chemisorption process, hence the chemical attachment was the rate determining step. This data was critical in determining the dye addition stage in filament production. Additionally, it was observed that conjugating DAC with a diamine significantly reduced high temperature solubility, a property that is significant in textiles.

In Chapter 5, a concerted mildly multi-functionalized cellulosic product containing carboxyl groups, aldehydes and a Schiff base was produced. Based on the discussion in Chapter 4, it was imperative that the dye be applied to the fibers prior to extrusion. This change is a major shift in the current industrial practice. The relocation of dyeing step prevents generation of waste products since only the desired amount of dye, based on the amount of available aldehyde groups, is added to the reaction mixture. It was also observed that the dye does not leach into the coagulation bath during extrusion, therefore, chemisorption improves the fiber fastness. A single-pot synthesis has the potential to improve production efficiency by eliminating purification of intermediate products, in addition to reduced water and solvent consumption.

Overall, the newly developed filament production attempts to minimize the quantities of solvents and reagents used via mild chemical modifications. This reduces makes the process economically viable and low environmental impact while to preserving most properties of cellulose, such as biodegradability and recyclability. This technology will be transformative once fully optimized.

6.2 Suggestions for future work

- An automated pilot scale spinneret (**Figure 6.1**) has been acquired and assembled, there is a need to get it operational.
- Optimize the process on the pilot spinneret.
- Use the pilot spinneret to produce kilogram quantities of CMF-based filaments and convert them into yarns.
- Explore blending of CMF-based filaments with other fibers or chemical modifications to enhance and develop materials with desired properties, such as reflective safety wear, fire resistance fibers.
- For the discussion in Chapter 3, there is need to further investigate if mechanical milling results in formation of nanoparticles and in general explore the characteristics of the milling product further.
- For the discussion in Chapter 5, further exploration on the fiber qualities and strength after multiple oxidations is necessary

Pilot scale wet spinning spinneret

Spinneret head with 300 of 70 µm holes

Figure 6.1: Automated pilot scale wet spinning spinneret for use in production of CMF textile filaments.